STEMM-CCS @ GHGT-14

Conference papers

14th International Conference on Greenhouse Gas Control Technologies, GHGT-14

21st -25th October 2018, Melbourne, Australia

Ensuring efficient and robust offshore storage – the role of marine system modelling.

Jerry Blackford[a], *, Guttorm Alendal[b], Yuri Artioli[a], Helge Avlesen[c], Pierre W. Cazenave[a], Baixin Chen[d], Andrew W. Dale[e], Marius Dewar[d], Maribel I. García-Ibáñez[c], Jonas Gros[e], Kristian Gundersen[b], Matthias Haeckel[e], Sorush Khajepor[d], Gennadi Lessin[a], Anna Oleynik[b], Abdirahman M. Omar[c], Umer Saleem[d].

[a] Plymouth Marine Laboratory, Prospect Place, Plymouth, PL1 3DH, UK
[b] Department of Mathematics, University of Bergen, Bergen, Norway
[c] Uni Research Climate, Bjerknes Centre for Climate Research, Bergen 5008, Norway
[d] Institute of Mechanical, Process and Energy Engineering, Heriot-Watt University, Edinburgh, EH14 4AS, UK
[e] GEOMAR Helmholtz Centre for Ocean Research Kiel, Wischhofstrasse 1-3, 24148 Kiel, Germany

Abstract

This paper describes the utility of developing marine system models to aid the efficient and regulatory compliant development of offshore carbon storage, maximising containment assurance by well-planned monitoring strategies. Using examples from several model systems, we show that marine models allow us to characterize the chemical perturbations arising from hypothetical release scenarios whilst concurrently quantifying the natural variability of the system with respect to the same chemical signatures. Consequently models can identify a range of potential leakage anomaly detection criteria, identifying the most sensitive discriminators applicable to a given site or season. Further, using models as in-silico testbeds we can devise the most cost-efficient deployment of sensors to maximise detection of CO_2 leakage. Modelling studies can also contribute to the required risk assessments, by quantifying potential impact from hypothetical release scenarios. Finally, given this demonstrable potential we discuss the challenges to ensuring model systems are available, fit for purpose and transferable to CCS operations across the globe.

Keywords: CCS; Offshore; Storage; Marine; Monitoring; Modelling

1. Introduction

Offshore geological storage options are available in many countries; however demonstrating robust storage poses some unique challenges in the marine environment. To comply with regulations and assure against false accusations, traditional seismic imaging of the storage complex and overburden can be complemented by monitoring at the sea floor for biochemical or physical anomalies, such as excess CO_2 concentrations or gas bubbles. Sea-floor techniques

* Corresponding author. Tel.: +44 (0)1752633462; fax: +44 (0)1752 633101.
E-mail address: jcb@pml.ac.uk

may have better sensitivity than seismics and contribute to all parts of the detection-location-verification-quantification process. Outstanding challenges include defining what constitutes an anomaly in a noisy time variant environment, and identifying optimal sensor combinations and deployment strategies to provide a sensitive, wide-ranging, accurate yet economic monitoring system. Here we demonstrate how marine modelling approaches are answering these challenges.

Developing a monitoring system requires that we meticulously understand the signals of leakage, and how these differ from natural, often highly-dynamic variability. For example, we need to predict the pathways of CO_2 transfer across the sediment-water interface, its phase chemistry under a variety of environmental conditions, the configuration of gas bubbles, their displacement and aqueous dissolution, the movement and dispersion of dissolved CO_2 plumes and their impact on the marine chemistry. In addition, we need to characterise how the same chemical and physical attributes evolve due to natural biological and physical processes. Understanding such "baselines", perhaps better termed natural variability, which will always be site- and season-specific, is critical to facilitate the successful detection and quantification of unintended emissions, for the application of corrective actions as well as the protection from false alarms.

Marine observations are generally expensive to undertake, requiring boat based surveys or the deployment of autonomous underway or fixed platforms. For scientific and practical reasons observations are biased towards the surface ocean and periods of poor weather are under-sampled. Consequently, sea floor marine systems are poorly described by direct observations, and the data that is available tends to be intermittent and sparse. However coastal regions are routinely described by marine system models – typically time evolving, 3D coupled hydrodynamic-biogeochemical systems which describe physical flows and biogeochemical fluxes, often explicitly modelling CO_2 chemistry (aka carbonate chemistry) and potentially hosting specialist modules, for example of bubble dynamics. Such models are run as decadal scale hind-casts and for short-term operational forecasts, both modes often using assimilation of observations to improve accuracy [1]. Models are also run in long-term climate forecast mode which allows for the assessment of impacts of increased atmospheric CO_2 emissions and other anthropogenic factors [2]. These models provide terabytes of internally-consistent, evaluated, skill-assessed [3] multi-variate data with comprehensive vertical, horizontal and temporal resolution – a virtual marine environment within which we can quantify baselines, simulate unplanned release and assess monitoring strategies.

2. Model developments and outcomes

Within a number of past and ongoing research and development projects, including STEMM-CCS [4], BayMoDe [5] and ECO2 [6,7,8,9] the research community has devoted considerable effort to developing and applying marine system models to advance offshore storage. We can now articulate the following understanding, advances and tools that will facilitate the development of geological storage in the marine domain.

2.1. Characterization of hypothetical release scenarios

In the absence of sufficient realistic analogues, models provide the only option to characterize the morphology of diverse hypothetical release events via sediments and water column (Fig 1), and thereby quantify detection targets. Offshore analogues of CO_2 release (natural seeps) do exist and can be helpful in establishing broad scale understanding of phenomena, however these are substantially variant from a CCS scenario. For example methane seeps, often biogenic in nature, are common, but methane has distinctly different solubility characteristics in seawater compared to CO_2 [10]. CO_2 seeps are also found in the marine environment, but often associated with volcanic activity, such that their location and environmental characteristics are not a close match with existing and potential storage sites. Controlled deliberate injection/release experiments are expensive and therefore rare [11] and whilst informative [12] deliver limited scenario variability.

A number of studies have used combinations of sediment, hydrodynamic and biogeochemical models to

characterise a wide variety of "leakage" scenarios. The primary varient between these studies is the spatial model resolution and the release rate tested. A-priori information on potential leak scenarios is by definition scant as the only expected scenario is no release. Consequently modelled scenarios range from the smallest rates that could be sensibly resolved by a particular model system to upper limits defined by injection rates, or especially in early research even more extreme releases, designed to demonstrate certain environmental consequences rather than be constrained by the operational reality of storage. Typically operational shelf models have resolutions of the order of 10 *km* in the horizontal, which are only suitable to represent dissolved phase plumes with footprints an order of magnitude larger [13]. However shelf scale models with resolutions approaching 1 *km* [14] have been applied as have sub-regional model domains whose resolution can be as fine as 1 *m* [15,16] , which allow very small release rates to be tested. These ultra-high resolution models also allow multiphase simulations, including the dynamics of bubble plumes as well as the dissolved phase [17]. Models of the upper layers of unconsolidated sediments [18] further enable the characterisation of multiphase flow and inform the morphology of leakage, in particular the nature of flow across the sediment-water interface which can modify the distribution of CO_2 plumes in the vicinity of the release point(s) and crucially affects the initial plume height with implications for broader scale dispersion and outgassing to the atmosphere as well as the visibility of gas bubble plumes to acoustic detection.
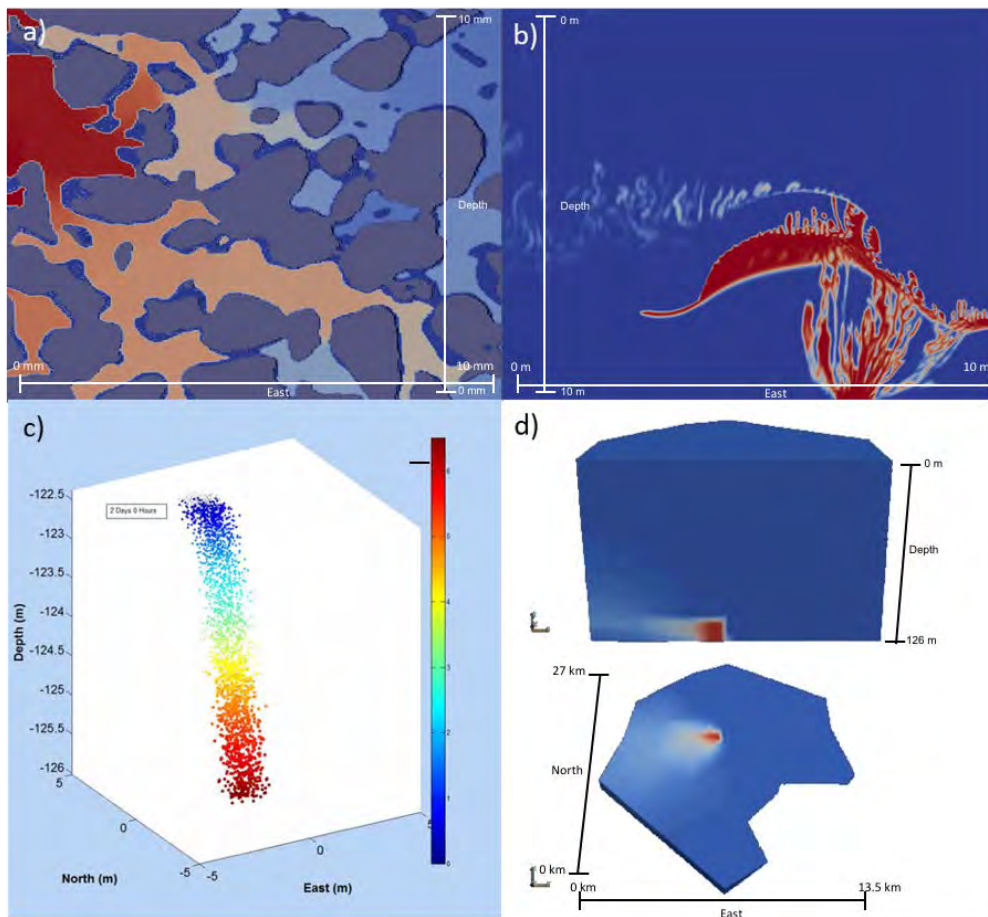

Figure 1. a) Flow through porous media in the pore scale (by a Lattice Boltzmann model, shown in terms of fluid pressures); b) Flow through porous media (red) and into the water column (white) in the meter scale (by a Navier-Stokes Darcy model shown in terms of void fraction); c) CO_2 bubble plumes rising and dissolving in the water column (by a multiphase plume model shown in terms of bubble size – mm); d) flow of dissolved CO_2 solution in the water column (by a multiphase plume model shown in terms of dissolved mass concentration).

As a result of this combined body of work we have a growing set of quantified release scenarios, ranging over at least seven orders of magnitude (see Fig 5). Primarily plume size (and therefore impact and detectability) relates to release rate according to a power law, consistent with the general dispersion of substances in marine environments [19]. However very significant variability of plume morphology is driven by the spatially and temporally varying tidal mixing vectors and seasonal weather-related phenomenon such as the degree of stratification and wind-induced mixing. Plumes are highly dynamic in space and time, often circulating around a release point on a tidal ellipse, with the strength of the perturbation decreasing with distance from the release point (Fig 1d).

2.2. Understanding and quantifying natural variability

Natural variability of marine CO_2 (Fig 2) may mask the signal from an unplanned release, and can also help to define the unperturbed state should an environmental impact assessment be necessary. Observational studies have demonstrated that the degree of variability itself varies according to location and season and is driven by a complex range of factors, which may include advection of water masses of different origin, influence of nearby riverine plumes, atmospheric CO_2, temperature, biological activity and in-situ mixing [20]. Conducting a comprehensive survey of the carbonate system to characterize the diurnal-seasonal-inter-annual and spatial variability of a particular storage site could be prohibitively expensive. However coupled model systems, which include sufficient process definition enable us to predict, extrapolate and quantify natural variability and its heterogeneity. A sufficient model system should include fully 3-dimensional hydrodynamics, riverine inputs, exchanges with open ocean boundaries and the atmospheric system, representation of biogeochemical processes especially community respiration and primary production and a fully resolved implementation of carbonate chemistry [21].
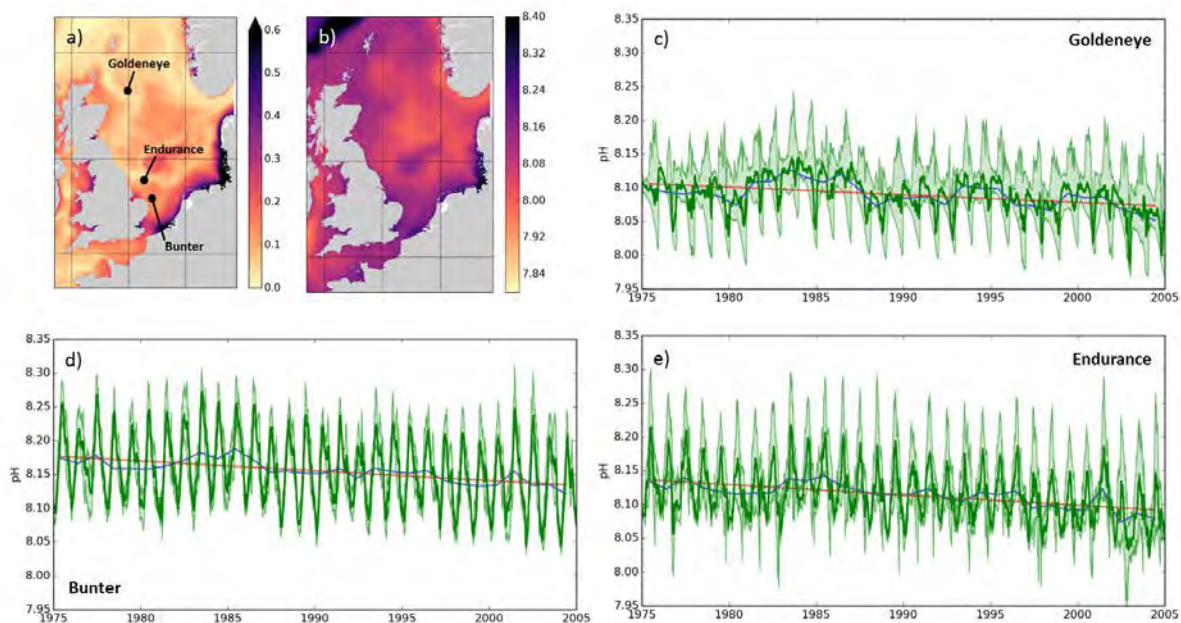

Figure 2. a) Annual range of seafloor pH (indicating CO_2 concentration) in the North Sea and b) mean pH using the NEMO-ERSEM model; c-e) contrasting evolution of baseline chemistry at different North Sea sites extracted from the model. Green shading shows the local variability, lines: green - daily mean, blue – annual mean, orange – acidification trend.

The example shown in figure 2 illustrates that within one regional sea, there are very distinct short-term, seasonal and inter-annual CO_2 dynamics, here using pH as a measure of concentration of CO_2. The annual range of pH varies between 0.5 pH units or more in shallow near shore environments where riverine influences are high, as are productivity cycles, to 0.1 pH units in deeper more oceanic conditions, where external influences and productivity

are minimized. Variability in shallow coastal regions tends to be dominated by seasonality whilst offshore, inter-annual variability and climate oscillations tend to be more influential. Only the long-term trend associated with ocean acidification is relatively constant across the region as this is a broad scale phenomenon driven by atmospheric CO_2 concentrations. On sub-diurnal timescales variability is driven by a combination of tidal mixing and the light-dark cycle of production/respiration. In the same region, changes within 24-hour periods are predicted to be of the order of 0.01-0.05 pH units, with maxima associated with peak biological and physical events [22].

2.3. Defining anomaly criteria

Perturbations arising from a release may be small, and of a similar magnitude to natural changes in CO_2 concentration especially if monitored at some distance from a release point. The challenge therefore is to develop highly sensitive criteria that identify anomalous chemistry as distinct from natural dynamics, minimizing the chance for false positives. By combining models of release scenarios and natural variability we can use these models to identify optimal detection criteria, identifying the most sensitive discriminators applicable to a given site or even season and identify the site-specific detection threshold.

A number of criteria have been investigated, falling into two categories. The first is based on detecting departures from normal stoichiometric relations. Natural changes in CO_2 concentration occur because of biological, chemical or physical processes, all of which create signals in other measurable variables. For example, the biological uptake of CO_2 during primary production is always accompanied by an equivalent release of oxygen, vice-versa for respiration. Such biological processes also affect nutrient concentrations. Natural changes in CO_2 arising because of mixing or advection of different water masses will also be accompanied by changes in temperature and or salinity. Although definition of natural stoichiometric relationships has been based on observational data sets [23,24] , models of sufficient complexity can be used to extend these definitions dynamically over larger areas and longer time periods [25], as well as defining the optimal combination of variables [26].
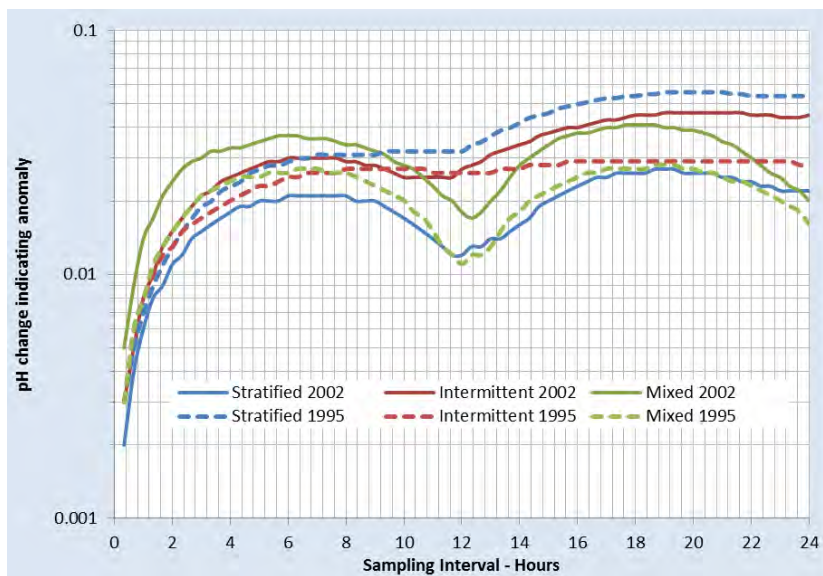

Figure 3. Theoretical anomaly detection thresholds, expressed as the rate of pH change relative to the sampling interval. Any rate change larger than indicated would suggest an anomaly requiring further investigation. Lines represent three different sites and two different years.

The second category utilizes the fact that given the mobility of CO_2 plumes, sensors (whether fixed or themselves mobile) are likely to be exposed to fluctuations in CO_2 over space and timescales that are different from the spatiotemporal gradients that result from natural processes [22,27]. By using models to define these natural

spatiotemporal gradients it is possible to then identify gradient-based thresholds which can be used to identify anomalous signals. For example if monitoring can approach sub-hourly frequencies, which is entirely within the capability of existing platforms, then criteria as sensitive as a change of pH of 0.01 unit over 20 minutes or less could be a reliable indicator of a release (Fig 3).

2.4. Optimizing sensor deployment and locating leaks

Designing monitoring programs to detect discharges which could theoretically occur anywhere within an area of several hundred square kilometres is challenging, one must take into account the variability of the marine environment and ocean dynamics. However, even if one can distinguish between CO_2 from a release from that due to natural variability, it is an additional challenge to identify the leak location. Building on knowledge of leak morphology, natural variability and anomaly criteria, models allow us to devise the most cost-efficient deployment of sensors to maximise detection. By quantifying how water movement impacts dispersion of CO_2 plumes, models can determine the minimum number of sensors and their optimal locations [28,29,30] , or the optimal deployment pathway of Autonomous Underwater Vehicles (AUVs) to maximise the likelihood of detection using Bayesian techniques [31] (Fig 4). Research is underway to develop machine learning techniques [32], inverse methods [33] and "greedy set" algorithms [34] to further optimise survey design.
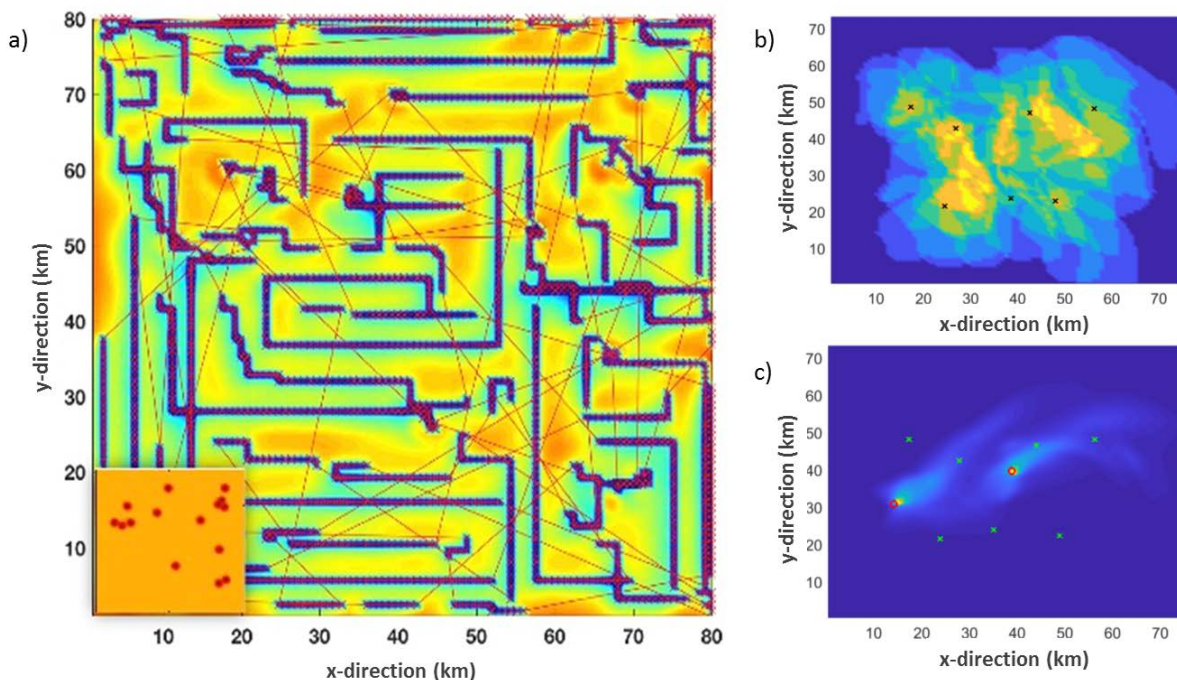

Figure 4. a) Optimal Autonomous Underwater Vehicles (AUV) route for rapid detection in an area with 15 wells (lower left corner) derived from Bayesian analysis. Measurement locations are shown in blue, AUV pathways as red lines whilst the background colour represents the probability of a leak at that location. b) Optimal sensor placements using simulation of 36 leaks at different locations with constant flow-rate and fixed detection threshold. Sensors placed such that any of 36 leaks would be detected while keeping the number of sensors minimal. c) Pseudo-colour plot of the averaged (in time) concentration c(x; t), measurement locations (crosses) and estimated leak locations (circles) using linear transport equation with sparse optimization method.

Model simulations suggest that a release event of 1 T day^{-1} may be detectable at 50 m distance, scaling to 5 km distance for a 100 T day^{-1} release, although local hydrodynamics would cause significant variability in the detection length-scale.

2.5. Risk assessments and communication

Environmental risk assessments are generally required by permitting authorities [35]. If required, marine models could contribute by quantifying potential impact from hypothetical release scenarios. These can utilize either the established relation between leak rate and affected area (Fig 5) or where specific risks are identified involve more detailed model studies in which impacts to species are explicitly coded into simulation models [36]. Such models can also consider other existing or potential stressors on a particular environment, as multiple stressors are generally recognized as more than cumulatively impactful on ecosystems. Additionally the accumulation of model scenario assessments can be used to inform stakeholders, including the public, regarding risks. Studies show that the potential impact from a small CCS leak will be very local (Fig 5), and that only catastrophic scale releases are likely to have some degree of regional scale impact. Importantly risks from CCS must be contrasted with risks of not performing climate mitigation, which are likely to be global and severe.
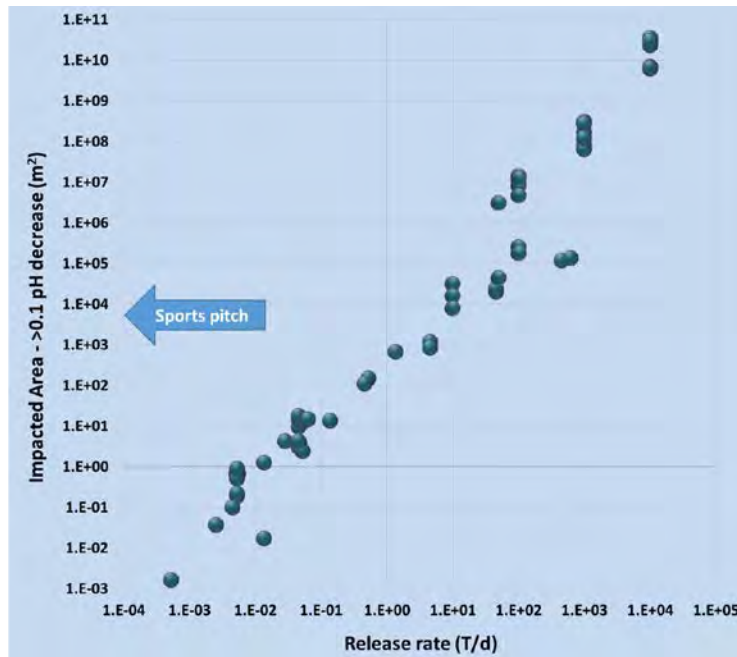

Figure 5. Model ensemble relationship between CO_2 release rate and impacted area. The size of a typical sports pitch (e.g. football) is indicated as a reference point. A decrease of 0.1 pH unit is a conservative indicator of impact potential.

3. Translation to operational capability and further challenges

The bad news for offshore CCS storage operations is that marine environments are so diverse that a generic definition of baselines, anomaly criteria and monitoring strategies will have little value, although the fundamental principles will be transferable from location to location. The positive outcome is that we can use models, ideally coupled with some observational data to ensure accuracy, to work out optimal criteria and strategies for individual storage sites, which will both minimise the cost of such monitoring whilst maximising rigour and thereby public acceptance.

It is the case that suitable marine models require a significant effort to develop, evaluate and interpret. They are often computationally expensive to run and models that are bespoke to particular storage sites are necessary. However, it is also the case that the majority of sites under consideration for offshore storage are already described by relevant model systems that at least resolve 3D hydrodynamics, boundary forcing and some degree of

biogeochemistry; such systems are already used for a variety of research and operational purposes. Many model systems now explicitly model carbonate chemistry, given the research interest in ocean acidification, and new model systems with high resolution are becoming more common. There are several examples cited here where existing model systems have been adapted to address CCS challenges, and where models are not yet optimal, code transfer can generally minimise further development effort.

   Using appropriately skilled models to derive baseline understanding, explore release scenarios and optimal site specific detection criteria is far more cost effective than deploying large observational programmes. However, model evaluation and quality assessment require in-situ environmental data, and establishing environmental baselines should be an intrinsic part of site characterisations. To assure adequate yet inexpensive baseline observations, early involvement of the marine modelling community is recommended, such that observational programmes can be targeted efficiently. However, there is much to gain by ensuring that national scientific monitoring programmes facilitate the monitoring required for CCS activities. Key parameters for CCS are common to those required for many other research purposes, e.g. temperature, salinity, pH, pCO_2, O_2, productivity, nutrients, etc. Perhaps the harder challenge is to reduce the bias towards sea surface measurements and to increase the frequency of observations such that variability on all scales is adequately captured.
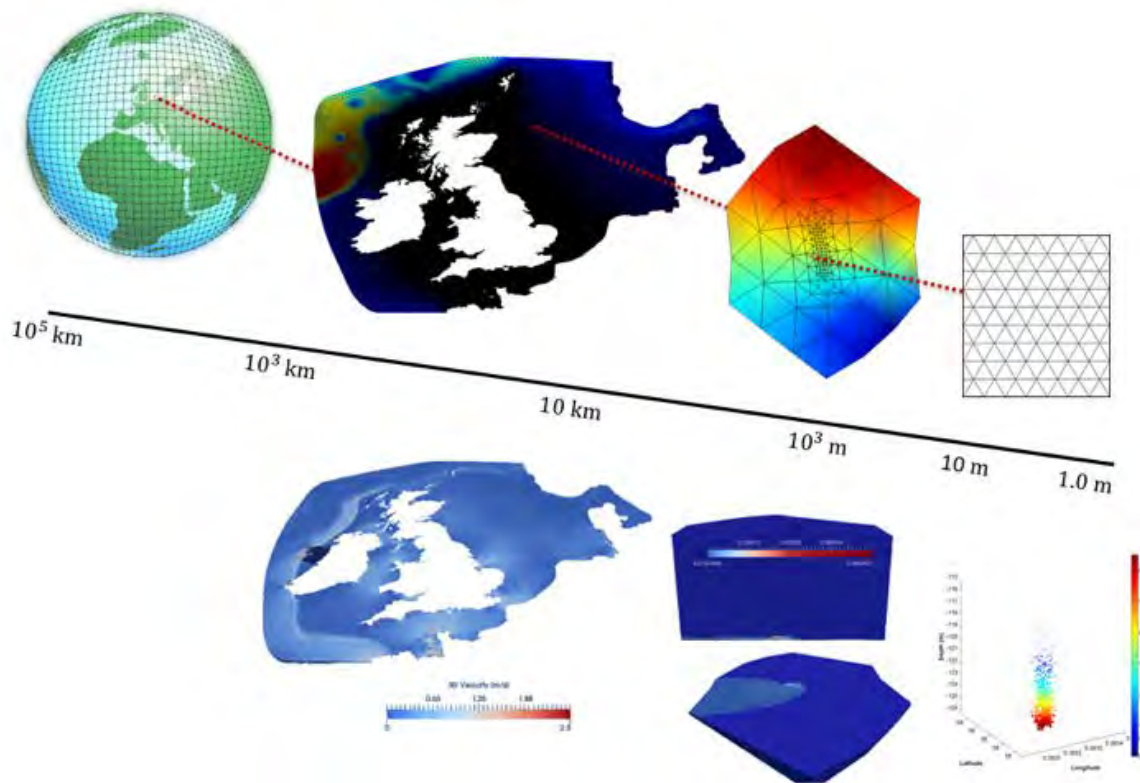

Figure 6. The multi-scale, multiphase numerical model, with forcing down from global scale data (the top left); into the shelf-seas / coastal scale (top middle shows the mesh, bottom left shows sample currents); with a nested ghost model reducing the scale to the meter scales (top left showing the mesh, bottom middle shows the flow of dissolved CO_2 solution); including an example CO_2 leakage plume module (bottom left, providing the dissolved solution distribution and dynamics of the bubble plume in the model).

In terms of further model development, a number of initiatives are underway. One such (Fig 6) is aiming to combine an ability to accurately represent currents and ocean scale mixing phenomena with an ability to model the ultra-fine scale of bubble dynamics and multiphase chemistry. Other initiatives are developing an ability to simulate high-resolution leakage scenarios with concurrent simulation of natural biogeochemical processes. Whilst such models are not necessarily optimal for operational use currently, due to computational costs, they do allow for testing and hypothesis development and the production of sufficiently accurate simpler models.

Models can therefore address all aspects of the detection, confirmation/localisation and quantification processes required as part of a comprehensive monitoring system. However, models cannot completely supplant in-situ measurements, observed data will be essential for model validation and quality assessments. A symbiosis between seagoing research and theoretical modellers will be a win-win situation, providing data for model assessments and development generating further process understanding and iteratively optimising measurement programs. We argue that it is critical to ensure that observational programmes, models and their data products that are already delivered by national science programmes for a variety of uses are optimised for CCS applications, where necessary. Open source software tools that enable bespoke analysis of variability, leak morphology, monitoring strategies and impact assessment on a site-by-site basis can then be developed, providing the base data requirements are met.

Acknowledgements

References

[1] Ciavatta, S., Kay, S., Saux-Picart, S., Butenschon, M., Allen, J.I., 2016. Decadal reanalysis of biogeochemical indicator and fluxes in the North West European shelf-sea ecosystem. *Journal of Geophysical Research – Oceans* 121, 1824–1845. doi:10.1002/2015JC011496

[2] Holt, J., Schrum, C., Cannaby, H., Daewel, U., Allen, J.I., Artioli, Y., Bopp, L., Butenschon, M., Fach, B.A., Harle, J., Pushpadas, D., Salihoglu, B., Wakelin, S., 2016. Potential impacts of climate change on the primary production of regional seas: A comparative analysis of five European seas. *Progress in Oceanography* 140, 91–115. doi:10.1016/j.pocean.2015.11.004

[3] Allen, J.I., Somerfield, P.J., 2009. A multivariate approach to model skill assessment. *Journal of Marine Systems* 76, 83–94. doi:10.1016/j.jmarsys.2008.05.009

[4] STEMM-CSS; Strategies for Environmental Monitoring of Marine Carbon Capture and Storage, an EU Horizon 2020 funded project. http://stemm-ccs.eu

[5] BayMoDe, Bayesian Monitoring Design, A Research Council of Norway (CLIMIT program) funded project: https://www.forskningsradet.no/prosjektbanken/#/project/NFR/254711/Sprak=en

[6] ECO2, Sub-seabed CO2 Storage: Impact on Marine Ecosystems. http://www.eco2-project.eu/

[7] Haeckel M., Blackford J., 2015. CCT2 Synthesis report on predicted impacts and uncertainties, ECO2 Deliverable D12.3, 42 p. DOI: 10.3289/ECO2_D12.3

[8] Alendal, G., Omar, A., Denny, A. R., Baumberger, T., Beaubien, S. E., Vielstädte, L., Dewar, M., Chen, B., Pedersen, R. B., De Vittor, C. and Johannessen, T. (2013) Technical synthesis report on droplet/bubble dynamics, plume dynamics and modelling parameters, use of hydro-acoustics to quantify droplet/bubble fluxes, and carbonate system variable assessment. ECO2 Deliverable, D3.1, 51 pp. DOI 10.3289/ECO2_D3.1.

[9] Dewar, M., Chen, B., Evgeniy, Y., Avlesen, H., Alendal, G., Ali, A. and Vielstädte, L., 2013. Technical report on *verified and validated application of droplet/bubble plume-, geochemical- and general flow- models*. ECO2 Deliverable, D3.3, 81 pp. DOI 10.3289/ECO2_D3.3.

[10] McGinnis, D. F., M. Schmidt, T. DelSontro, S. Themann, L. Rovelli, A. Reitz, and P. Linke, 2011. Discovery of a natural CO2 seep in the German North Sea: Implications for shallow dissolved gas and seep detection, *J. Geophys. Res.*, 116, C03013, doi: 10.1029/2010JC006557.

[11] Roberts, J.J., Stalker, L., 2017. What have we learned about CO2 leakage from field injection tests? *Energy Procedia* 114, 5711–5731. doi:10.1016/j.egypro.2017.03.1710

[12] Blackford, J.C., Stahl, H., Bull, J.M., Bergès, B.J.P., Cevatoglu, M., Lichtschlag, A., Connelly, D.P., James, R.H., Kita, J., Long, D., Naylor, M., Shitashima, K., Smith, D., Taylor, P., Wright, I., Akhurst, M., Chen, B., Gernon, T.M., Hauton, C., Hayashi, M., Kaieda, H., Leighton, T.G., Sato, T., Sayer, M.D.J., Suzumura, M., Tait, K., Vardy, M.E., White, P.R., Widdicombe, S., 2014. Detection and impacts

of leakage from sub-seafloor deep geological carbon dioxide storage. *Nature Climate Change* 4, 1011–1016. doi:10.1038/NCLIMATE2381

[13] Blackford, J.C., Jones, N., Proctor, R., Holt, J.T., 2008. Regional scale impacts of distinct CO₂ additions in the North Sea. *Marine Pollution Bulletin* 56, 1461–1468. doi:10.1016/j.marpolbul.2008.04.048

[14] Phelps, J.J.C., Blackford, J.C., Holt, J.T., Polton, J.A., 2015. Modelling Large-Scale CO₂ Leakages in the North Sea. *International Journal of Greenhouse Gas Control* 38, 210–220. doi:10.1016/j.ijggc.2014.10.013

[15] Blackford, JC; Torres, R; Artioli, Y; Cazenave, P. 2013. Modelling dispersion of CO₂ plumes in sea water as an aid to monitoring and understanding ecological impact. *Energy Procedia* 37, 3379–3386. doi:10.1016/j.egypro.2013.06.226

[16] Dewar, M., Saleem, U., Khajepor, S., Chen, B. Prediction of Greenhouse Gas Leakages from Potential North Sea Storage Sites into Coastal Waters by an Unstructured, Multi-Scale and Multi-Phase Flow Model, *this issue*.

[17] Dewar, M., Wei, W., McNeil, D., Chen, B., 2013. Small-scale modelling of the physiochemical impacts of CO₂ leaked from sub-seabed reservoirs or pipelines within the North Sea and surrounding waters. *Marine Pollution Bulletin* 73, 504–515. doi:10.1016/j.marpolbul.2013.03.005

[18] Saleem, U., Dewar, M., Chen, B. Numerical Modelling of CO₂ Flow through Sediments into Water Column, *this issue*.

[19] Elliot, A.J., Wallace, D.C., 1989. Dispersion of Surface Plumes in the Southern North Sea, Dt. Hydrogr. Z., 42, 16.

[20] Hofmann, G.E., Smith, J.E., Johnson, K.S., Send, U., Levin, L.A., Micheli ,F., Paytan, A., Price, N. N., Peterson, B., Takeshita, Y., Matson, P.G., Crook, E.D., Kroeker K.J., Gambi , M.C., Rivest, E.B., Frieder, C.A., Yu, P.C., Martz, T.R., 2011. High-Frequency Dynamics of Ocean pH: A Multi-Ecosystem Comparison. *PLoS ONE* 6(12), e28983. doi:10.1371/journal.pone.0028983

[21] Artioli, Y., Blackford, J.C., Butenschon, M., Holt, J.T., Wakelin, S.L., Thomas, H., Borges, A.V., Allen, J.I., 2012. The carbonate system of the NW European shelf: sensitivity and model validation. *Journal of Marine Systems* 102–104, 1–13. doi:10.1016/j.jmarsys.2012.04.006

[22] Blackford, J.C., Artioli, Y., Clark, J., de Mora, L., 2017. Monitoring of offshore geological carbon storage integrity: implications of natural variability in the marine system and the assessment of anomaly detection criteria. *International Journal of Greenhouse Gas Control* 64, 99–112. doi:10.1016/j.ijggc.2017.06.020

[23] Uchimoto, K., Nishimura, M., Kita, J., Xue, Z., 2018. Detecting CO₂ leakage at offshore storage sites using the covariance between the partial pressure of CO₂ and the saturation of dissolved oxygen in seawater. *International Journal of Greenhouse Gas Control* 72, 130–137. doi:10.1016/j.ijggc.2018.03.020

[24] Botnen, H., Omar, A.M., Throseth, I., Johannessen, T., Alendal, G., 2015. The impact of submarine CO₂ vents on seawater: implications for detection of subsea carbon sequestration leakage. *Limnology and Oceanography* 60, 402–410. doi:10.1002/lno.10037

[25] Omar, A.M., García-Ibáñez, M.I., Alendal, G. C$_{seep}$ as a stoichiometric tool to distinguish a seep signal from the natural variability, *this issue*.

[26] Lessin, G., Artioli, Y., Bruggeman, J., Blackford, J. Can we use departure from natural co-variance relationships for monitoring of offshore carbon storage integrity? *this issue*.

[27] Alendal, G., Blackford, J., Chen, B., Avlesen, H., & Omar, A., 2017. Using Bayes Theorem to Quantify and Reduce Uncertainties when Monitoring Varying Marine Environments for Indications of a Leak. *Energy Procedia*, *114*, 3607–3612. http://doi.org/10.1016/j.egypro.2017.03.1492

[28] Greenwood, J., Craig, P., Hardman-Mountford, N., 2015. Coastal monitoring strategy for geochemical detection of fugitive CO₂ seeps from the seabed. *International Journal of Greenhouse Gas Control* 39, 74–78. doi:10.1016/j.ijggc.2015.05.010

[29] Hvidevold, H.K., Alendal, G., Johannessen, T., Ali, A., Mannseth, T., Avlesen, H., 2015. Layout of CCS monitoring infrastructure with highest probability of detecting a footprint of a CO₂ leak in a varying marine environment. *International Journal of Greenhouse Gas Control* 37 274–279. doi:10.1016/j.ijggc.2015.03.013

[30] Ali, A., Frøysa, H.G., Avlesen, H., Alendal, G., 2016. Simulating spatial and temporal varying CO₂ signals from sources at the seafloor to help designing risk-based monitoring programs. *Journal of Geophysical Research-Oceans 121*(1), 745–757. doi:10.1002/2015JC011198

[31] Alendal, G. (2017). Cost efficient environmental survey paths for detecting continuous tracer discharges. *Journal of Geophysical Research-Oceans*, *122*(7), 5458–5467. http://doi.org/10.1002/2016JC012655

[32] Gundersen, K., Oleynik, A., Alendal, G., Skaug, H.J., Avlesen, H., Berntsen, J., Blackford, J., Blaser, N., Cazenave, P. Combining models and machine learning techniques to design leak detection monitoring, *this issue*.

[33] Oleynik, A., Gundersen, K., Alendal, G., Skaug, H.J., Avlesen, H., Berntsen, J., Blackford, J., Blaser, N., Cazenave, P. Simplified modelling as a tool to locate and quantify fluxes from a CO₂ seep to marine waters, *this issue*.

[34] Cazenave, P., Torres, R., Blackford, J., Artioli, Y. Regional modelling to inform the design of sub-sea CO₂ storage monitoring networks, *this issue*.

[35] Dixon, T., McCoy, S.T., Havercroft, I., 2015. Legal and Regulatory Developments on CCS. *International Journal of Greenhouse Gas Control* 40, 431–448. doi:10.1016/j.ijggc.2015.05.024

[36] Lessin, G., Artioli, Y., Queirós, A.M., Widdicombe, S., Blackford, J.C., 2016. Modelling impacts and recovery in benthic communities exposed to localised high CO₂. *Marine Pollution Bulletin* 109, 267–280. doi:10.1016/j.marpolbul.2016.05.071

14th International Conference on Greenhouse Gas Control Technologies, GHGT-14

21st -25th October 2018, Melbourne, Australia

Constraining the physical properties of chimney/pipe structures within sedimentary basins

Jonathan M. Bull[1]*, Christian Berndt[2], Timothy A. Minshull[1], Timothy J. Henstock[1], Gaye Bayrakci[1], Romina Gehrmann[1], Giuseppe Provenzano[1], Christoph Böttner [2], Bettina Schramm[2], Ben Callow[1], Mark Chapman[3], Hamza Birinci[1], Naima Yilo[1], Marius Dewar[4], Baixin Chen[4], Umar Saleem[4], Hector Marin-Moreno[5], Anna Lichtschlag[5] Ismael Falcon-Suarez[5], Ben Roche[1], Rachael James[1], Douglas P. Connelly[5], Juerg Matter[1], Judith Elger[2], Jens Karstens[2], Angus I. Best[5]

[1]*Ocean and Earth Science, University of Southampton, National Oceanography Centre Southampton, SO14 3ZH, U.K*
[2]*GEOMAR, Wischhofstr. 1-324148 Kiel, Germany*
[3]*School of Geosciences, University of Edinburgh, EH9 3JW, U.K.*
[4]*School of Engineering and Physical Sciences, Heriot-Watt University, Edinburgh, EH14 4AS, U.K.*
[5]*National Oceanography Centre Southampton, Southampton SO14 3ZH, U.K.*

Abstract

Evaluation of seismic reflection data has revealed structures cross-cutting the overburden within many sedimentary basins worldwide, including those in the North Sea and Norwegian Sea. These seismically-imaged pipes and chimneys are considered to be possible pathways for fluid flow. Natural fluids from deeper strata have migrated through these structures at some point in geological time. We test the hypothesis that many chimney and pipe structures imaged on seismic reflection profiles worldwide are the consequence of (1) a fracture network that has been reactivated by pore fluid pressure which facilitates the migration of fluids upwards; and (2) shallow sub-seafloor lateral migration of fluids along stratigraphic interfaces and near-surface fractures. An experimental approach to determine the physical properties of these structures beneath the sub-seafloor is described, with particular reference to an investigation of the Scanner Pockmark complex in the North Sea. The study is relevant to storage operators, policy-makers and those keen to demonstrate that it is possible to constrain and fully understand the physical properties and possible fluid flow pathways in the sedimentary overburden above sub-seafloor CO_2 storage reservoirs
Keywords: seismic chimney; pipe; fluid flow; fracture network

1. Introduction

Numerous geological structures within sedimentary basins can breach sealing sequences and facilitate the movement of fluids sub-vertically [1,2,3]. Seismic reflection data within sedimentary basins have been used to image the subsurface, allowing interpretation of potential migration pathways, and also to identify vertical fluid conduits, gas accumulations, and sediment mobilization (pockmarks etc.). There is agreement that there is ubiquitous evidence for focused fluid flow through low permeability sedimentary units.

Seismic chimneys and pipes (vertical seismic anomalies) are common in basins and they are interpreted as focused fluid flow structures which hydraulically connect deeper stratigraphic layers with the sediment overburden

*Corresponding author. Tel.: +44 (0) 2380593078.

E-mail address: bull@soton.ac.uk

(4,3]. The activity of vertical fluid conduits can be limited to blowout-like events, e.g. resulting in pipe structures offshore Norway [5], or fluid flow may be continuous and long-lasting, e.g. the chimney structures above the leaking hydrocarbon reservoir Tommeliten [6]. Understanding of these shallow fluid flow systems is critical for assessing the integrity of sub-seafloor CCS sites.

One of the most comprehensive analysis of a fluid migration features in the North Sea [3] analysed large 3D seismic reflection volumes within the South Viking Graben and found 46 large-scale chimney structures within the shallowest 1000 m of the overburden, most of which terminate at or close to the seabed. The most prominent features imaged had large-scale (500 – 800 m long, 100 to 1000 m wide) seismic anomalies, whose pipe or chimney-like seismic signatures were similar to those interpreted world-wide as being due to vertical fluid flow. Vertical seismic anomalies interpreted as being due to fluid flow are found throughout the North Sea [e.g. 7,3,2,6], and globally [e.g. 1,8].

Karstens and Berndt [3] describe three types of North Sea chimney structures. Type C anomalies are elongate and meandering in plan view, and are possibly seismic artefacts or related to underlying tunnel valleys, and are considered less important in vertical migration of fluids and seal bypass, and we do not consider further. Type A "columnar" anomalies, or pipe structures and type B more "chaotic" anomalies are interpreted as the seismic image of fluid conduits that have by-passed the sealing formation (Nordland Shales), with the presence of bright spots clearly indicating the presence of gas within the structures. Most authors attribute the formation of chimneys or pipes as being due to hydro fracturing of an impermeable cap rock [1,2,3] with breaching of the cap rock caused by either capillary or fracture failure. Localization of fluid flow is a common feature of fracture networks [9]. Both these mechanisms for cap rock breaching require high pore over pressure.

Field core from the North Sea overburden has revealed the Cenozoic section to be pervasively faulted and fractured, with extensive regions of well-connected polygonal faulting occurring immediately below the Utsira Formation [10]. The Utsira sand is a major reservoir (used at Sleipner), with high porosity (>30%) and permeability (>1000 mD or 10-12 m2). The overlying Nordland Shales provide a series of seals to this reservoir and has <<1mD matrix permeability and >2 MPa capillary pressure. The dynamics of the CO_2 plume in the Sleipner well suggest high horizontal permeabilities of >2000mD and, more significantly, high vertical permeability (~400 mD) or capillary pressures of >2000 kPa and 50 kPa, respectively. Vertical permeability in the Nordland suggests either lateral discontinuity of the shales (unlikely as some are several metres thick) or the presence of fractures (most likely). At Sleipner, there are no gas chimneys and the fracturing is attributed to microfracturing, possibly in response to the sudden removal of grounded ice [11].

2. Scanner Pockmark

This paper describes results from two geophysical cruises to the Scanner pockmark complexes in the North Sea. The Scanner pockmark complex is located in UK License Block 15/25 (Figure 1), around 190 km east of Scotland within the Witch Ground Basin close to a number of oil and gas condensate fields. The closest field to Scanner is the decommissioned Blenheim Oil Field, which is a heavily faulted Palaeocene sandstone play on the flank of the Fladen Ground Spur (Figure 1). Within the Blenheim field, structure maps of the Late Palaeocene Top Mey Sandstone [12] show a dominant NW-SE normal fault set.
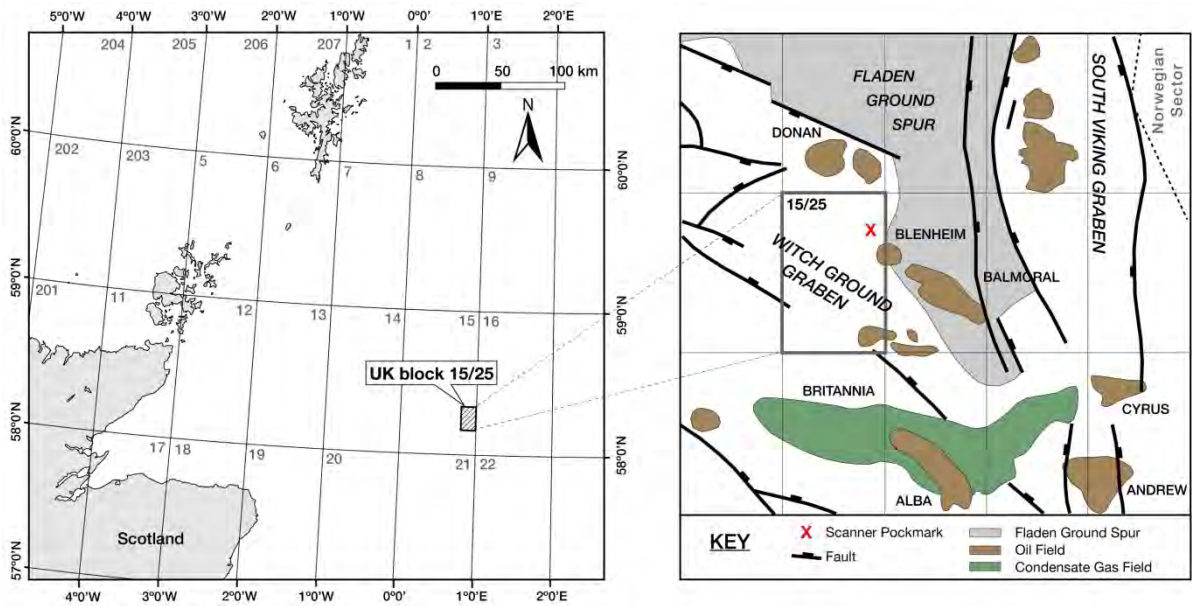
Fig. 1. Position of the Scanner Pockmark within the North Sea. The Scanner pockmark complex is within the Witch Ground Graben.

The Witch Ground Basin was the locus of rapid fine-grained sediment deposition between 15 and 13 ka after the end of the last glacial period. The soft muds of this formation are affected by large numbers of pockmarks [13]. Following the stabilisation of sea level after the last glaciation, the Witch Ground has been little affected by erosion or sedimentation, and hence pockmarks at the current seabed show the effects of gas escape over at least the last 6000 years. Although most pockmarks are small, less than 2 – 3 m, several studies have identified the presence of large pockmarks within Block 15/25 with very active methane venting [14,15].

The Scanner pockmarks are known to be the locations of vigorous and persistent methane venting, are associated with bright spots at shallow depth, and have chimney structures imaged on seismic reflection data to depths of several hundred metres. The Scanner pockmark is a composite feature involving two overlapping seabed pockmarks, each a few hundred metres in diameter, lying in c. 155 m water depth. Within the pockmarks samples of methane-derived authigenic carbonate (MDAC) have been recovered [16]. These MDAC deposits are formed by the anaerobic oxidation of escaping methane, cementing sediment grains just beneath the sea-bed, which with the process of continued gas movement across the seabed, become a hard ground.

In this paper we describe an experimental methodology to determine the physical properties and geometry of a representative chimney structure within the North Sea (Scanner Pockmark, Figure 1). The main aim of this study is to understand the physical properties of seismic chimney structures, develop appropriate methodologies which are widely applicable in the North Sea and elsewhere, and to model gas flux for realistic scenarios. The structure of the chimney may contribute to the understanding of causes of breaching, but this is not a primary aim of this paper.

3. Evidence for small scale seismic chimney formation - QICS

Although on a much smaller scale, some analogies can be made with the chimney structures induced during the QICS experiment. A shallow controlled sub-seabed CO_2 release to replicate small-scale, but realistic, leakage that has migrated into the near-seabed environment was completed on the west coast of Scotland [17]. A borehole was drilled from shore, to a depth of 11 m beneath the sea floor, in 12 m of water and 350 m offshore. A total of 4.2 tonnes of CO_2 was injected into the overlying sediments, over a 37-day period, during which flow was increased from 10 to 210 kg d^{-1}. Repeated seismic reflection imaging [18] demonstrated the formation of chimneys as gas

migrated upwards by fracture propagation and reactivation of pre-existing fractures, and subsequent spreading of gas along the shallow stratigraphy.

4. Models of Seismic Chimneys

Our hypothesis (Figure 2), based on previous literature, and the QICS experiment, is that seal breaching occurs due to reduced effective stress and leads to either reactivation of pre-existing fractures, or opening of new fractures and the generation of a localized connected fracture system. Gas-rich pore fluids then exploit these locations, with buoyancy causing vertical migration through the linked fracture system. It is this combination of localized vertical migration and lateral flow that is imaged from 4-D seismic (as in the plumes at Sleipner) as chimney structures. Thus the chimneys resolvable from seismic reflection data provide a first order prediction of potential areas of leakage, but the overlying sediment beds may disperse such vertical flow, making direct detection at the surface more difficult.
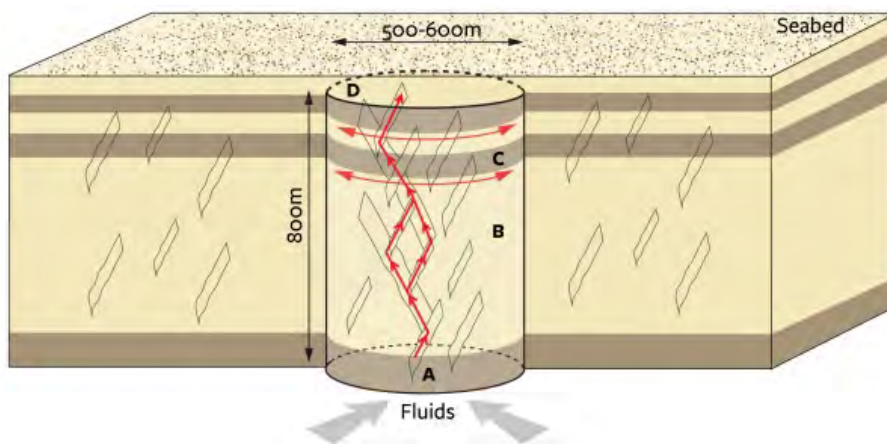

Fig. 2. Conceptual model for a seismic chimney structure which extends close to the seabed. The diagram shows that the overburden sediments are pervasively faulted. Where seal rupture occurs (A) pore fluids drive fracture propagation and linkage (B) allowing fluids to rise due to buoyancy and elevated fluid pressure. In the near surface fluids will migrate along impermeable stratigraphic interfaces (C). In rare situations fractures may propagate to the very near-surface (D) or even rupture the seabed.

5. Experimental Approach

Our experimental design uses multiple seismic sources with different frequency bandwidths to collect seismic reflection data on surface streamers and wide-angle data recorded on ocean bottom seismometers to characterize the fracture system within and around the Scanner pockmark gas chimney in the North Sea. We collected an innovative broadband multicomponent seismic dataset, and are performing a state-of-the-art anisotropy analysis to characterize the fracture system. The wide frequency-band (10 Hz – 6 kHz) in our data set will allow us to apply techniques based on the frequency-dependence of seismic anisotropy, allowing a more detailed picture of the fracture system to be developed than through conventional methods.

Our hypothesis on the formation of gas chimneys suggests that there should be a different fracture geometry outside the chimney compared to inside, with the chimney being associated with connected fracture sets, with possible concentric fracture distributions. To test this hypothesis requires state-of-the-art seismic techniques.

It is well established that the most accurate and reliable seismic fracture detection requires multicomponent data [19]. The measurement of seismic anisotropy, particularly using shear-wave splitting, has been established as a key technique to infer orientation and density of fracture networks [20]. Techniques such as estimation of the coherency

of stacked seismic images [21] are able to image larger fractures, but it is only through consideration of anisotropy that we can obtain information on the key features which are at sub-seismic resolution.

Theoretical work [22,23,24] predicts that properties such as fracture scale length and fluid saturation can be inferred from the frequency-dependence of anisotropic attributes. Recent work in Southampton and Edinburgh has established key relationships between fracture parameters, rock properties, fluid saturation and seismic anisotropy. The theoretically predicted relationship between shear-wave splitting and fracture density has been verified [25] through laboratory measurements on synthetic rock with controlled fracture geometry, and with fluid viscosity effects [26]. More recently, the impact of partial saturation on anisotropy and attenuation in fractured materials has been studied [27,28,29]. This latter work develops models that can link laboratory and field datasets

The excess permeability associated with a fracture system is likely to be strongly dependent on the degree of connectivity. This in turn is typically related to the range of fracture orientations, since fracture sets in multiple orientations may have more connections than a single aligned set. The greatest anisotropy is often associated with perfectly aligned fractures, and the most permeable zones show the least anisotropy in reservoir formations. Our hypothesis has unconnected vertical fractures outside the chimney that are preferentially aligned with the regional stress field, with connected and possibly concentric fracture systems within the chimney. If this is so, we would expect to see significant differences in anisotropy outside and inside the chimney. Such differences would include not only the strength of the anisotropy but also the symmetry system, with aligned fractures giving rise to azimuthal anisotropy, described by transverse isotropy with a horizontal symmetry axis, and concentric fractures showing little azimuthal anisotropy, with the response being described by transverse isotropy with a vertical symmetry axis. Our analysis will test our hypothesis by differentiating between these symmetry systems.

Our surveys used ocean bottom seismometers (OBS) to measure the converted waves which are known to be essential for characterizing fracture systems. A key component of our approach is to use three seismic sources with different frequencies, in the range 10 Hz to 6 kHz (low frequency airguns, GI guns, sparker systems). This approach will provide a unique opportunity to study the frequency-dependence of anisotropy over a much wider frequency range than has been used in previous studies. To our knowledge, this will be the first survey of its kind, and successful completion would likely lead to significant impact in the wider geophysical industry.

Our experimental design builds on that developed for a chimney structure in deeper water [30]. We deployed a grid of OBSs, centred on the chimney structure, with spacings increasing radially from c. 200 m to c. 400 m, with two OBS positioned 20 m apart in the main pockmark. In addition a smaller asymmetrical grid of OBS was positioned away from the pockmark to determine the background anisotropy (Fig. 3). These instruments recorded every shot from our range of seismic sources, using a hydrophone and three orthogonal geophones and a sample interval of 0.25 ms. We fired our seismic sources separately repeating grids of lines, with line spacing as close as 25 m.

6. Geophysical Experiment at Scanner Pockmark

RRS James Cook 152 (funded by NERC, CHIMNEY) successfully completed two anisotropy experiments over the Scanner and Challenger pock marks by shooting various seismic sources into a grid of 25 and 7 ocean bottom seismometers respectively (Figure 3). Five different seismic sources (Bolt airguns, GI guns, Squid surface sparker, Duraspark surface sparker, and Deep Tow Sparker) were recorded by the ocean bottom seismometers (Figures 4), and an acoustic recorder deployed c. 25 m above the seabed. Multichannel seismic reflection profiles were collected with GI guns (Figure 5) and both surface sparker sources, and single channel seismic reflection profiles were collected with the Deep Tow Sparker source. In addition data collected by Maria S. Merian (funded by STEMM-CCS) collected seismic reflection data using GI guns, and these sources were recorded on 18 Ocean bottom seismometers (OBS) around the Scanner pockmark. The results from the two cruises will be integrated together to test the chimney model hypothesis.
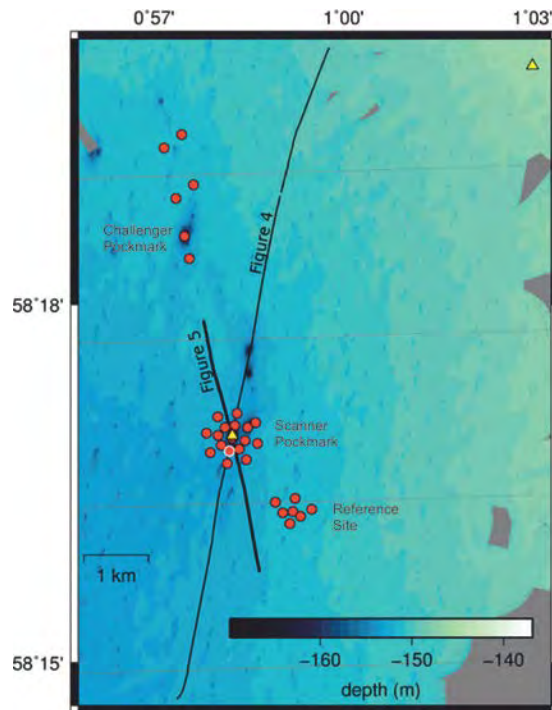
Fig. 3. Location of all instruments deployed during JC152 superimposed on the seabed bathymetry. The red circles show the position of the 25 ocean bottom seismometers (OBS) deployed at the Scanner pock mark and a reference site during the first part of the cruise, and the position of a further 7 OBS deployed around and north of the Challenger pock mark. The yellow triangles show the position of acoustic recorder deployments to record source signatures. The position of the OBS record illustrated in Figure 4 and seismic reflection profile shown in Figure 5 are shown.
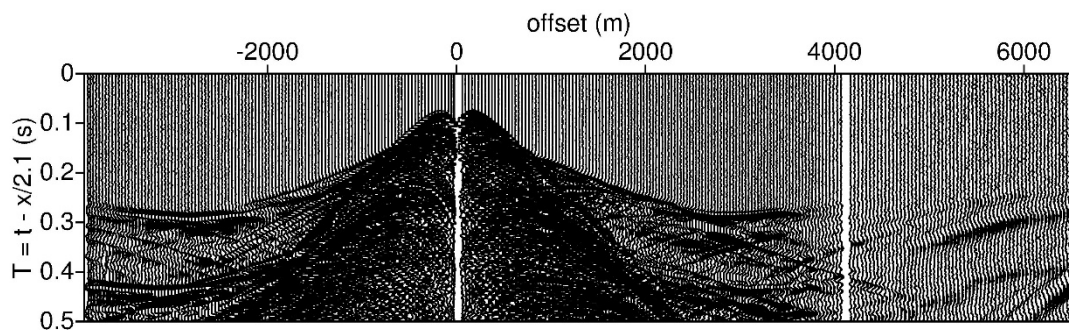

Fig. 4. Example Ocean Bottom Seismometer data collected close to Scanner Pockmark (position shown in Figure 3). This example is an in-line GI-gun profile from OBS8 of the Chimney OBS Network. A velocity reduction of 2.1 km/s has been applied.
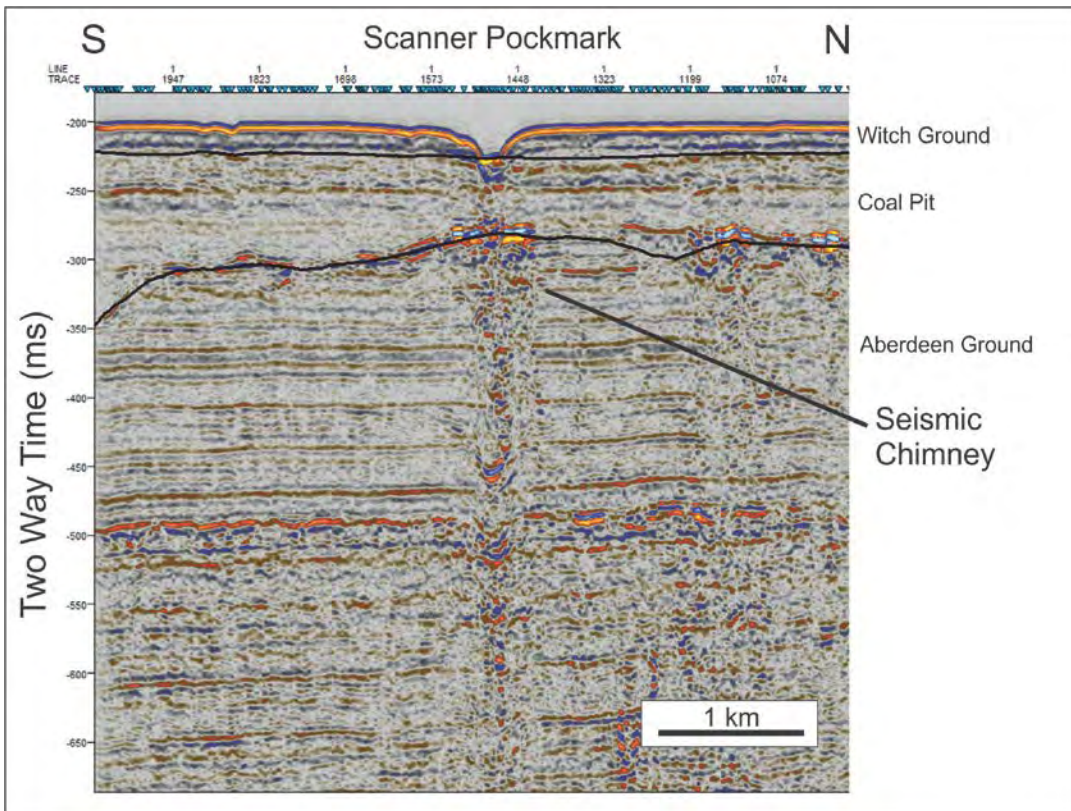
Fig. 5. Pre-stack depth migrated seismic reflection profile collected with a GI-gun source across the Scanner Pockmark during JC152 (position of profile shown in Figure 3). Note the position of the bright amplitude anomalies beneath the pockmark and a seismic chimney structure. The presence of gas in the sub-surface, and the chimney structure will be further tested by tomographic and anisotropic analyses.

7. Analysis and conclusions

Preliminary analysis of 2D seismic reflection profiles shows the overall shape of the sedimentary succession in the Scanner pockmark region. Between the seafloor and the well-stratified sediments of the Nordland formation (200-350 ms TWT) clear indications for several stages of deposition and erosion are visible. A characteristic tunnel valley with steep flanks and several phases of deposition and erosion is located SW of the Scanner pockmark. This new high resolution seismic reflection data acquired with the various seismic sources is of high quality, and indicates the presence of gas at several different levels and complex areas of gas blanking. The new data reveal a complex fluid migration system in the sub-surface which comprises fluids that rise from > 500 m depth as well as gas produced within the shallowest post-glacial sediments resulting in a variety of fluid pathways and seep sites at the seabed. Seismic anisotropy analysis using the broad band data collected by the ocean bottom seismometer data is on-going.

Acknowledgements

References

[1] Cartwright J, Huuse M, Aplin A, 2007. Seal bypass systems. Am. Assoc. Pet. Geol. Bull. 91, 1141–1166

[2] Løseth H, Gading M, Wensaas L., 2009. Hydrocarbon leakage interpreted on seismic data. Mar. Pet .Geol. 26, 1304–1319.

[3] Karstens J, and Berndt C, 2015. Seismic chimneys in the Southern Viking Graben – Implications for palaeo fluid migration and overpressure evolution. Earth Planet. Sci. Lett. 412, 88-100.

[4] Berndt C 2005. Focused fluid flow in passive continental margins. Phil. Trans. R. Soc. A, Math. Phys. Eng. Sci. 363, 2855-2871.

[5] Bünz S, Mienert J, Berndt C, 2003. Geological controls on the Storegga gas-hydrate system of the mid-Norwegian continental margin Earth Planet. Sci. Lett. 209, 291-307.

[6] Arntsen B, Wensaas L, Loseth H, Hermanrud C, 2007. Seismic imaging of gas chimneys. Geophysics 72, 251-259.

[7] Cathles, L.M., et al., 2010. The physics of gas chimney and pockmark formation, with implications for assessment of seafloor hazards and gas sequestration. Mar. and Petrol. Geol. 27, 82-91.

[8] Foschi M, Cartwright JA, Peel FJ, 2014. Vertical anomaly clusters: Evidence for vertical gas migration across multilayered sealing sequences. AAPG Bull. 98, 1859–1884.

[9] Zhang X and Sanderson DJ, 2002. Numerical Modelling and Analysis of Fluid Flow and Deformation of Fractured Rock Masses, Pergamon, 288pp.

[10] Cartwright JA and Lonergan L, 1996. Volumetric contraction during the compaction of mudrocks: A mechanism for the development of regional-scale polygonal fault systems. Basin Res. 8, 183–193.

[11] Cavanagh, AJ & Haszeldine, RS, 2014. The Sleipner storage site: Capillary flow modeling of a layered CO_2 plume requires fractured shale barriers within the Utsira Formation. Intl. J. Greenh. Gas Cont. 21, 101-112.

[12] Dickinson B, Waterhouse M, Goodall J, and Holmes N, 2001. Blenheim Field: the appraisal of a small oil field with a horizontal well. Petrol. Geoscience. 7: 81-95.

[13] Gafeira J and Long D, 2015. Geological investigation of pockmarks in the Scanner Pockmark SCI area. JNCC Report No 570. JNCC Peterborough

[14] Hovland M and Sommerville, 1985. Characteristics of two natural gas seepages in the North Sea. Mar. Petrol. Geol. 2, 319-326.

[15] Judd AG, Long D, and Sankey M, 1994. Pockmark formation and activity, UK block 15/25, North Sea. Bull. Geol. Surv. Denmark 41, 34-49.

[16] Judd AG, and Hovland M, 2009. Seabed Fluid Flow: the impact on geology, biology and the marine environment. Cambridge University Press.

[17] Blackford J, Stahl H, Bull JM et al., 2014. Detection and impacts of leakage from sub-seafloor deep geological Carbon Dioxide Storage. Nature Climate Change 4, 1011-1016.

[18] Cevatoglu M, Bull JM, Vardy ME, Gernon TM, Wright IC, Long D, 2015. Gas migration pathways, controlling mechanisms and changes in sediment acoustic properties observed in a controlled sub-seabed CO_2 release experiment. Intl. J. Greenh. Gas Cont. 38, 26-43.

[19] Li X-Y, 1997. Fractured reservoir delineation using multicomponent seismic data. Geophys. Prospect. 45, 39-64.

[20] Liu E and Martinez A 2012. Seismic Fracture Characterization. EAGE Education Tour Series, Vol. 8.

[21] Bahorich M and Farmer S, 1995. 3D Seismic Discontinuity for Faults and Stratigraphic Features: The Coherence Cube. The Leading Edge 14, 1053-1058.

[22] Chapman M, 2003. Frequency-dependent anisotropy due to meso-scale fractures in the presence of equant porosity. Geophys. Prospect., 51, 369-379.

[23] Chapman M, 2009. Modeling the effect of multiple sets of mesoscale fractures in porous rock on frequency-dependent anisotropy. Geophysics 74, D97-D103.

[24] Jakobsen M and Chapman M, 2009. Unified theory of global flow and squirt flow in cracked porous media. Geophysics 74, WA65-WA76.

[25] Tillotson P, Sothcott J, Best AI, Chapman M and Li X-Y, 2012. Experimental verification of the fracture density and shear-wave splitting relationship using synthetic silica cemented sandstones with a controlled fracture geometry, Geophys, Prospect., 60, 516-525

[26] Tillotson P, Chapman M, Sothcott J, Best AI, Li X-Y, 2014. Pore fluid viscosity effects on P and S wave anisotropy in synthetic silica cemented sandstone with aligned fractures. Geophys. Prospect. 62, 1238-1252.

[27] Amalokwu K., Best AI, Southcott J, Chapman M., Minshull TA, Li X-Y, 2014. Water saturation effects on elastic wave attenuation in porous rocks with aligned fractures Geophys. J. Int. 197, 943-947.

[28] Amalokwu K., Best AI, Southcott J, Chapman M., Minshull TA, Li X-Y, 2015a. Water saturation effects on P-wave anisotropy in synthetic sandstone with aligned fractures. Geophys. J. Int. 202, 1088-1095.

[29] Amalokwu K, Chapman M., Best AI, Southcott J, Minshull TA, Li X-Y, 2015b. Experimental observation of water saturation effects on shear wave splitting in synthetic rock with fractures aligned at oblique angles. Geophys.J. Int. 200, 17-24.

[30] Plaza-Faverola A, Westbrook, GK, Ker, S, Exley, RJK, Gailler A, Minshull, TA, Burto K., 2010. Evidence from three‑dimensional seismic tomography for a substantial accumulation of gas hydrate in a fluid‑escape chimney in the Nyegga pockmark field, offshore Norway. J. Geophys. Res. 115, B08104

Regional modelling to inform the design of sub-sea CO_2 storage monitoring networks

Pierre Cazenave[a]*, Ricardo Torres[a], Jerry Blackford[a], Yuri Artioli[a], Jorn Bruggeman[a]

aPlymouth Marine Laboratory, Plymouth, PL1 3DH, UK

Abstract

A 3D hydrodynamic model (FVCOM) coupled to a carbonate system (ERSEM) has been used to model a number of seabed CO_2 release scenarios ranging from 3 to 3000 t d^{-1} for the Goldeneye complex in the northern North Sea. The results of the scenario runs were used to characterise the fate of CO_2 in the water column in space and time. A new approach to designing monitoring networks has been implemented and compared with a simple approach. A weighted greedy set algorithm is used to identify the positions within the model domain which yield the greatest combined coverage for the smallest number of sampling stations, further limited by selecting only a feasible number of sample sites. The weighted greedy set algorithm incorporates the effect of the unstructured grid in FVCOM as well as the proximity of the candidate sample locations to the Goldeneye complex. For the range of release rates simulated, the design of the optimal sampling strategy changes depending on the magnitude of the release. The role of the tides discriminates the four release scenarios into two categories: for the lower release rates (3 and 30 t d^{-1}), the effect of the tide is relatively unimportant in the distribution; for the larger release rates (300 and 3000 t d^{-1}), the direction of the principal tidal axis controls the distribution of the sampling stations more strongly. Comparison of the weighted greedy set approach shows it is able to identify releases sooner and with a stronger signal than a simple regular sampling approach.

Keywords: carbon capture and storage; FVCOM; offshore geological storage; monitoring; marine; climate change

1. Introduction

Carbon Capture and Storage (CCS) involves preventing CO_2 emissions to the atmosphere, most commonly by capturing it at fossil fuel energy generation sites or other industrial sources, and compressing and sequestering the CO_2 in depleted oil and gas reservoirs and saline aquifers. The Intergovernmental Panel on Climate Change (IPCC) reports indicate that CCS is an important strategy in reducing mitigation measure costs around fossil fuel usage [1] if atmospheric CO_2 emissions are to be reduced by 80-95% before 2050 as required to keep rising average global temperatures below 2°C.

* Corresponding author. Tel: +44(0)1752633448; fax: +44 (0)1752633101
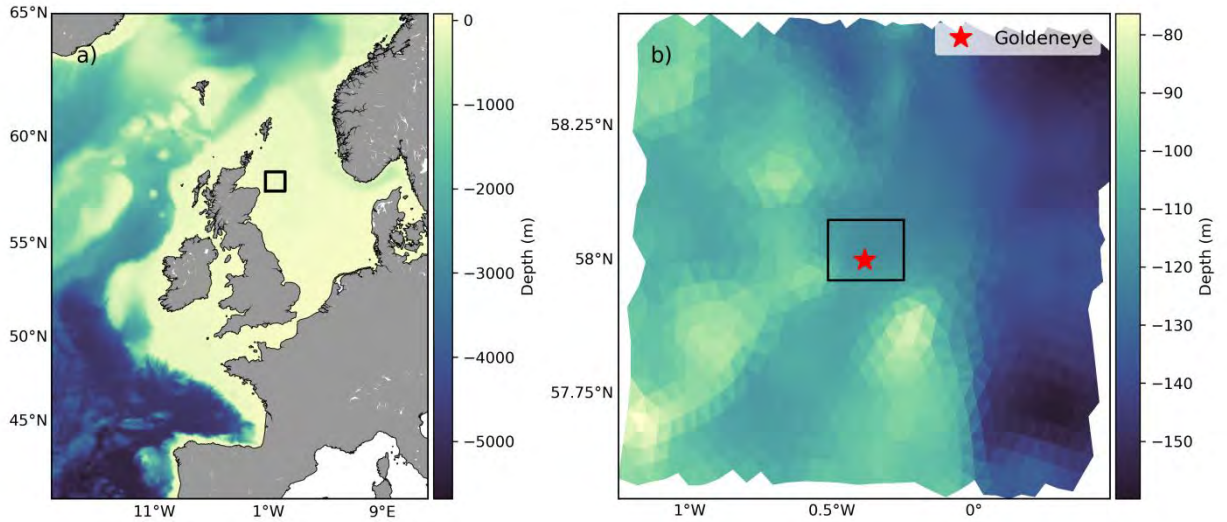 *E-mail address:* pica@pml.ac.uk

Figure 1 a) FVCOM domain used in which resolution varies from 15 km at the open boundaries to 0.5 km at the release site. The black box indicates the extents of the grid shown in (b). b) The nested domain with resolution from 0.5 km at the boundary to 3 m at the release site (red star). The black box in (b) indicates the extent of the Goldeneye complex

Many potential storage sites are situated offshore, generally in shelf sea settings. Whilst seismic techniques will be used to monitor reservoir conformance, marine based monitoring will be required to provide additional assurance that storage is robust and environmental impacts low. The use of numerical marine system models provides a mechanism by which impacts can be assessed and monitoring strategies designed whilst minimising cost [2]–[6]. [3] and [2] have investigated approaches to monitoring CO_2 based on the optimal deployment of limited available instrumentation, considering the sensitivity of those instruments to changes in a number of parameters (particle density, CO_2 concentration). Here we extend this approach using a method more commonly used for identifying optimal sampling strategies for large ocean basins [7].

2. Hydrodynamic Modelling

The Finite Volume Community Ocean Model (FVCOM) [8] has been coupled with the biogeochemical European Regional Seas Ecosystem Model (ERSEM) [9] through the Framework for Aquatic Biogeochemical Models (FABM) coupler [10] to provide a fully coupled 3D time evolving simulation capability that includes hydrodynamic, carbonate chemistry and biologically driven biogeochemical processes [11]. A fully-forced hydrodynamic model provides the setting for modelling sub-sea CO_2 reservoir release scenarios. Atmospheric forcing is supplied from a custom Weather Research and Forecasting (WRF) [12], [13] model. This model system can therefore simulate the chemical signature of a range of hypothetical leakage scenarios within the context of natural variability of the system. This combination is crucial as the key challenge is to distinguish anomalous signals from what can be considerable natural variability.

The large shelf model domain in Figure 1a is driven at its boundary by a predicted sea surface elevation time series derived from 11 tidal constituents (M_2, S_2, N_2, K_2, K_1, O_1, P_1, Q_1, M_4, MS_4, MN_4) from the TPXO data set [14]–[16]. In order to accurately model the carbonate system in ERSEM, depth-resolved temperature, salinity and non-tidal velocity inputs are sourced from the $1/15 \times 1/10°$ north-west European continental shelf operational Forecast Ocean Assimilation Model (FOAM) and interpolated onto the FVCOM open boundary nodes. A nested Weather Research and Forecasting (WRF) model [12], [13] of the model domain supplies surface wind, heating and

precipitation. Sea surface temperature is nudged to remotely sensed SST in FVCOM from the Group for High Resolution Sea Surface Temperature (GHRSST) Level 4 G1SST Global Foundation Sea Surface Temperature Analysis daily data [17]. Although the unstructured grid of FVCOM allows for increases in resolution in areas of interest, FVCOM also incorporates a nesting module with which smaller FVCOM models can be run using the outputs of a larger domain. The target region for the modelling described here is the Goldeneye complex in the northern North Sea (Figure 1b) which is implemented as a nested grid forced by boundary conditions from the larger grid (Figure 1a). The nested grid resolution varies from 0.5km at its boundaries to 3m at the release location.

The CO_2 release is modelled in FVCOM-FABM-ERSEM as a flux from the seabed into the bottom element where it is subject to the advection and diffusion calculated by FVCOM. The bottom element at which the CO_2 is released has a volume of 39-40 m^3 depending on the state of the tide. Release scenarios are designed to encompass the range of hypothetical potential releases for CCS sites in the North Sea (Table 1). To simulate a non-catastrophic failure of the CCS storage (since a large instantaneous release is more readily identifiable), the initial release is tapered with a hyperbolic tangent over a period of a day until the maximum release rate is attained, after which the rate remains constant for the remainder of the model run. The model pH outputs as an indicator of CO_2 concentration are used as a test dataset to generate a monitoring network.

Table 1 CO_2 release scenarios

CO_2 (t d^{-1})	CO_2 (mmol m^{-2} s^{-1})
3	91.1
30	911.4
300	9114.1
3000	91140.6

3. Sampling strategy

The sampling strategy employed here is a development of the technique developed for the OPEC project [7], [18]. The OPEC method investigates monitoring in terms of the spatial distribution of sampling points required to capture some threshold of the signal being monitored to enable the design of an optimal monitoring network, which may include realistic constraints such as a limited number of sensors. This important caveat can have significant associated cost savings compared with less optimal sampling designs.

In the OPEC tool, an initially regular sampling grid is overlaid on the model grid with a specified sampling radius with staggered alternate rows to maximise coverage for each location. Within each radius at each regular grid position, the model grid closest to each position in the uniform grid is identified and used as a base time series against which all remaining nodes in the model domain are compared. A range of statistics is able to be calculated (root mean square error, standard deviation, correlation coefficient, variance etc.) to calculate what percentage of the model time series inside the radius for the regular sampling position can explain the variability seen compared with the base time series. Based on the statistical values at each regular grid sampling location, those with similar values are merged to form regions of the domain where the properties of the water are similar and which can then be sampled with a single time series.

This method was designed with remote sensing and regularly gridded model results in mind and is less well suited to outputs from an unstructured grid model such as FVCOM. As such, it has had to be modified for use with FVCOM. As with the OPEC approach, a regularly spaced grid is overlaid on the model grid and the closest model node to each regular position is used as the base time series. Rather than comparing only those positions which fall inside a pre-defined radius, each base time series is compared against all other nodes in the model grid starting with those closest to the base time series location and moving away. The radius of similarity for the time series at each of the remaining model nodes is instead computed dynamically based on a threshold statistical value. The approach described here uses the Pearson correlation coefficient of the base time series and the other time series in the model domain with a threshold of 0.5. Once the correlation coefficient decreases below the threshold, the analysis flags the remaining nodes as outside the radius of similarity. This approach means that each position in the regular grid has a radius of similarity which is dependent on the base time series. However, the result produces a large number of overlapping regions.
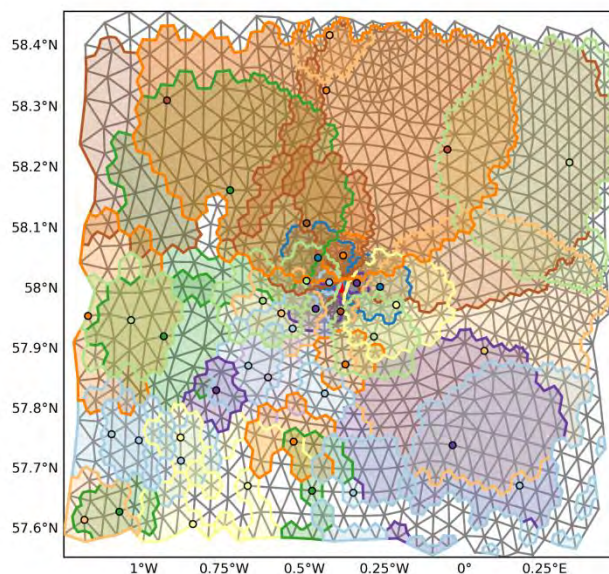

Figure 2 The results of the weighted greedy set algorithm applied to the regions for all the locations in the initial uniform grid. Each coloured polygon represents the coverage of the correspondingly coloured dot.
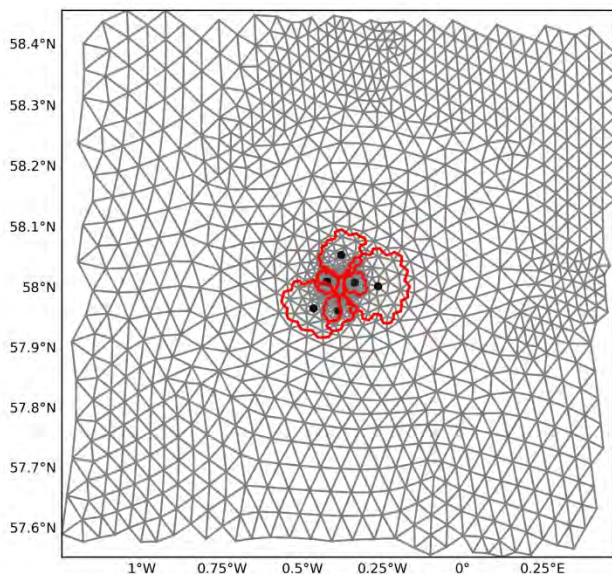

Figure 3 Coverage of similar water properties for the given domain for a limited number of sites for a finite number of sampling stations from the results in Figure 2).

A greedy set algorithm [19] is able to identify the smallest number of sampling locations which provide the largest set of nodes. Whilst this approach is suitable for a regularly gridded model, the unstructured nature of FVCOM means that a greedy set algorithm would generally favour regions of higher resolution. A weighted greedy set algorithm [19] uses a weight to modify the behaviour by selecting the set of similarity radiuses at the regular grid positions which minimises the total weights. In this instance, the weights are a combination of the distance from the Goldeneye complex (black box in Figure 1b) and the coverage of each region. In this manner, a monitoring network can be designed which will provide the maximum likelihood of identifying a sub-sea release of CO_2 into the water column (Figure 2). The number of locations is artificially restricted to six to mimic a finite number of in situ sensors to yield an optimal sampling strategy (Figure 3).

4. Sampling validation

Although it is tempting to assume a complex method for identifying optimal sampling must be better than a simple approach, it is important to ensure this is the case, especially given the potential real costs associated with monitoring in ocean environments.

To validate the weighted greedy set approach to designing optimal monitoring networks in Figure 3, a simpler uniform distribution of the same number of sampling stations was generated for the Goldeneye complex (Figure 4). Time series of the difference in pH between a no release run and the 30 t d^{-1} release at the relevant sampling stations are shown in Figure 5.

Using the first deviation from baseline in pH, the regular sampling network is able to identify a signal from the released CO_2 on 2015-01-02 17:00:00. For the weighted greedy set network, the first non-zero value occurs at 2015-01-02 10:00:00, 7 hours earlier. Whilst a non-zero ΔpH is technically identifiable, in reality, the variability in the natural system means that such small thresholds are impractical for monitoring purposes [20]. What the weighted greedy set
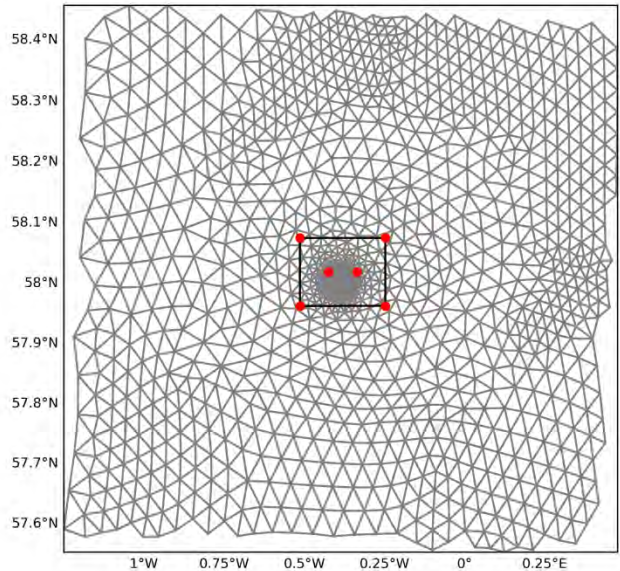

Figure 4 Regular sampling stations (red dots) within the Goldeneye complex (black box) to illustrate a simpler sampling strategy with the same number of stations as the optimised approach (Figure 3).
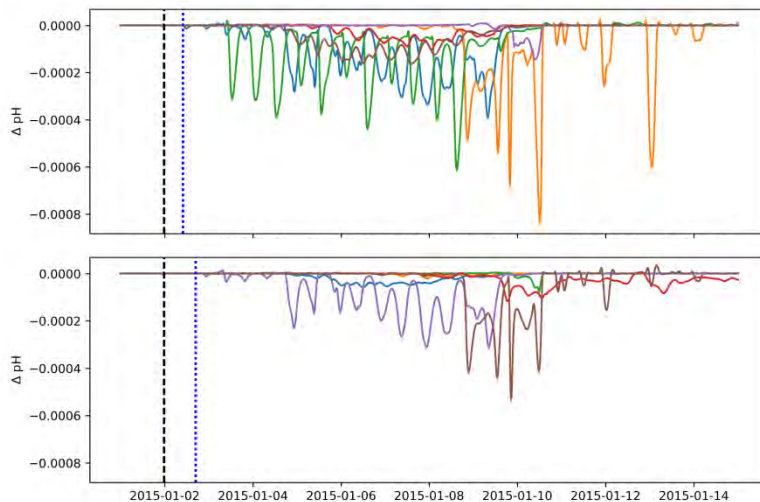
monitoring network also shows is a greater magnitude of signal: the top panel in Figure 5 shows the weighted greedy set ΔpH for the 30 t d^{-1} release where pH drops relative to the no release scenario are of the order 0.0004; in contrast, the pH drops in the lower panel in Figure 5 for the regular sampling are of order 0.0001, four times lower. These changes are two orders of magnitude lower than detection thresholds of current sensors, indicating larger impacts from the released CO2 are confined to a radius of fewer than 5km.

Figure 5 Comparison of time series of ΔpH from the weighted greedy set (Figure 3) and regular approaches (Figure 4) for a 300 t d^{-1} release to compare a simpler and more complex sampling approach. The dashed black vertical line indicates the start of the release and the dotted blue vertical line the time at which the release is first encountered by a sampling station.

5. Conclusions

Effective monitoring of CCS is required to ensure the integrity of the reservoir and thus the long term CO_2 storage. The monitoring which is put in place must include geological (both consolidated and unconsolidated sediments) and water column monitoring at the very least, and monitoring water column chemistry is a critical part of a baseline monitoring strategy. Critical to effective monitoring is an optimal sampling strategy, one which is cognisant of the cost of such operations but also of the importance of timely detection.

We present the application of a monitoring tool which extends an existing in situ sensor network design tool [7], [18]. Based on a uniform grid, pH time series correlation coefficients at the model grid nodes closest to the regular grid positions and all the nodes in the model domain are calculated. Those which fall within a given threshold coefficient are grouped to identify regions of similar properties. The weighted greedy set algorithm then groups these sets of model nodes in combination with a weighting (the distance outside the Goldeneye complex and the coverage of each region of similarity at each regular grid position). This provides an optimal sampling strategy with no limitations on the number of sampling stations; the weighted greedy set algorithm merely aims to maximise coverage whilst minimising the number of sampling stations required.

To replicate more real-world limitations, where cost per sampling station is a valid criterion, a limited number of sampling stations are extracted from the weighted greedy set algorithm results to design a pragmatic monitoring network. The changes in pH from the pragmatic network are compared with those from a simple sampling strategy and show that the weighted greedy set positions are able to both identify releases sooner and produce stronger signals in ΔpH over the duration of the CO_2 release. Previous work has shown that the sensitivity to changes in pH is strongly correlated with the likelihood of a true positive release identification [20], so optimising the sampling locations to maximise the potential changes in observed pH increases the chances of identifying a release correctly.

The weighted greedy set algorithm is shown to be able to design monitoring networks for tracers released from point sources in tidally dominated coastal seas. Its application, however, is not limited to such environments since the analysis is performed on model outputs. The algorithm is implemented to show how a monitoring network can be designed which improves release detection timelines compared with a simpler scheme.

Acknowledgements

References

[1]   R. K. Pachauri et al., Climate change 2014: synthesis Report. Contribution of working groups I, II and III to the fifth assessment report of the intergovernmental panel on climate change. IPCC, 2014.
[2]   J. Greenwood, P. Craig, and N. Hardman-Mountford, 'Coastal monitoring strategy for geochemical detection of fugitive CO2 seeps from the seabed', Int. J. Greenh. Gas Control, vol. 39, pp. 74–78, Aug. 2015.
[3]   H. K. Hvidevold, G. Alendal, T. Johannessen, A. Ali, T. Mannseth, and H. Avlesen, 'Layout of CCS monitoring infrastructure with highest probability of detecting a footprint of a CO2 leak in a varying marine environment', Int. J. Greenh. Gas Control, vol. 37, pp. 274–279, Jun. 2015.
[4]   J. C. Blackford, R. Torres, P. Cazenave, and Y. Artioli, 'Modelling Dispersion of CO2 Plumes in Sea Water as an Aid to Monitoring and Understanding Ecological Impact', Energy Procedia, vol. 37, pp. 3379–3386, Jan. 2013.

[5]   J. J. C. Phelps, J. C. Blackford, J. T. Holt, and J. A. Polton, 'Modelling large-scale CO2 leakages in the North Sea', Int. J. Greenh. Gas Control, vol. 38, pp. 210–220, Jul. 2015.

[6]   J. C. Blackford, N. Jones, R. Proctor, and J. Holt, 'Regional scale impacts of distinct CO2 additions in the North Sea', Mar. Pollut. Bull., vol. 56, no. 8, pp. 1461–1468, Aug. 2008.

[7]   J. She et al., 'OPerational ECology: Effectiveness of routine monitoring of ecosystem properties in European regional seas', 283291, Aug. 2014.

[8]   C. Chen, H. Liu, and R. C. Beardsley, 'An Unstructured Grid, Finite-Volume, Three-Dimensional, Primitive Equations Ocean Model: Application to Coastal Ocean and Estuaries', J. Atmospheric Ocean. Technol., vol. 20, no. 1, pp. 159–186, Jan. 2003.

[9]   M. Butenschön et al., 'ERSEM 15.06: a generic model for marine biogeochemistry and the ecosystem dynamics of the lower trophic levels', Geosci. Model Dev., vol. 9, no. 4, pp. 1293–1339, 2016.

[10]   J. Bruggeman and K. Bolding, 'A general framework for aquatic biogeochemical models', Environ. Model. Softw., vol. 61, pp. 249–265, Nov. 2014.

[11]   J. C. Blackford, J. I. Allen, and F. J. Gilbert, 'Ecosystem dynamics at six contrasting sites: a generic modelling study', J. Mar. Syst., vol. 52, no. 1–4, pp. 191–215, Dec. 2004.

[12]   J. Michalakes et al., 'Development of a next generation regional weather research and forecast model', in Developments in Teracomputing: Proceedings of the Ninth ECMWF Workshop on the use of high performance computing in meteorology, 1998, vol. 1, pp. 269–276.

[13]   C. Skamarock et al., 'A Description of the Advanced Research WRF Version 3', 2008.

[14]   G. D. Egbert and S. Y. Erofeeva, 'Efficient Inverse Modeling of Barotropic Ocean Tides', J. Atmospheric Ocean. Technol., vol. 19, no. 2, pp. 183–204, Feb. 2002.

[15]   G. D. Egbert, S. Y. Erofeeva, and R. D. Ray, 'Assimilation of altimetry data for nonlinear shallow-water tides: Quarter-diurnal tides of the Northwest European Shelf', Cont. Shelf Res., vol. 30, no. 6, pp. 668–679, Apr. 2010.

[16]   G. D. Egbert, A. F. Bennett, and M. G. G. Foreman, 'TOPEX/POSEIDON tides estimated using a global inverse model', J. Geophys. Res., vol. 99, no. C12, pp. 24821–24852, 1994.

[17]   Y. Chao, Z. Li, J. D. Farrara, and P. Hung, 'Blending Sea Surface Temperatures from Multiple Satellites and In Situ Observations for Coastal Oceans', J. Atmospheric Ocean. Technol., vol. 26, no. 7, pp. 1415–1426, Jul. 2009.

[18]   W. Fu, J. L. Høyer, and J. She, 'Assessment of the three dimensional temperature and salinity observational networks in the Baltic Sea and North Sea', Ocean Sci., vol. 7, no. 1, pp. 75–90, Jan. 2011.

[19]   N. E. Young, 'Greedy Set-Cover Algorithms', in Encyclopedia of Algorithms, M.-Y. Kao, Ed. Boston, MA: Springer US, 2008, pp. 379–381.

[20]   J. Blackford, Y. Artioli, J. Clark, and L. de Mora, 'Monitoring of offshore geological carbon storage integrity: Implications of natural variability in the marine system and the assessment of anomaly detection criteria', Int. J. Greenh. Gas Control, vol. 64, pp. 99–112, 2017.

[21]   E. Jones, T. Oliphant, P. Peterson, and others, SciPy: Open source scientific tools for Python. 2001.

[22]   S. van der Walt, S. C. Colbert, and G. Varoquaux, 'The NumPy Array: A Structure for Efficient Numerical Computation', Comput. Sci. Eng., vol. 13, no. 2, pp. 22–30, Mar. 2011.

[23]   F. Perez and B. E. Granger, 'IPython: A System for Interactive Scientific Computing', Comput. Sci. Eng., vol. 9, no. 3, pp. 21–29, May 2007.

[24]   J. D. Hunter, 'Matplotlib: A 2D Graphics Environment', Comput. Sci. Eng., vol. 9, no. 3, pp. 90–95, Jun. 2007.

[25]   O. Tange, 'GNU Parallel - The Command-Line Power Tool', Login USENIX Mag., vol. 36, no. 1, pp. 42–47, Feb. 2011.

Prediction of greenhouse gas leakages from potential North Sea storage sites into coastal waters by an unstructured, multi-scale and multi-phase flow model

Marius Dewar[a]*, Umer Saleem[a], Sorush Khajepor[a], Baixin Chen[a]*

[a]Institute of Mechanical, Process and Energy Engineering, Heriot-Watt University, Edinburgh, EH14 4AS, UK

Abstract

This paper reports the development of a multi-scale, multi-phase modules for bubble plume dynamics within the FVCOM numerical model to investigate the fate of CO_2 leakage into the water column from potential carbon storage sites. The model is capable of analysing the fluid dynamics, dissolution and leakage impacts, including seawater pH and pCO2 changes, at scales ranging from the leakage site in the order of meters, up to the regional and coastal ocean scale in the order of thousands of kilometres for a wide range of leakage scenarios, from bubbly seeps to well blowouts. The developed model is tested to predict the fate of leakage of CO_2 from the Goldeneye area of the North Sea, a potential site for CO_2 storage. Results show that the bubble modules are successfully coupled with the ocean model and predicted, from 3 leakage ports within a 5x5 m^2 area at a rate of 0.3 Tons/day, the maximum increases of concentration of dissolved CO_2 (DIC) reaches to 0.03kg/m^3 at the leakage sites within an area of 2.5 km^2, with DIC increases of 0.01 kg/m^3 at a leakage time of 5 hours. The CO_2 bubble plume reaches to a steady state at the height of 13 m and moves with the ocean current horizontally within a 2.2 m in diameter. The DIC plume then further develops to an area of 93 km^2 within one day and circulates periodically around the leakage site with the tidal currents.

Keywords: FVCOM Numerical Model; Multi-Phase Flow; Plume Dynamics; CO_2 Bubble Dynamics; Carbon Capture and Storage;

1. Introduction

To reduce greenhouse gas levels in the atmosphere and to mitigate anthropogenic carbon dioxide (CO_2) emissions, Carbon dioxide Capture and Storage (CCS) has been identified as a vital component, removing CO_2 from large emission sources such as fossil fuel burning power stations and disposing of it in storage sites and geological formations deep underground on or offshore. A large concern in offshore CCS is the ability of the storage reservoirs to retain the CO_2, and preventing any risk of leakage traveling through the geoformations into the water column and atmosphere. Another issue is the lack of studies into the impacts a leak would have on local and coastal marine ecosystems; requiring development of new monitoring techniques, testing in low risk in-situ experiments, and utilising modelling techniques to best define monitoring strategies, determine the impact of leakage, and upscaling from the small-scale experiments to full scale analysis. Without significant realistic analogues, modelling systems are the only method of characterising the diverse "hypothetical" release events that can occur through sediments and into the water column [1].

---

* Corresponding authors. Baixin Chen, Tel.: +44 131 451 4305 and Marius Dewar, Tel.: +44 131 451 3779;
 E-mail addresses: B.Chen@hw.ac.uk and Marius.Dewar@hw.ac.uk

A two-phase regional ocean model is developed aiming to predict, under a range of leakage and seasonal conditions, the CO_2 bubble/droplet plume developments coupled with the chemistry and dispersion of the dissolved CO_2 solution, along with the subsequent impacts in terms of changes in pCO_2 or pH from baseline measurements on ocean physicochemical environments.

Existing regional leakage models have a number of shortcomings beyond that of the lack of in-situ experimental data required to test and calibrate the modelling systems. There are shortfalls of modelling the multi-phase flows that aim to predict leakages from gas bubbles and liquid droplets, with/without hydrate formations; along with low depth, dissolving, bubbly flow in CO_2 leakage scenarios [2]. Further to this, looking at wider impact zones also requires analysis in multiple scales, investigating the local impacts in the order of meters and larger scale impacts in the order of tens of kilometres. Except for the structured mesh models by Sato et al. [3], [4], there are a lack of nested modelling systems developed allowing data transfer between these different scales.

Typical oceanic shelf models have resticted horizontal resolutions, either in the order of 10km or larger, that, clearly, is unable to predict the impacts of the near leakage plumes that are in an order of magnitude smaller [5]. Therfore, there has always been treatement to de-couple these models from those of the fine scale providing bubble plumes in the order of meters. To investigate the fate of CO_2 leakage into the water column in the local environment (meters) to oceanic scale (thousand kilometres), the small scale impacts of the bubble plume are required, giving the plume rise height, rate of dissolution, distribution and concentration of the dissolved solution [6-9]. On the other hand, the small scale impacts are affected greatly by oceanic tides, currents and ocean turbulence cascaded from those generated in the global and coastal scales. Therefore, a new numerical modelling system requires to be developed to fit these gaps.

2. FVCOM Leakage Plume Module

In this study, a multi-scale and multi-phase prediction module is developed based on the Unstructured Grid Finite Volume Community Ocean Model (FVCOM) [10] for predictions of the fate of CO_2 leakage into the ocean. The model aims of coupling the hydrodynamics and mixing phenomena from the oceanic scale, with the bubble dynamics and the multi-phase physicochemistry in the ultra-fine scale, including analysis of leakage impacts and fluid dynamics ranging from leakage site (m - km) up to the regional and coastal scale (10^3 km) in the North Sea, as shown on the top of Figure 1 (a). The model is designed initially for the North Sea, where it has been considered to store carbon in the undersea bed oil and gas reservoirs, utilising grid system and regional boundary forcing data from the Scottish Shelf Model [11]. The model is capable of simulating the CO_2 plumes from multiple leakage sites, which may move within the North Sea. It should be noted that the methodology and the model system are not limited to the North Sea, but can be applied to other regional oceans and global ocean as required.

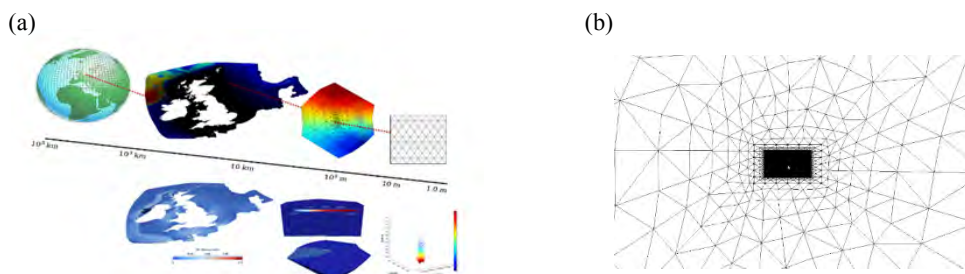(a)   (b)

Fig. 1.   The developed multi-scale, multi-phase numerical model, a). with forcing down from global scale data (the top left); into the coastal scale in the SSM (top middle shows the mesh, bottom left shows sample currents); with a nested ghost model reducing the scale to the meters (top left showing the mesh, bottom middle shows the flow of dissolved CO_2 solution); including an example CO_2 leakage plume module (bottom left, providing CO_2 bubble plumes rising and dissolving in the water column (shown in terms of bubble size – mm), and flow of dissolved CO_2 solution in the water column (shown in terms of dissolved mass concentration). b). the unstructured grid around the CO_2 leakage sites, where the black area reduces to a grid size of 1.0m x 1.0m.

As the particle tracking module build into FVCOM only allows movements with the water column [10], a new module is developed to cover the rising and dissolving gas dynamics and their impact on the water column dynamics. This is achieved through developing a module that links the individual bubble model from Chen et al. [6] to FVCOM in a two-way coupling scheme that not only solves the bubble dynamics, but provides source terms for changes in mass, momentum and Dissolved Inorganic Carbon (DIC) in the water column, from which the further developments of the CO_2 solution can be simulated up to the regional ocean model [12]. The module is developed through a Lagrangian-Eulerian approach, where the dynamics of the leaked CO_2 are modelled by the Lagrangian scheme that interacts with the turbulent ocean, modelled by the Eulerian scheme, through two-way coupling of mass and momentum. Therefore, in addition to the dynamic models of CO_2 bubble interactions with the water, a high level of modification has been made in FVCOM's coding and design to allow multi-phase flow for gas leakage. Further details of the CO_2 bubble/droplet models, parameters and their respective values and correlations are found in Chen et al. [6].

3. Model Test Set up

The developed model is tested, setting the leakage of CO_2 at a rate of 0.3 tons/day from 3 leakage ports within 5x5 m^2 of sea floor at near the Golden Eye platform in the North Sea at a depth of 126m, refer to the top part of Figure 1 (a). The unstructured grid system has the fine mesh sizes of 1.0m x1.0 m horizontally and 2.0m vertically at CO_2 leakage ports area as shown in Fig 1 (b). The simulation is performed for a test case of 7 days leakage of CO_2. The bubble plumes and the development of the CO_2 solution distribution within this period are examined to demonstrate how the model works. The code was running using a 16 core workstation.   Results and Discussion

The leaked bubbles fully dissolve within 15 meters height from the seafloor at an initial size of 2 ~ 12 mm in diameter randomly leaked from sediment pockmarks. This indicates a dissolution rate of ~0.64 mm/s in diameter. No significant horizontal movements, but about 2.0 m in diameter around the leakage pockmarks, of the bubble plume have been observed due to the relatively larger velocity ratio of bubble rising (u_b ~ 12 cm/s) to that of current at the bottom boundary layer (u_c ~ 1.0 cm/s).

The CO_2 enriched seawater (or the dissolved inorganic carbon, DIC) plume developed by the flow of the ocean current, are demonstrated within the domain of 27.1 km (East to West) and 13.5 km (north to south) centred at the leakage pockmarks in the first grid from sea floor. The results of CO_2 enriched water plume shown by the CO_2 concentration normalized by the maximum concentration of 0.03kg/m^3 are presented in Figure 2 at 8 different leakage times.

Fig. 2.   The developments of CO_2 enriched seawater plume within an area of 27.1 km x 13.5km centred to the leakage pockmarks in the first grid from sea floor at a series of times and the scale bar can be used as reference for the dissolved CO_2 concentration normalized by the maximum value of 0.03 kg/m^3.

The CO_2 enriched water plume reaches the maximum concentration (0.03 kg/m^3) within 5.0 hours at the leakage sites from the horizontal dispersion though flow of the seawater. The oceanic currents within the leakage period is, in

general, towards the North-East (can be seen from the plume of 4.2 day in Fig. 2), however this circulates with the tidal frequency. The development of the plume of this circulation can be found from the snapshots taken at 20 hr, 1.2 days, to 6.3 days. As such, when the current turns to the South-West, the DIC at the North-East side of the leakage site is transferred past the leakage site, creating a temporal relatively larger area of high DIC concentration, as shown in the snapshots at 1.2 day, 3.5 day and 6.3 day in Fig 2. The area of the CO_2 enriched water with concentrations larger than 0.01 kg/m^3 is less than 2.5 km^2 through to the end of the simulation on day 7.

It has to be mentioned that the results discussed in this paper are from early preliminary analysis on the data obtained from the simulation. The aim is to demonstrate how the developed model works. The details on the structure and the dynamics of bubble plume and the CO_2 enriched water plume will be reported when the data from the simulations are analysed in the following papers.

4. Conclusion

A multiscale and multiphase regional ocean model is developed on the basis of the Unstructured Grid Finite Volume Community Ocean Model (FVCOM) [10] for predictions of the fate of CO_2 leakage into the ocean. The test simulation shows that the model is capable to simulate the interactions between the leaked bubbles with turbulent ocean to predict the potential impacts of leaked CO_2 on ocean. The model will be developed to simulate the leakage plume dynamics from CO_2, CH_4, and oil transportation pipelines.

Acknowledgements

References

[1] Blackford J, Alendal G, Artioli Y, Avlesen H, Cazenave P, Chen B, Dale A, Dewar M, Gundersen K, Haeckel M, Khajepor S, Lessin G, Oleynik A, Saleem U, García-Ibáñez MI, Omar AM. Ensuring efficient and robust offshore storage – the role of marine system modelling, this issue.
[2] Dewar M. Modelling the two-phase plume dynamics of CO_2 leakage into open shallow waters, Thesis, Heriot-Watt University, 2016.
[3] Kano Y, Sato T, Kita J, Hirabayashi S, Tabeta S. Multi-scale modeling of CO_2 dispersion leaked from seafloor off the Japanese coast, Marine Pollution Bulletin, vol. 60, no. 2, pp. 215–224, Feb. 2010.
[4] Mori C, Sato T, Kano, Y, Oyama H, Aleynik D, Tsumune D, Maeda Y, Numerical study of the fate of CO_2 purposefully injected into the sediment and seeping from seafloor in Ardmucknish Bay, International Journal of Greenhouse Gas Control, vol. 38, pp. 153–161, Jul. 2015.
[5] Blackford JC, Jones N, Proctor R, Holt J T, Regional scale impacts of distinct CO_2 additions in the North Sea. Marine Pollution Bulletin; 2008. 56. 1461 - 1468.
[6] Chen B, Nishio M, Song Y, Akai M. The fate of CO_2 bubble leaked from seabed. Energy Procedia. vol. 1. no. 1. pp. 4969–4976. Feb. 2009.
[7] Dewar M, Sellami N, Chen B. Dynamics of rising CO_2 bubble plumes in the QICS field experiment: Part 2 – Modelling. International Journal of Greenhouse Gas Control; 2015. vol. 38. pp. 52–63.
[8] Dewar M, Wei W, McNeil D, Chen B, Small-scale modelling of the physiochemical impacts of CO_2 leaked from sub-seabed reservoirs or pipelines within the North Sea and surrounding waters. Marine Pollution Bulletin; 2013. vol. 73. no. 2. pp. 504–515.
[9] Dewar M, Wei W, McNeil D, Chen B. Simulation of the Near Field Physiochemical Impact of CO_2 Leakage into Shallow Water in the North Sea. Energy Procedia; 2013. vol. 37. pp. 3413–3423.
[10] Chen C, Liu H, and Beardsley RC. An Unstructured Grid, Finite-Volume, Three-Dimensional, Primitive Equations Ocean Model: Application to Coastal Ocean and Estuaries. J. Atmos. Oceanic Technol; 2003. vol. 20. no. 1. pp. 159–186.
[11] CH2M -. The Scottish Shelf Model. Part 1: Shelf-Wide Domain. Marine Scotland Science. 2016.
[12] Dewar M. Modelling the two-phase plume dynamics of CO_2 leakage into open shallow waters. Thesis. Heriot-Watt University. 2016.

14th International Conference on Greenhouse Gas Control Technologies, GHGT-14

21st -25th October 2018, Melbourne, Australia

Ensuring efficient and robust offshore storage - use of models and machine learning techniques to design leak detection monitoring.

Kristian Gundersen[1], Anna Oleynik[1], Guttorm Alendal[1], Hans J. Skaug[1], Helge Avlesen[2], Jarle Berntsen[1], Nello Blaser[1], Jeremy Blackford[3], Pierre Cazenave[3].

[1]Department of Mathematics, University of Bergen, Bergen, Norway
[2] Uni Research, Bergen, Norway,
[3]Plymouth Marine Laboratory, Plymouth, UK

Abstract

The use of machine learning techniques to identify CO_2 seeps to marine waters is assessed. These techniques require a large amount of data for training, here obtained through model predictions on how CO_2 seeps behave in the water column. Goldeneye, off the coast of Scotland, has been used as area of study. It is shown that Convolutional Neural Networks (CNN) are able to, with high confidence, to classify time series from the model simulations into leak and no-leak situations. CNN in data analysis can increase the detectability of CO_2 seeps, and thus the optimization of sensor deployment and monitoring design.

Keywords: Convolutional neural networks, Time series classification, CO_2 leak detection, Goldeneye, CCS, Marine Monitoring

1. Introduction

Carbon, Capture and Storage (CCS) projects will be designed to keep the stored CO_2 within the intended formations, and the injection wells and the formation will be monitored by standard technologies to assure detection of unexpected events [1]. However, due to the large amount of CO_2 that needs to be stored and, as a consequence, the large area needed to be monitored, there is always that CO_2 may migrate toward the sea floor undetected. As a precaution, the marine environment will have to be monitored for indications of a leak, we argue that monitoring of the surface are necessary in order to compile with the regulations[1].

The marine component of the monitoring program assures that a storage project can coexist with other offshore activities, and the associated environmental monitoring can be beneficial for other purposes. For instance, tools are under development for assessing the total environmental stress imposed on the oceans, e.g. Cumulative Effects Assessments (CEA), in view of Marine Spatial Planning and ecosystem services framework [2-4], and a potential stress

---

[1] https://eur-lex.europa.eu/legal-content/EN/TXT/PDF/?uri=CELEX:32009L0031&from=EN

Corresponding author. Tel +47 92066620
E-mail address: Kristian.Gundersen@uib.no

added from CO_2 storage projects need to be documented. The marine monitoring program also assures against un-justified accusations for having adverse environmental effects [5], but will impose additional costs and challenges to the storage project [6-8].

Environmental changes, e.g. changes in bottom fauna or in the pelagic ecosystem [9, 10], detection of bubbles from ship sonars [15, 16], or elevated concentration of dissolved gases [11-15], can be used as indicators of marine gas re-leases. However, the real challenge is the high variability of the marine environment, both in current conditions [16] and in biochemical activities [11, 17].

Monitoring an unsteady marine environment for changes in variables that are a naturally present is a classification problem, we need to classify data streams into seep/no-seep situations. A false positive, i.e. indications of a leak that is not there, can become costly, the monitoring program will enter the locating and confirmation mode, but also false negatives (i.e. undetected seeps) may impose undetected additional stress to the environment.

Machine learning techniques are well suited to classify data streams collected from sensory systems that are ubiquitous today. Recently we have seen efforts for finding better techniques for identifying anomalies in pH by look at the difference between lags for the purpose of detecting anomalies and thus potential CO_2 leakages [18].

The learning process for the machine learning technique will require time series for both situations, i.e. time series of the variables in question for no-seep and seep conditions. The no leak situation represents natural environmental statistics, i.e. the baseline. These statistics must be based on in-situ measurements, preferably supplemented with model simulations [19]. Time series for the seep situations must rely on process modelling, simulating the different processes involved during a seep [13, 20]**,** preferably supported by in-situ and laboratory experiments [14]**.**

In anticipation of real experimental data, this study is based on simulations from the Finite-Volume Coastal Ocean Model (FVCOM) [21] coupled with European Regional Seas Ecosystem Model (ERSEM) [22]. Data at the Goldeneye site have been extracted from the regional model. Different scenarios have been created in a statistically sound manner to train the network. Other model results have subsequently been used to test the network. This study is a part of our preparation for the large-scale field study planned at Goldeneye in 2019 within the STEMM-CCS project (http://www.stemm-ccs.eu).

2. Time series classification

Monitoring of a CCS storage site will provide sensory time series from fixed installations on the seabed. The challenge is to classify these time series into a leak or no leak class. We define a time series **x** as follows:

$$\mathbf{x}^{(j)} = \{x_1^{(j)}, ..., x_m^{(j)}\}$$

where *m* is the number of observations in the time series, and $x_i^{(j)}$ is the value at time *i*. An instance is a pair {$\boldsymbol{x}^{(j)}$, $y^{(j)}$}, where $y^{(j)}_i$ is a discrete class variable which is a categorical value in *C* where $C \in \mathbb{Z}$. A dataset with *N* instances is denoted, $D = \{X^{(j)}, y^{(j)}\}$ where *j=1,2,...,N*, $X^{(j)}$ is a set of *j* time series and $y^{(j)}$ is a the corresponding class variable for the *j*th time series. The dataset *D* is split into a training and test dataset $D^V = \{X^{(1,...,j-m)}, y^{(1,...,j-m)}\}$ and $D^T = \{X^{(j-m,...,j)}, y^{(j-m,...,j)}\}$, respectively, where *m* represents the number of instances included in the training dataset, and *N-m* the test dataset. The time series classification problem consists of constructing a model based on the training dataset D^V, with the ability to predict a class label $y^{(j)} \in C$ given the input instances D^T.

Time series classification have been dominated by two different approaches, namely distance and feature based methods. Distance based methods takes untreated time series and exploits the fact that time series within a class can be interpreted as observations that arise from an underlying process. These methods depend on calculating the distance, or similarity, between unprocessed time series, and combine them with a classifier, e.g. k-nearest-neighbour (k-NN). Dynamic Time Warping (DTW) and Euclidean Distance (ED) are typically methods for calculating metrics for distances between time series. DTW seems to be the most successful distance based method,

as it allows for perturbations, shifts, variations and in the temporal domain [23, 24].

Feature based methods withdraw features from the time series and use traditional classification methods based on the extracted features. As an example, Bag-of-Words models, where countenance of the features extracted from the time series are feed to a classifier, have been extensively used in time series classification [25]. Recently, several efforts have used Artificial Neural Networks (ANN) for time series classification [16, 17]. Here we investigate how Convolutional Neural Networks (CNN) performs to the task of classify time series in the context of CO_2 leak detection.

3. Models and Simulations

The simulations used in this study are performed with FVCOM [21], coupled via FABM (Framework for Aquatic Biogeochemical Model) [26] with the ERSEM [22] model, thus enabling complex biogeochemical models to be developed as sets of stand-alone, process-specific modules. In these numerical simulations, ERSEM is run with only the carbonate system parameters enabled. Several simulations are performed, with and without CO_2 seeps present. We are studying the Goldeneye area in the North Sea and the simulations used are summarized in Table 1. The North West Europe model is run over a two-year period, while the model of the Goldeneye area is run for approximately 14 days. The North West Europe model is used as initial conditions and forcing for the Goldeneye set up. Model parameters for these simulations are shown in Table 1.

Table 1: Simulations used in the study with descriptions and key figures

Simulations	Description	Grid/Area	Size/Node/Grid
North-west-Europe	A large model is run for North-west Europe for 2015 and 2016. Data from the model is used as initial conditions and forcing for the model on the Goldeneye region	Only physical model run. Include wind forcing. FVCOM	
No Leak – Baseline simulation	**Training dataset,** no-leakage simulation with FVCOM and ERSEM including the Carbonate system at the Goldeneye region.	Physical and carbonate system, FVCOM ver4.0-ERSEM with nesting,	24 horizontal layers, 1736, nodes, 3357 Triangles, 1345 time steps with 15 minutes interval, 100x100 km area,
Goldeneye area, Small leak simulation (30T)	**Training dataset**, Small leak (30 Ton CO2 per day) simulation with FVCOM and ERSEM including the Carbonate system at the Goldeneye region.	Physical and carbonate system, FVCOM ver4.0-ERSEM with nesting,	24 horizontal layers, 1736, nodes, 3357 Triangles, 1345 time steps with 15 minutes interval, 100x100 km area,
Goldeneye area, Large leak simulation (3000T)	**Training dataset**, Large leak (3000 Ton CO2 per day) simulation with FVCOM and ERSEM including the Carbonate system at the Goldeneye region.	Physical and carbonate system, FVCOM ver4.0-ERSEM with nesting,	24 horizontal layers, 1736, nodes, 3357 Triangles, 1345 time steps with 15 minutes interval, 100x100 km area,
Goldeneye area, Medium leak simulation (300T)	**Test dataset**, Medium leak (300 Ton CO2 per day) simulation with FVCOM and ERSEM including the Carbonate system at the Goldeneye region.	Physical and carbonate system, FVCOM ver4.0-ERSEM with nesting,	24 horizontal layers, 1736, nodes, 3357 Triangles, 1345 time steps with 15 minutes interval, 100x100 km area,

4. Data Pre-processing

In the real-world information collected are in general incomplete, are often boisterous, lacking attributes and consists of false values and errors, include outliers and have incorporated inconsistencies. Data pre-processing is the task of preparing data before it is feed to a machine learning algorithm, that aim to facilitate and optimize the accuracy of the algorithm.

The pre-processing can be divided into two main tasks, data preparation and data reduction, with associated subtasks. Preparation of data includes among others, data cleaning, data integration, data normalization and transformation, as well as missing data imputation. Instance selection, data discretization, feature selection and feature construction are part of the data reduction process. The most important aspects of the data pre-processing steps are described in [27] and [28].

Since we use gridded data from numerical simulations, which often are uniform and regular, many of the steps in the data pre-processing stage described in [28] are unnecessary. The main pre-processing step for this particular data is the cleaning step, i.e. removing time series that do not contain traces of the leakage and to transform them with simple techniques such as normalization or standardization [29]. Here we first compared and subtracted the baseline simulation from the leak simulations and generated a footprint of the leakage (See Figure 2). Secondly, we clean the dataset by only label time series as leak above a threshold, here we use the maximum value of the concentration of 1 (mmol C/m^3). Thirdly, we standardized [30] the training data and test data separately. The training data is then fed to the neural network while we leave out the test dataset for validation of the model.

5. Method: Artificial Neural Networks (ANN)

An ANN consists of a finite number of inputs and outputs, neurons, connections between neurons, the influence of the connections, i.e. weights, a propagation function and a learning rule. An artificial neuron, here denoted g, is the mathematical function that computes a weighted sum of its inputs signals, x_i, $i=1,...,n$ and generate output based on the, linear or non-linear, activation function K [15],

$$g = K \left(\sum_{i=0}^{n} w_i x_i - b \right)'$$

w is the coefficients or weights of the, while b is the bias. One of the most commonly used activation functions has been the sigmoid function (logistic function), recently variants of the Rectified Linear Unit (ReLu) have become popular [31]. The artificial neurons are organized in layers and the output of the neurons in one layer are connected to the input of the next layer. The process of updating and optimizing the weights and thresholds in the artificial neural network is called the learning process. For this optimization task we need to define a cost or loss function that typically is a measure of the true value against the predicted estimate, i.e. mean squared error, hinge loss or cross entropy [30]. This optimization task is usually solved by gradient-decent-methods such as backpropagation [32]. CNN have been successful in many applications such as image recognition [33], video analysis [34] and natural language processing [35].

5.1. Convolutional Neural Networks

CNNs utilize the grid structures in the data to be analysed, i.e. in 1-D the regular sampling in time series data, or in 2-D the fixed structure of pixels in an image and use convolutions instead of matrix multiplication in at least one of its layers. The convolution operation is defined as the function *s(t)* such that:

$$s(t) = \int x(a)w(t-a)da$$

where *x(a)* is an observation or input, and *w(a)* is a weighting function. The convolution operation will typically generate a less noisy dataset *s(t)*, as the observations *x(a)* will be averaged with the weighting function *w(t)*. The output of a convolution operation is often referred to as the feature map, while the function *w* is called the kernel.

Normally implementations of CNNs do not actually use regular convolution, use but instead cross correlation. Cross-correlation and convolutions are very alike, and the major difference in definition is that the weighting function *w(t-a)* is altered to *w(t+a)*. During a convolution operation we have to flip either the input or the kernel, while this is not necessary in the cross-correlation operation. Optimization will lead to the same final results with both methods and thus, by using cross-correlation, simpler implementation of the CNN is possible. The main reasons for using convolutions in neural networks are; sparse interactions, parameter sharing and equivariant representation [30, 36].

Sparse interactions are a consequence of the convolutional operation and occur when the kernel *w* is smaller than the input *x*, i.e. interactions between layers in the CNN are limited by the kernel size [30]. For instance, in a time series setting it is with the convolution possible to detect meaningful and small features that occur only in a fraction of the original time series. The convolution operation enables for parameter sharing in the network, which in essence reduce the parameters of the model and thus reduces memory requirements and improves the quality of the model/estimator [30]. The convolutional operation is equivariance to translation [30], which means that a translation of input features results in an equivalent translation of output. For time series, the convolution generates a record of when different features appear, and the feature will be represented similarly regardless of where it appears. This is particular good property for CO_2 leak detection, it does not matter when the feature occurs. A great benefit with the convolutional neural networks is the fact that they utilize spatial or temporal relationships to reduce learning requirements [37].

The architecture of a fully CNN consists in general of three important steps that are repeated; the convolution operation, a non-linear transformation via the activation function and a pooling operation. The convolution enables for detection of feature on a smaller scale, the non-linear activation ensures that non-linear relationships in the data are accounted for and the pooling operation reduce overfitting, the spatial size and the number of parameters in the network. Dropout is applied after the last convolutional layer and it is a regularization method which removes features in the network [38] with the intent of reduce overfitting. Stochastic gradient-decent-method Adam [39] is used as optimization method. Table 2 shows the most important aspects of the neural networks used here.

We use the two simulations with 30T and 3000T as training dataset. The 300T simulation is used to verify the neural network by predicting both false-positive rate and probability for detection. Table 3 shows an overview of the layers, shape of the layers and parameters. In total there are 72 986 trainable parameter in the neural network.

Table 2: The most important aspects of the architecture of the neural network used in the study.

Architecture	Description
Pre-processing	Cleaning and standardization of data
Input data	1-D time series of length 1345, time step 15 minutes
Samples/Instances	83328
Test split	33 %
Validation split	33 %
Validation dataset (leak/no-leak ratio)	17 %

Prediction dataset (leak/no-leak ratio)	24 %
Layers	All convolutional layers, 3 in total
Activation function	ReLu for all CNN layers
Pooling	Max-pooling after each CNN layer
Regularization	Drop-out (60 %)
Loss function	Binary cross-entropy [3]
Optimizer	Stochastic Gradient decent – Adam [3, 42]
Output	Binary, Softmax [3] activation function

Table 3: Overview of parameters to be optimized in the CNN.

Layer	Output of Layer (shape)	Parameter figures	Parameters in total
Convolution - 1	(None, 1344, 24)	Filters: 24, Kernel size: 2	72
Max pooling - 1	(None, 672, 24)	Pool size: 2, Strides: 2	0
Convolution - 2	(None, 669, 48)	Filters: 48, Kernel size: 4	4656
Max pooling - 2	(None, 334, 48)	Pool size: 2, Strides: 2	0
Convolution - 3	(None, 327, 96)	Filters: 96, Kernel size: 8	36960
Max pooling - 3	(None, 163, 96)	Pool size: 2, Strides: 2	0
Flatten - 5	(None, 15648)	-	0
Dropout 6	(None, 15648)	Dropout rate: 0.6	0
Dense 7	(None, 2)	-	31298

6. Results

Figure 1 shows the validation and test loss, and validation and test accuracy, from the trained convolutional neural network model. The training dataset is the majority of the data available, and it is used to update the weights or parameters in the model. The validation dataset is used to tune the hyperparameters of the network, while the test dataset is independent of the training data and used to verify that the fitting of the model is robust. When both the training and test dataset fits the model, it is a good indication of minimal overfitting. We have used the cross entropy as loss function and the model convergence towards a validation loss close to zero and a test loss around 0.025. Test loss is expected to have a higher loss than validation, because in the test phase the model encounters "new" time series.

We observe that both the test and validation loss convergence, indicating that the model is not overfitted. Further, this indicates that the network is able to construct features with distinctiveness for each class, that allows for good classification. The classification is dependent on how the data have been cleaned. A high threshold for what time series to include in the training dataset will result in strong classification probability, with low false-positives. The drawback is that the classifier, by excluding the time series with lower threshold, do not capture the nuances that can be important to classify weaker signals, hence the probability for detecting a leakage decrease. A lower threshold will increase the false-positive rate since time series from both classes are getting more equal to each other.

Figure 1: **Left panel:** Validation loss and test loss. The loss used in this analysis is cross entropy. **Right panel:** Validation accuracy and test accuracy.

Figure 2 shows the actual footprint due to a leakage of size 300 Tonnes per day in the centre of the domain. The difference between the concentration from the leakage, and the same model run without leakage is calculated and plotted to the left. This is what we refer to as the footprint of the leakage. The time series that are feed to the CNN include background variability as shown in the left panel.

The rate of false positives for the non-leak time series fed to the network is given in the left panel of Figure 3. The corresponding rate of correct positives, i.e., the detection of a 300 T/d leak, is shown in the right panel of Figure 3. Although the simulations and data used for training the neural network have been limited, we see that the area of detectability are relatively large, when compared against the footprint on the right panel in Figure 2. Figure 3 shows the false-positive-rate of the model on the seabed. Here we have fed the model only time series that do not contain leakages, and obsereve how the model classifies between leak and no-leak. With limited data available and minimal optimization of other parameters than the weights, theses initial results gives a good indication that CNN is a suitable method for classifying time series that arise in a typical CO_2 monitoring setting.

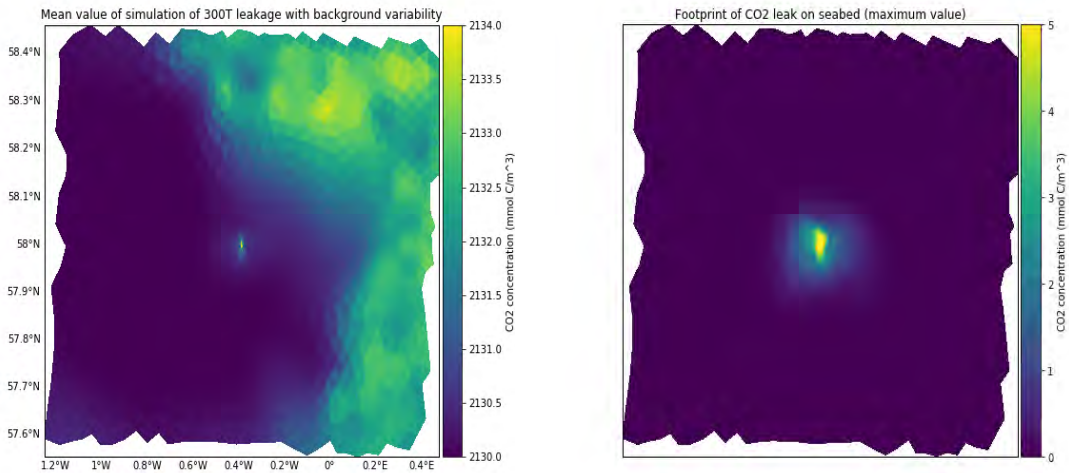Figure 2: **Left Panel:** Mean value of CO2 concentration of the 300T simulation with background variability.
Right panel: Maximum value of the concentration in each triangle of the footprint, i.e. the difference between a leak and no-leak situation. Here we have used 1 mmol C/m^3 when cleaning the data, i.e. only time series that are above a threshold of 1 mmol C/m^3 are labeled as a leak.
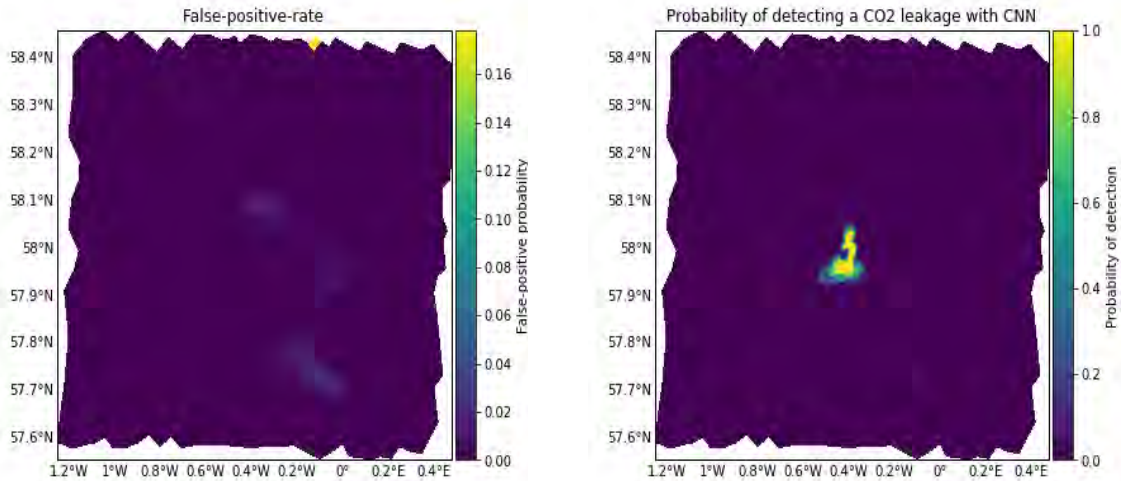
Figure 3: **Left Panel:** False positive rate of the seabed. **Right panel:** Area of detectability and probability of detection of a 300T leakage on the Goldeneye area.

7. **Discussion**

This small test of using convolutional neural networks in time series classification of CO_2 seepage signals shows promising results. We observe that the model converges and are able to distinguish time series between leak and no-leak class. Due to the limited amount of data and relatively low variability, results should be viewed with care. Thus, we need to investigate further how these methods work on more complex model runs and with real data where the variability and complexity is higher. New simulations with more variability are under development. There are many ways of improving the results, expanding the network and optimizing hyperparameters are two obvious ways forward.

Acknowledgements

References

[1]   Strickland, C.E., et al., *Geophysical Monitoring Methods Evaluation for the FutureGen 2.0 Project.* Energy Procedia, 2014. **63**: p. 4394-4403.

[2]   Jones, D.G., et al., *Developments since 2005 in understanding potential environmental impacts of CO2 leakage from geological storage.* International Journal of Greenhouse Gas Control, 2015. **40**: p. 350-377.

[3]   Marine Spatial Planning Programme, M.S.P. *IOC-UNESCO the Intergovernmental Oceanographic Commission of UNESCO* Available from: http://msp.ioc-unesco.org.

[4]   Menegon, S., et al., *Addressing cumulative effects, maritime conflicts and ecosystem services threats through MSP-oriented geospatial webtools.* Ocean & Coastal Management, 2018. **163**: p. 417-436.

[5]   Boyd, A.D., et al., *Controversy in technology innovation: Contrasting media and expert risk perceptions of the alleged leakage at the Weyburn carbon dioxide storage demonstration project.* International Journal of Greenhouse Gas Control, 2013. **14**: p. 259-269.

[6]   Oldenburg, C.M. and J.L. Lewicki, *On leakage and seepage of CO2 from geologic storage sites into surface water.* Environmental Geology, 2006. **50**(5): p. 691-705.

[7]   Blackford, J., et al., *Marine baseline and monitoring strategies for carbon dioxide capture and storage (CCS).* International Journal of Greenhouse Gas Control, 2015. **38**: p. 221-229.

[8]   Blackford, J., et al., *Monitoring of offshore geological carbon storage integrity: Implications of natural variability in the marine system and the assessment of anomaly detection criteria.* International Journal of Greenhouse Gas Control, 2017. **64**: p. 99-112.

[9]   Wegener, G., et al., *Biogeochemical processes and microbial diversity of the Gullfaks and Tommeliten methane seeps (Northern North Sea).* Biogeosciences Discussions, 2008. **5**(1): p. 971-1015.

[10]   Blackford, J., et al., *13 - Environmental risks and performance assessment of carbon dioxide (CO2) leakage in marine ecosystems*, in *Developments and Innovation in Carbon Dioxide (CO2) Capture and Storage Technology*, M.M. Maroto-Valer, Editor. 2010, Woodhead Publishing. p. 344-373.

[11]   Botnen, H.A., et al., *The effect of submarine CO2 vents on seawater: Implications for detection of subsea carbon sequestration leakage.* Limnology and Oceanography, 2015. **60**(2): p. 402-410.

[12]   Drange, H., G. Alendal, and O.M. Johannessen, *Ocean release of fossil fuel CO2: A case study.* Geophysical Research Letters, 2001. **28**(13): p. 2637-2640.

[13]   Alendal, G. and H. Drange, *Two-phase, near-field modeling of purposefully released CO2 in the ocean.* Journal of Geophysical Research: Oceans, 2001. **106**(C1): p. 1085-1096.

[14]   Vielstädte, L., et al., *Quantification of methane emissions at abandoned gas wells in the Central North Sea.* Marine and Petroleum Geology, 2015. **68**: p. 848-860.

[15]   Jain, A.K., M. Jianchang, and K.M. Mohiuddin, *Artificial neural networks: a tutorial.* Computer, 1996. **29**(3): p. 31-44.

[16]   Zheng, Y., et al. *Time Series Classification Using Multi-Channels Deep Convolutional Neural Networks*. in *Web-Age Information Management*. 2014. Cham: Springer International Publishing.

[17]   Wang, Z., W. Yan, and T. Oates. *Time series classification from scratch with deep neural networks: A strong baseline*. in *2017 International Joint Conference on Neural Networks (IJCNN)*. 2017.

[18]   Jeremy Blackford, H.S., Jun Kita, Toru Sato, *CCS and the Marine Environment.* International Journal of Greenhouse Gas Control 38, 2015. **38**(Special Issue): p. 1-230.

[19]   Siddorn, J.R., et al., *Modelling the hydrodynamics and ecosystem of the North-West European continental shelf for operational oceanography.* Journal of Marine Systems, 2007. **65**(1-4): p. 417-429.

[20]   Dewar, M., N. Sellami, and B. Chen, *Dynamics of rising CO2 bubble plumes in the QICS field experiment: Part 2 – Modelling.* International Journal of Greenhouse Gas Control, 2015. **38**: p. 52-63.

[21]   Chen, C., *An Unstructured-grid, Finite-volume Community Ocean Model: FVCOM User Manual*. 2012: Sea Grant College Program, Massachusetts Institute of Technology.

[22]   Butenschön, M., et al., *ERSEM 15.06: a generic model for marine biogeochemistry and the ecosystem dynamics of the lower trophic levels.* Geoscientific Model Development, 2016. **9**(4): p. 1293-1339.

[23]   Berndt, D.J. and J. Clifford, *Using dynamic time warping to find patterns in time series*, in *Proceedings of the 3rd International Conference on Knowledge Discovery and Data Mining*. 1994, AAAI Press: Seattle, WA. p. 359-370.

[24]   Ratanamahatana, C. and E. Keogh, *Three Myths about Dynamic Time Warping Data Mining*, in *Proceedings of the 2005 SIAM International Conference on Data Mining*. 2005, Society for Industrial and Applied Mathematics. p. 506-510.

[25]   Bagnall, A., et al., *The great time series classification bake off: a review and experimental evaluation of recent algorithmic advances.* Data Mining and Knowledge Discovery, 2017. **31**(3): p. 606-660.

[26]   Bruggeman, J. and K. Bolding, *A general framework for aquatic biogeochemical models.* Environmental modelling & software, 2014. **61**: p. 249-265.

[27]   Garca, S., J. Luengo, and F. Herrera, *Data Preprocessing in Data Mining*. 2016: Springer Publishing Company, Incorporated. 320.

[28]   Kotsiantis, S., D. Kanellopoulos, and P. Pintelas, *Data preprocessing for supervised leaning.* International Journal of Computer Science, 2006. **1**(2): p. 111-117.

[29]   Brockwell, P.J., R.A. Davis, and M.V. Calder, *Introduction to time series and forecasting*. Vol. 2. 2002: Springer.

[30]   Goodfellow, I., Y. Bengio, and A. Courville, *Deep Learning*. 2016: The MIT Press. 800.

[31]   Nair, V. and G.E. Hinton. *Rectified linear units improve restricted boltzmann machines*. in *Proceedings of the 27th international conference on machine learning (ICML-10)*. 2010.

[32]   Werbos, P.J., *Backpropagation through time: what it does and how to do it.* Proceedings of the IEEE, 1990. **78**(10): p. 1550-1560.

[33]   Krizhevsky, A., I. Sutskever, and G.E. Hinton. *Imagenet classification with deep convolutional neural networks*. in *Advances in neural information processing systems*. 2012.

[34]   Baccouche, M., et al. *Sequential deep learning for human action recognition*. in *International Workshop on Human Behavior Understanding*. 2011. Springer.

[35]   Collobert, R., et al., *Natural language processing (almost) from scratch.* Journal of Machine Learning Research, 2011. **12**(Aug): p. 2493-2537.

[36]   LeCun, Y., et al., *Gradient-based learning applied to document recognition.* Proceedings of the IEEE, 1998. **86**(11): p. 2278-2324.

[37]   Arel, I., D.C. Rose, and T.P. Karnowski, *Deep machine learning-a new frontier in artificial intelligence research.* IEEE computational intelligence magazine, 2010. **5**(4): p. 13-18.

[38]   Hinton, G.E., et al., *Improving neural networks by preventing co-adaptation of feature detectors.* arXiv preprint arXiv:1207.0580, 2012.

[39]   Kingma, D.P. and J. Ba, *Adam: A method for stochastic optimization.* arXiv preprint arXiv:1412.6980,   2014.

Can we use departure from natural co-variance relationships for monitoring of offshore carbon storage integrity?

Gennadi Lessin*, Yuri Artioli, Jorn Bruggeman, Jerry Blackford

Plymouth Marine Laboratory, Plymouth PL13DH, UK

Abstract

Carbon capture with offshore storage may take place at various geographical locations, characterized by diverse physical and biogeochemical properties and dynamics of the overlying water. In order to ensure storage integrity, baseline conditions must be carefully assessed for each potential storage area, which will allow design and deployment of optimal monitoring and sampling programs and establish appropriate site-specific criteria for anomaly detection, to allow timely reaction and necessary remedial measures.

Within this paper, we assess applicability of using outputs of coupled hydrodynamic-biogeochemical models for the selection of appropriate variables to describe baseline variability and, consequently, strategies for the following monitoring. Via application of multivariate linear regression we identify combinations of modelled variables that best predict variability in pCO_2 at a location corresponding to the potential storage site at Goldeneye Field in the Central North Sea. Although some variable pairs better predict pCO_2 variability, we focus on a combination of oxygen saturation and silicate, as variables that can potentially be frequently and accurately monitored over long periods. In this work we employ highly simplified leakage scenarios to highlight the accuracy of baseline characterization and implications for establishment of thresholds for anomaly detection in highly dynamic marine environments. We conclude that hydrodynamic-biogeochemical models are invaluable tools for informing cost-effective monitoring strategies regarding the optimal number and combination of parameters surveyed and for establishing appropriate anomaly criteria for each potential storage location.

Keywords: Carbon capture and storage, baseline monitoring, leak detection, ecosystem modelling, ERSEM, multivariate regression

1. Introduction

Carbon capture with offshore storage may take place at various geographical locations, characterized by diverse physical and biogeochemical properties and dynamics of the overlying water. Baseline conditions, including any periodic (e.g. seasonal) and episodic (e.g. due to lateral advection) temporal variability, must be carefully assessed for each potential storage area, which will allow design and deployment of optimal monitoring programs for storage integrity [1]. Baseline characterization is also a necessary prerequisite for establishing appropriate site-specific criteria for anomaly detection that would ensure timely reaction and appropriate remedial measures.

---

* Corresponding author. Tel.: +441752633429; fax: +441752 633 101.
 E-mail address: gle@pml.ac.uk

Using covariance between the partial pressure of CO_2 (pCO_2) and the saturation of dissolved oxygen in seawater to characterize baseline conditions has been proposed previously, and several options to establish thresholds for anomaly detection have been discussed [2, 3]. In terrestrial systems departure from rigid co-variance relationships of a few easily measurable variables provides natural baseline and has been successfully implemented to indicate anomalies which may result from a CO_2 release [4]. However, dynamic and diverse nature of marine environments hinders our ability to establish thresholds universally valid at different locations and time instances.

Thorough characterization of any marine region requires simultaneous assessment of many variables over a sufficiently long time period, which is usually a costly and time consuming task. However, coupled hydrodynamic-ecosystem models set up for an area of interest, can produce a high amount of data at appropriate spatial and temporal resolution, allowing description of the system at a level of detail not attainable with traditional sampling techniques. Therefore, modelling products carefully validated against observational data can be particularly applicable for the selection of appropriate variables to describe baseline variability and, consequently, establish optimal monitoring strategies.

To test the applicability of models for this task, in this pilot study we applied simulation outputs of a well-established biogeochemical-ecological model ERSEM for baseline characterization at a potential CCS site in Central North Sea. Building and expanding on previous approaches, we test if co-variance of pCO_2 with two variables could lead to improved accuracy of baseline description and, consequently, anomaly detection.

2. Model description

For the purpose of our study we use the coupled hydrodynamic-biogeochemical modelling suite NEMO-FABM-ERSEM configured on the Atlantic Meridional Margin (AMM7) domain, which extends from 20°W to 13°E and 40°N to 65°N, and has a horizontal resolution of 1/15 of a degree in latitudinal and 1/9 of a degree in longitudinal direction, corresponding to ~7 km. Vertically, the model is resolved into 50 sigma layers. The model is initialized in 1981 and is forced with ERA interim reanalysis of European Centre for Medium-Range Weather Forecasts [5].

ERSEM (Fig. 1) is a generic model of marine biogeochemistry and the ecosystem dynamics of the lower trophic levels. ERSEM simulates planktonic and benthic parts of the marine ecosystem and includes the cycles of the major chemical elements of the ocean (carbon, nitrogen, phosphorus, silicate, and iron), the microbial food web, a sub-module for the carbonate system, calcification, and a full benthic model [6].

For the purpose of this study, time-series of near-bottom daily mean modelled variables covering a 10-year period (01.01.2000-31.12.2009), at a location corresponding to the potential CCS site at Goldeneye Field in the Central North Sea (58.00°N, 0.35°W, depth ~120 m), were extracted from the model.
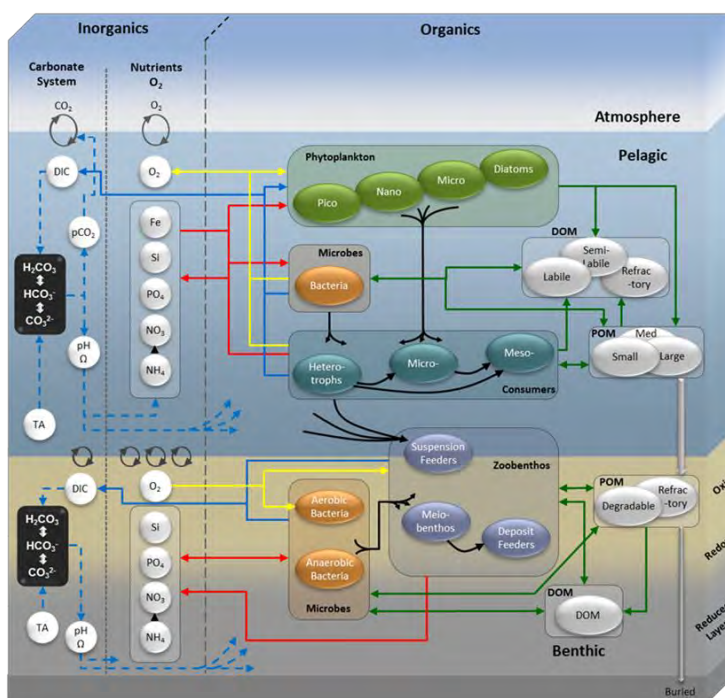
Figure 1. Conceptual diagram of ERSEM

3. Results and discussion

3.1. Baseline characterization

Time-series of near-bottom pCO_2 (Fig. 2, blue line) show distinct seasonal variability: high values are typical in autumn, while low values during winter (maximum range 165.6 µatm). Steady build-up of pCO_2 in the near-bottom waters during the course of a year is fuelled by mineralization of sedimented organic matter (OM), while abrupt decline is caused by breakup of water column stratification. Despite similarity in general seasonal pattern, there is a considerable degree of inter-annual variability caused by interplay of physical and biogeochemical dynamics.

As a first step towards baseline characterization, we establish which variables are best at explaining variability of pCO_2 in the near-bottom layer of the model (Table 1). While oxygen saturation explains 43.4% of variability in pCO_2, inorganic nutrients – phosphate, nitrate and silicate, explain 55.7, 59.5 and 68.9% of variability, respectively. Inorganic nutrients tend to follow pCO_2 dynamics (positive correlation), as they are released into near-bottom water following degradation of sedimented OM, and are consecutively mixed up with the breakdown of stratification. Strong correlation with silicate (0.83) is indicative of substantial contribution of diatoms to benthic OM, while stronger correlation with nitrate than with ammonium suggests high nitrification activity within our study area.
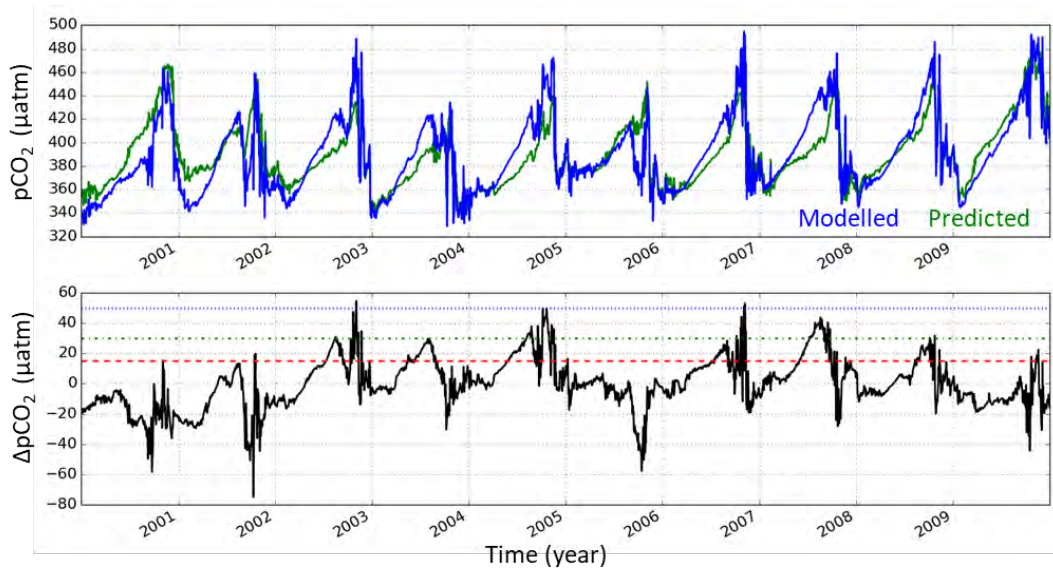
Table 1. Variables exerting strongest correlation with pCO_2 in the model

Variable	Variability explained (%)
Pelagic bacteria	41.4
Oxygen saturation	43.4
Phosphate	55.7
Nitrate	59.5
Silicate	68.9

Table 2. Pairs of variables exerting strongest correlation with pCO_2 in the model

Variable 1	Variable 2	Variability explained (%)
Porewater ammonium	Bacteria	72.1
Bacteria	Silicate	72.2
Oxygen saturation	Silicate	72.3
Total organic carbon	Silicate	72.3
Ammonium	Bacteria	74
Meiofauna	Bacteria	75
Porewater nitrate	Bacteria	78.2
Porewater oxygen	Bacteria	79.1

Following this initial model-based finding that near-bottom inorganic nutrients can be better indicators than oxygen saturation for baseline characterization at our study area, we test if regression using combination of two variables to explain variability in pCO_2 can lead to further improvement in accuracy. For this purpose, correlations of modelled time-series of pCO_2 with combinations of two other variables were calculated. Table 2 shows pairs of variables that explain variability in pCO_2 better than any single variable tested. Pelagic bacteria or silicate in combination with other variables were found to be the best predictors of pCO_2 variability, with porewater oxygen - pelagic bacteria combination explaining 79.1% of variability. However, since our aim is to inform monitoring programs, it is rational to establish a baseline based on a combination of variables that can be easily, frequently and cost-effectively monitored over long periods of time. Recent first deployments of *in situ* silicate sensors showed good results and demonstrated great potential [7].Therefore in the following examples we focus on combination of silicate concentration and oxygen saturation, which explain 72.3% of variability in pCO_2 in the model (Fig. 2, green line).

Figure 2. Time-series of modelled and predicted near-bottom pCO_2 (upper panel) and their difference (lower panel)

Applied for anomaly detection, maintenance of correlation between predicted and modelled (observed) pCO_2 at any point in time would lead to some level of confidence of storage integrity. Increase in modelled (observed) compared to predicted pCO_2 above certain threshold (ΔpCO_2) could thus indicate a possibility of leakage. Notably, however, the difference between modelled and predicted values is not constant due to high variability of the system (Fig 2, black line), which will have implication for anomaly detection. Here we test a selection of constant detection thresholds (Table 3). A threshold of 15 µatm was often exceeded in summer-autumn months; a higher threshold of 30 µatm was exceeded less often, while a difference higher than 50 µatm was observed only 1% of a time in November. This implies that more stringent thresholds will increase probability of false leakage detection, especially during summer-autumn period. On the other hand too high threshold can leave leaks of lower intensity undetected.

Table 3. Detection of false leaks (% of time per months) for selected thresholds.

Threshold	Jan	Feb	Mar	Apr	May	June	July	Aug	Sept	Oct	Nov	Dec
15	0.3	0	0	0	5.5	27.3	41.9	54.2	34	28.7	17	0
30	0	0	0	0	0	0	7.4	18.4	4.7	12.3	7.3	0
50	0	0	0	0	0	0	0	0	0	0	1	0

3.2. Simplified leak scenarios

To illustrate the potential of multivariate baseline characterization for anomaly detection, and to highlight implications of natural variability of the system on the choice of detection thresholds, we applied highly simplified leakage scenarios to the modelled pCO_2 time-series, where concentrations are increased by 10% either every June or every October. For simplicity, thresholds of 15, 30 and 50 µatm difference between modelled (observed) and predicted pCO_2 were assessed initially.

In case of June leaks (Fig. 3), background pCO_2 is usually high and increasing steadily, so a further 10% increase is clearly noticeable. In October, however, background conditions are highly variable (Fig. 4), and contribution of 10% increase can be either clearly manifested (e.g. in 2002, 2004) or almost undetectable (e.g. in 2000 and 2005). This has direct implications for detection levels (Table 4): a more stringent 15 µatm threshold allows detection of leaks in June 99% of the time, but only 81% in October with its high inter-annual variability. Higher threshold of 30 µatm allows to detect leaks in June 79.7%, and in October 61.3% of the time. In case of 50 µatm threshold, leaks in June and October can be detected 46 and 40.6% of the time, respectively. At other times (i.e. period without imposed leakage), the more stringent thresholds would lead to increase in detection of false leaks (e.g. for 15 µatm 16.6 and 16.5% for June and October scenarios, respectively), as a consequence of natural system variability and accuracy of prediction metric.

Table 4. Detection of true positives (TP) and false positives (FP) for each scenario

	Hypothetical leak			
	June		October	
Threshold	%TP	%FP	%TP	%FP
15	99.0	16.6	81.3	16.5
30	79.7	4.6	61.3	3.5
50	46.0	0.1	40.6	0.1

Figure 3. Modelled pCO$_2$ with 10% increase each June (blue lines) and predicted pCO$_2$ (green line)

Figure 4. Modelled pCO$_2$ with 10% increase each October (blue lines) and predicted pCO$_2$ (green line)

This trend of increased frequency of true leak detection with consecutively smaller thresholds is illustrated on Fig. 5 for both June and October cases. Concurrently, however, increases the frequency of false leak detections. From the perspective of monitoring of site integrity and preparedness for mitigation, a threshold which minimizes false positives and maximizes detectability of true positive is required. Optimal threshold selection will thus be

dictated by accuracy of baseline description as well as by acceptable frequency of false positives, in particular in terms of costs of undertaking confirmation monitoring in the case of a false leak prediction.

Figure 5. Detectability of true and false leaks (%) for comprehensive range of thresholds

4. Conclusions

Model results have shown that due to high environmental variability, strong correlation between near-bottom pCO_2 and dissolved oxygen proposed as a storage site integrity criterion ear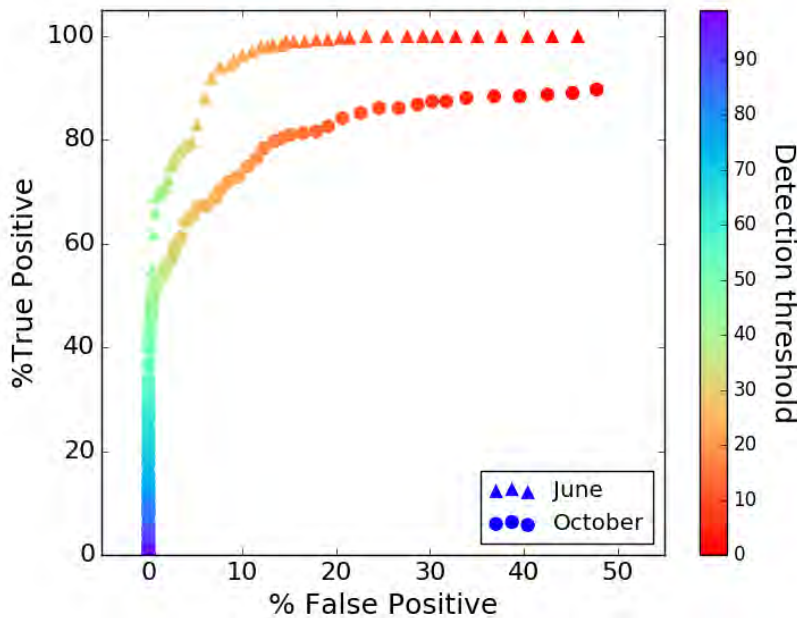lier [2, 3], is not the best descriptor of baseline conditions for our study area, where correlation with inorganic nutrients is stronger. To assist with selection of optimal number of monitoring parameters for baseline monitoring, we applied multivariate linear regression to identify combinations of variables that best predict local variability in pCO_2. Concentrating on variables that are relatively easily measured on a long-term basis, our results suggest using a combination of oxygen saturation and silicate concentration to explain variability of pCO_2 with high accuracy. Further tests showed that only slight improvement in accuracy of baseline description could be achieved when using a combination of three rather than two variables (not shown), which suggests that long-term monitoring of a limited set of variables with high frequency might be sufficient for baseline characterization. Clearly, due to strong dynamic nature and diversity of physical and biogeochemical conditions, combinations of different variables will be identified as optimal for different locations.

Compared to multivariate characterization in terrestrial environment, which uses fixed gas composition in the atmosphere as a starting point to baseline description and anomaly detection [4], rigid relationships are not characteristic for marine environments. Therefore using models has a clear advantage in terms of spatial and temporal coverage, as well as large number of variables. However, model accuracy in reproducing each modelled process, as well as representation of different areas (e.g. coastal zone) can vary, which requires attention. ERSEM configuration applied for our study does not include parameterizations of methane dynamics, which could be used to explain increase in pCO_2 due to oxidation processes within sediments.

In this study we introduced a method to detect baseline conditions for offshore storage sites based on covariance of several variables with observed pCO_2. Simplified leak scenarios were used merely to illustrate the accuracy of

baseline description and highlight variability of the marine environment. We intend to expand this work in the future by comparing several contrasting sites and propose generic method for establishing detection thresholds.

Our main conclusion is that hydrodynamic-biogeochemical models are invaluable tools for informing cost-effective monitoring strategies on optimal number and combination of parameters surveyed and for establishing appropriate anomaly criteria for each potential storage location.

Acknowledgements

References

[1] Blackford J, Bull JM, Cevatoglu M, Connelly D, Hauton C, James RH, Lichtschlag A, Stahl H, Widdicombe S, Wright IC. Marine baseline and monitoring strategies for carbon dioxide capture and storage (CCS). International Journal of Greenhouse Gas Control. 2015; 38:221-9.

[2] Uchimoto K, Kita J, Xue Z. A novel method to detect CO2 leak in offshore storage: focusing on relationship between dissolved oxygen and partial pressure of CO2 in the sea. Energy Procedia. 2017; 114:3771-7.

[3] Uchimoto K, Nishimura M, Kita J, Xue Z. Detecting CO 2 leakage at offshore storage sites using the covariance between the partial pressure of CO 2 and the saturation of dissolved oxygen in seawater. International Journal of Greenhouse Gas Control. 2018; 72:130-7.

[4] Romanak KD, Bennett PC, Yang C, Hovorka SD. Process-based approach to CO2 leakage detection by vadose zone gas monitoring at geologic CO2 storage sites. Geophysical Research Letters. 2012; 39(15)

[5] Dee DP, Uppala SM, Simmons AJ, Berrisford P, Poli P, Kobayashi S, Andrae U, Balmaseda MA, Balsamo G, Bauer DP, Bechtold P. The ERA-Interim reanalysis: Configuration and performance of the data assimilation system. Quarterly Journal of the royal meteorological society. 2011; 137(656):553-97.

[6] Butenschön M, Clark J, Aldridge JN, Allen JI, Artioli Y, Blackford J, Bruggeman J, Cazenave P, Ciavatta S, Kay S, Lessin G. ERSEM 15.06: a generic model for marine biogeochemistry and the ecosystem dynamics of the lower trophic levels. Geoscientific Model Development. 2016; 9(4):1293-339.

[7] Barus C, Chen Legrand D, Striebig N, Jugeau B, David A, Valladares M, Munoz Parra P, Ramos ME, Dewitte B, Garçon V. First Deployment and Validation of in Situ Silicate Electrochemical Sensor in Seawater. Frontiers in Marine Science. 2018; 5:60.

Simplified modeling as a tool to locate and quantify fluxes from CO$_2$ seep to marine waters

[a]Anna Oleynik[*], [a]Kristian Gundersen, [a]Guttorm Alendal,
[a]Hans J. Skaug, [b]Mårten Gullliksson, [c]Helge Avlesen, [a]Jarle Berntsen,
[d]Jeremy Blackford, [d]Pierre Cazenave

[a]*Department of Mathematics, University of Bergen, Bergen, N-5020, Norway*
[b]*School of Science and Technology, Örebro University, Örebro, SE-701 82 Sweden*
[c]*Uni Research, Bergen, N-5020, Norway*
[d]*Plymouth Marine Laboratory, Prospect Place, Plymouth, PL1 3DH, UK*

Abstract

An adequate monitoring program will be an intrinsic part of all CO$_2$ storage projects, as required by regulations. This program must involve a surface monitoring component in addition to the subsurface methods. Should anomaly be detected, the monitoring program enters the costly confirmation modus, i.e., surveys to localize or dispel suspicion of an ongoing seep. Inverse methods applied to the tracer transport equation, using proper current statistics, are demonstrated here as a valuable tool to make predictions on where a seep might be located, and the flux associated with the source. The framework can be updated as new measurements are being collected.

Keywords: CO$_2$ seep localization; CCS; marine monitoring; inverse problems; Bayesian methods.

1. Introduction

Monitoring the injection formation with geophysical monitoring technologies, assuring that the injected CO$_2$ behaves as expected and to detect any CO$_2$ migrating out of the formation, will be the backbone of the monitoring program for offshore CO$_2$ storage projects [1,2]. We argue that monitoring of the surface for any unexpected seeps of CO$_2$ and other substances, as indications of a leak, are necessary in order to comply with the regulations, see [3].

Since the storage site must be monitored for a long period of time after injection is stopped, and the area in which migrating CO$_2$ might reach the seafloor is large, the marine monitoring program will impose additional costs and challenges to the storage project [4–6].

Environmental changes, e.g. changes in bottom fauna or in the pelagic ecosystem [7,8], detection of bubbles from ship sonars [9,10], or elevated concentration of dissolved gases [11–15], can be used as indicators of marine gas releases. However, the real challenge is the high variability of the marine environment, both in current conditions [16] and in biochemical activities [13,17]. Hence environmental monitoring poses new challenges compared to the

---

* Corresponding author. Tel.: +47 55 58 47 91; fax: +47 55 58 28 38
E-mail address: anna.oleynik@uib.no

classical environmental monitoring procedures developed during decades of offshore petroleum activities.

Communicating CCS monitoring for assuring purposes might be challenging [18] and even the successful history of offshore oil and gas exploration give no guarantee for public acceptance, [19]. Tools are under development for assessing the total environmental stress imposed on the oceans, e.g. Cumulative Effects Assessments in view of Marine Spatial Planning and ecosystem services framework [20–22]. The monitoring program also have a role in communicating risks and benefits for storage projects and assures against unjustified accusations for having adverse environmental effects [23].

Studies on how to design monitoring programs for detecting a seep, incorporating the natural variabilities, for fixed installations have been performed in [24–27] and for Autonomous Underwater Vehicles (AUV) [28]. It is a challenge to quantify the uncertainties involved, and how to make a decision on upscaling to the confirmation phase based on available data [29]. These studies have to rely on simulated data, both for the environmental baseline and predictions on the signature from a seep of stored CO_2 to the water column. The European Union funded project STEMM-CCS (http://www.stemm-ccs.eu) addresses procedures on how to obtain a proper environmental baseline. The role of numerical modelling in this context is summarized in [30]. A combination of measurements and model predictions is also necessary for utilizing machine learning techniques as a tool to analyse time series from the monitoring [31].

Here we address how times series from the monitoring program, together with a reduced transport equation, can assist in giving estimates of the location and rate of seeps through the seafloor. We present two approaches using the velocity field generated by the Bergen Ocean Model (BOM) as reported in [15].

2. Methods and results

The field of inverse problems has a long history in mathematics and engineering providing tools for estimating parameters in a model given some measured quantities, see [32]. In the classical settings, the goal is to find the optimal set of the parameters that minimize a cost function, which typically measures the distance from the model solution to the observations. In the case of point-leak scenarios, the locations and intensities of the sources are the desired unknown model parameters. The minimization of the cost function is performed by using an iterative method such as, e.g., a gradient descent search where the parameters are updated in every iteration.

In recent years, the Bayesian formulation of inverse problems has become more popular partially due to growing available computing resources, see [33]. Compared to the classical approach, the parameters are not deterministic but considered to be random variables whose probability distribution (posterior distribution) we would like to obtain based on the observations, an underlying model and a-priori information. In order to single out the representative parameter values one could for example identify the maximum-a-posteriori estimate (MAP) of the posterior distribution. Under some assumptions on the error distributions and prior information, the two approaches coincide.

Both approaches however rely on being able to perform simulations of the underlying model multiple times. The transport of CO_2 in the ocean is typically modelled using general circulation models with additional balance equations for tracers, such as CO_2. These models are computationally demanding and often require supercomputers. In particular, using a grid resolution better than 1 km, a single realization of a period of a few months can require more than a 100 000 simulation hours. This makes it practically impossible to use the general circulation model for the above mentioned approaches.

However, under the assumption that CO_2 is a passive tracer, i.e. the CO_2 concentration does not influence on seawater density, the advection-diffusion equation and the ocean dynamics model have only one-directional coupling. This allows us to use velocity fields obtained from ocean circulation models as input to the advection-diffusion model, reducing the computational cost enough to use classical optimization methods to minimize a cost function or a Markov Chain Monte Carlo method for sampling from a posterior distribution. The advection-diffusion model can also be used to create various leak scenarios, e.g. different locations and fluxes, including time varying fluxes, to add scenarios to the data sets needed for other methods of analysis [31].

Let $c(x, t)$ be the concentration of a contaminant at the position x and time t. Knowing the water flow in the area of interest Ω and the diffusivity of the contaminant, transport of the contaminant in the ocean environment can be

described by the advection-diffusion equation

$$\frac{\partial c}{\partial t} = D \, \Delta \, c - w \cdot \nabla c + f, \; x \in \Omega, t \in [0, T],$$ (1)

with some appropriate boundary and initial conditions. Here Ω is a bounded connected domain in $\boldsymbol{R}^n$, $w = w(x, t) \in \boldsymbol{R}^n$ $(n = 2,3)$ is a divergence free velocity field that describes the water flow, and D is a diffusion coefficient. The source term $f(x, t)$ is assumed to be in the form

$$f(x, t) = \sum_{j=1}^{N_s} q_j \, \delta(x - \xi_j),$$ (2)

where δ is the n-dimensional Dirac -delta function, ξ_j are the source locations and a_j are the corresponding intensities.

In applications, the point sources ξ_i are substituted by small regions around ξ_i which amounts to replacing $\delta(x - \xi_j)$ with functions of small support. Thus, the $\delta(x - \xi_j)$ can be viewed as a limiting case of a point source.

To advect the concentration $c(x, t)$ forward in time, it is important to apply a numerical scheme that is gradient preserving to capture possible sharp fronts. At the same time, the advection schemes need to be monotonic to avoid artificial over- and undershooting, see [34,35]. The BOM, see [36,37], has been used to compute the velocity field $w(x, t)$ [15]. It applies a monotonic TVD (Total Variance Diminishing) scheme with a superbee limiter for advection, see the test of advection schemes in [38].

Assuming that the time series of the CO_2 concentration is available at M different locations $\{\chi_1, \ldots \chi_M\}$ and is cleaned from natural variability (with some error), we would like to estimate the location of leaks and their intensity. To be more strict, let $\boldsymbol{\theta}$ be the vector of all unknown parameters q_j and ξ_j, see in (2), and the data is given as $d_{mk} = c(\chi_m, t_k; \boldsymbol{\theta}_{true}) + error, k = 1, \ldots, K$. Then our goal is to minimize the difference between the data and the model predictions, i.e.,

$$J(\boldsymbol{\theta}) = \sum_{m,k} (c(\chi_m, t_k; \boldsymbol{\theta}) - d_{mk})^2 \rightarrow min,$$

such that $\boldsymbol{\theta}$ satisfies some constraints, that is, $\xi_j \in D \subset \Omega$ and $q_j \geq 0$.

The fact that, not only the location and intensity but also, the number of leaks are unknown substantially complicates the problem. In order to deal with this complication we simplify the model even further. We fix all the possible leak locations $x_1, \ldots, x_N, N \geq N_s$, see Fig.1 (left), and then simulate one leak at a time with fixed intensity which we set, without loss of generality, to one. That is, we obtain $c_1(x, t), \ldots, c_N(x, t)$, as the solutions of (1) with $f = \delta(x - x_i), i = 1, \ldots, N$, see example in Fig.1 (right). Since the advection-diffusion model is linear, any solution to (1)-(2) is given as a linear combination

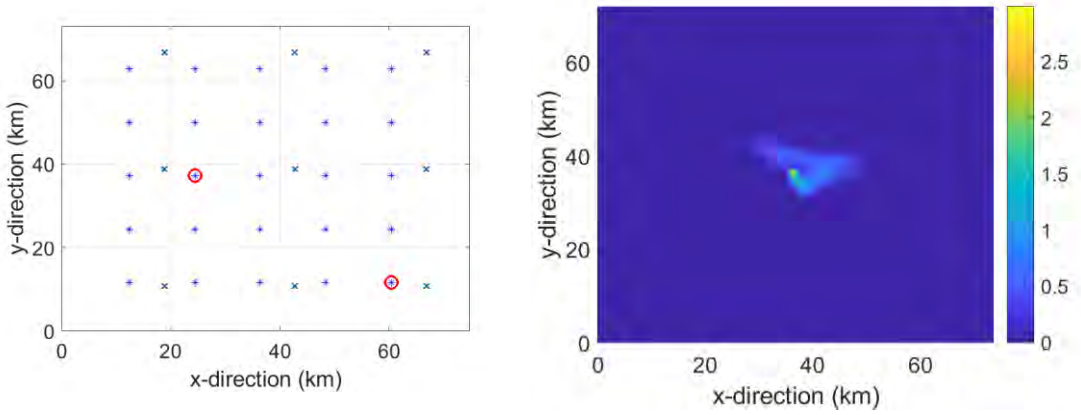$$c(x, t; \boldsymbol{a}) = \sum_{i=1}^{N} a_i \, c_i(x, t),$$ (3)

Fig. 1. (Left) The studied domain with potential seep locations, stars, measurement points, crosses, and the locations of the two seeps, red circles; (Right) Snapshot of the concentration at the central location, $c_{13}(x,t)$, at $t = 100h$.

where $\boldsymbol{a} = (a_1, \ldots, a_N)$, and $a_i = 0$ if the corresponding leak location x_i is inactive, and $a_i = q_j$ if $x_i = \xi_j$. Note that $\boldsymbol{a}$ is dimensionless as, formally, $a_i = q_j/1$. We assume in this paper that the list of all possible leak locations is complete and the two models are equivalent.

Here we use a deterministic and a Bayesian approach, using a Hamiltonian Monte Carlo (HMC) sampling [39], to estimate the parameters $\boldsymbol{a}$. Obviously, the number of sensors and their placement affects the solution outcome as it is possible that the data does not capture the signal of one or several possible leaks. The placement of sensors is an important and difficult problem than can be addressed in an extension of this work.

In the deterministic case, we can easily reformulate the problem as linear least squares problem with constrains

$$\min_{\boldsymbol{a}} \parallel \boldsymbol{Ca} - \boldsymbol{d} \parallel^2, \ \boldsymbol{C} \in \boldsymbol{R}^{MK \times N}, \boldsymbol{d} \in \boldsymbol{R}^{MK}$$
$$s.t. \, \boldsymbol{0} \leq \boldsymbol{a} \leq \boldsymbol{a}_{max}. \tag{4}$$

However, solution to the problem above does not contain information about uncertainties. Therefore, we also use a Bayesian approach. Using Bayes theorem we define the probability density function for $\boldsymbol{a}$ given the data $\boldsymbol{d}$ as

$$p(\boldsymbol{a}|\boldsymbol{d}) = C_p p(\boldsymbol{d}|\boldsymbol{a}) p(\boldsymbol{a}),$$

where $p(\boldsymbol{d}|\boldsymbol{a})$ and $p(\boldsymbol{a})$ are the likelihood function and prior density, respectively, and C_p is a normalization constant. For independent unbiased normally distributed measurement errors we have

$$p(\boldsymbol{d}|\boldsymbol{a}) \propto \exp\left(-\frac{1}{2}(\boldsymbol{Ca} - \boldsymbol{d})^T \boldsymbol{\Sigma}^{-1}(\boldsymbol{Ca} - \boldsymbol{d})\right),$$

where $\boldsymbol{\Sigma}$ is a diagonal covariance matrix of the noise introduced in $\boldsymbol{d}$, if the elements of the noise vector are independent. Otherwise $\boldsymbol{\Sigma}$ is a positive definite symmetric matrix.
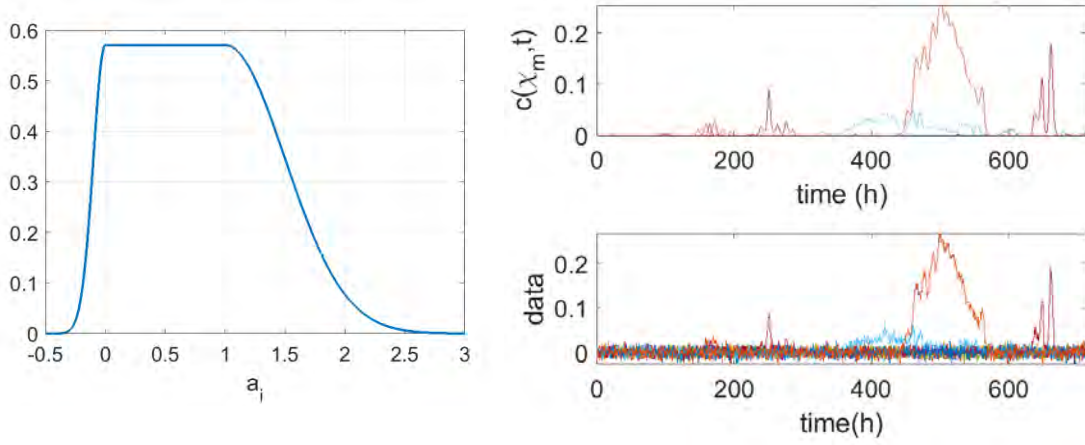

Fig. 2. (Left) Assumed prior for the flux rates $p(a_i)$; (Right) The time series of concentration at nine considered locations without (upper panel) and with (lower panel) added Gaussian noise.

The prior, here $p(\boldsymbol{a}) \propto \prod_{i=1}^{N} p(a_i)$, should incorporate a-priori information on the leaks and their intensities. To mimic the constrains in (4) we choose $p(a_i)$ as in Fig.2 (left). Finally, a series of sampling methods could be used to sample from the posterior probability density $p(\boldsymbol{a}|\boldsymbol{d})$. Their efficiency could vary depending on the problem.

For the numerical example we used the velocity fields from the 800 meters resolution BOM simulation on a 72.8×74.4 squared kilometers domain centered at Sleipner A (1.94 E 58.36 N), see [15]. For simplicity we considered only the bottom layer, that is, $n = 2$.

We choose 25 potential leak locations indicated by blue stars in Fig.1(left) numbered column-wise starting from the bottom left one. In Fig.1 (right) one can see the snapshot of the leak #13 with intensity $a_{13} = 1$ at $t = 100h$. Sensors were placed at nine different locations, blue crosses in Fig.1(left). Active seeps were chosen to be at #8 and #21 with intensities $a_8 = 0.3$ and $a_{21} = 0.8$, respectively. For this set up, the time series $c(\chi_i, t)$ are plotted in the upper panel of Fig.2 (right), the lower panel is similar but with Gaussian noise added. In Fig.3 we have plotted the results of both constrained least squares method (3) with $\boldsymbol{a}_{max} = 2$ and the Bayesian approach. The black circles are the solutions of the former approach and are in the excellent agreement with the real solution, in particular, $\max|\boldsymbol{a}_{estimated} - \boldsymbol{a}_{true}| = 0.0047$. The central red mark in Fig.3 indicates the median, the bottom and top edges of the box indicate the 25th and 75th percentiles, respectively, for the Bayesian method. The whiskers extend to the most extreme points, not considered outliers. While all a_i are supposed be nonnegative, the negative values of a_i here are consistent with the noise introduced. For this method $\max|\boldsymbol{a}_{median} - \boldsymbol{a}_{true}| = 0.0475$ and $\max|\boldsymbol{a}_{MAP} - \boldsymbol{a}_{true}| = 0.0065$, where $\boldsymbol{a}_{MAP}$ is the MAP of the log probability density $p(\boldsymbol{a}|\boldsymbol{d})$ obtained by the limited memory Broyden-Fletcher-Goldfarb-Shanno quasi-Newton optimizer, see [40]. We do not plot $\boldsymbol{a}_{MAP}$ as it is almost not distinguishable from the least squares and true solutions. The two active seeps are in locations #8 and #21, correctly predicted by both methods

3. Discussion

Obviously, a solution to (3) is only an approximation of a solution to (1)-(2) if the possible leak locations are not fully known. In this case, the positions and number of possible leaks could be chosen such that the model error in (3) is sufficiently small, and then further reduced by refining the position set-up iteratively. The Bayesian approach could further be used to design the efficient sensors layout and to optimize the AUV search path.
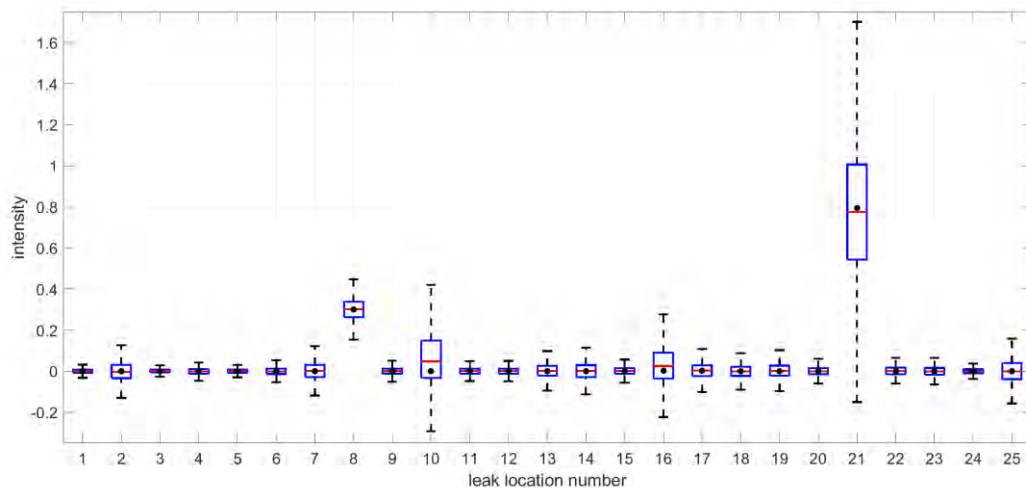
Fig. 3. Box plot of HMC sampling and the least squares estimate (circles). The central red mark indicates the median, the bottom and top edges of the box indicate the 25th and 75th percentiles. The whiskers extend to the extreme points, not considered outliers.

The lack of data due to, e.g., inefficient sensors layout, would lead to an under-determined system in (4). This issue could be solved by introducing a regularization term, e.g., Lasso. The regularization term could be incorporated to the prior $p(a)$ as well to obtain a similar solution. We would like to emphasize however, that the Bayesian approach with a proper choice of prior could allow a better judgment regarding the quality of the data.

Acknowledgements

References

[1] Lien, M. (2013). Simultaneous joint inversion of amplitude-versus-offset and controlled-source electromagnetic data by implicit representation of common parameter structure. Geophysics *78*, ID15–ID27.

[2] Strickland, C.E., Vermeul, V.R., Bonneville, A., Sullivan, E.C., Johnson, T.C., Spane, F.A., and Gilmore, T.J. (2014). Geophysical monitoring Methods Evaluation for the FutureGen 2.0 Project. Energy Procedia *63*, 4394–4403.

[3] Dixon, T., McCoy, S.T., and Havercroft, I. (2015). Legal and regulatory developments on CCS. International Journal of Greenhouse Gas Control *40*, 431–448.

[4] Oldenburg, C.M., and Lewicki, J.L. (2006). On leakage and seepage of CO_2 from geologic storage sites into surface water. Environmental Geology *50*, 691–705.

[5] Blackford, J., Bull, J.M., Cevatoglu, M., Connelly, D., Hauton, C., James, R.H., Lichtschlag, A., Stahl, H., Widdicombe, S., and Wright, I.C. (2015). Marine baseline and monitoring strategies for carbon dioxide capture and storage (CCS). International Journal of Greenhouse Gas Control *38*, 221–229.

[6] Blackford, J., Artioli,Y., Clark, J., and Mora, L.(2017). Monitoring of offshore geological carbon storage integrity: Implications of natural variability in the marine system and the assessment of anomaly detection criteria. International Journal of Greenhouse Gas Control *64*, 99–112.

[7] Wegener, G., Shovitri, M., Knittel, K., Niemann, H., Hovland, M., and Boetius, A. (2008). Biogeochemical processes and microbial diversity of the Gullfaks and Tommeliten methane seeps (Northern North Sea). Biogeosciences Discussions *5*, 971–1015.

[8] Blackford, J.C., Widdicombe, S., Lowe, D., and Chen, B. (2010). Environmental risks and performance assessment of carbon dioxide (CO_2) leakage in marine ecosystems. In Developments and Innovation in Carbon Dioxide (CO_2) Capture and Storage Technology, Volume 2, Carbon Dioxide (CO_2) Storage and Utilisation. (Woodhead Publishing Limited), pp. 344–373.

[9] Brewer, P.G., Chen, B., Warzinki, R., Baggeroer, A., Peltzer, E.T., Dunk, R.M., and Walz, P. (2006). Three-dimensional acoustic monitoring and modeling of a deep-sea CO_2 droplet cloud. Geophysical Research Letters *33*, 5.

[10] Noble, R.R.P., Stalker, L., Wakelin, S.A., Pejcic, B., Leybourne, M.I., Hortle, A.L., and Michael, K. (2012). Biological monitoring for carbon capture and storage a review and potential future developments. International Journal of Greenhouse Gas Control *10*.

[11] Alendal, G., and Drange, H. (2001). Two-phase, near-field modeling of purposefully released CO_2 in the ocean. Journal of Geophysical

Research *106*.

[12] Drange, H., Alendal, G., and Johannessen, O. (2001). Ocean release of fossil fuel CO2: A case study. Geophysical Research Letters *28*, 2637–2640.

[13] Botnen, H., Omar, A., Thorseth, I., Johannessen, T., and Alendal, G. (2015). The effect of submarine CO_2 vents on seawater: Implications for detection of subsea Carbon sequestration leakage. Limnology and Oceanography *60*.

[14] Vielstädte, L., Karstens, J., Haeckel, M., Schmidt, M., Linke, P., Reimann, S., Liebetrau, V., Mcginnis, D.F., and Wallmann, K. (2015). Quantification of methane emissions at abandoned gas wells in the Central North Sea. Marine and Petroleum geology.

[15] Ali.,A, Frøysa, H.,Avelsen, H., and Alendal, G. (2016). Simulating spatial and temporal varying CO_2 signals from sources at the seafloor to help designing risk-based monitoring programs. Journal of Geophysical Research: Oceans *121*, 745–757.

[16] Alendal, G., Berntsen, J., Engum, E., Furnes, G.K., Kleiven, G., and Eide, L.I. (2005). Influence from 'Ocean Weather' on near seabed currents and events at Ormen Lange. Marine and Petroleum Geology *22*, 21–31.

[17] Omar, M.O., Garcia-Ibanez,M.I., and Alendal, G. (2018). C-seep as a stoichiometric tool to distinguish a seep signal from the natural variability.

[18] L'Orange Seigo, S., Wallquist, L., Dohle, S., and Siegrist, M. (2011). Communication of CCS monitoring activities may not have a reassuring effect on the public. International Journal of Greenhouse Gas Control *5*, 1674–1679.

[19] Mabon, L., Shackley, S., and Bower-Bir, N. (2014). Perceptions of sub-seabed carbon dioxide storage in Scotland and implications for policy: A qualitative study. Marine Policy *45*, 9–15.

[20] Jones, D., Beaubien, S., Blackford, J., Foekema, E., Lions, J., Vittor, C.D., West, J., Widdicombe, S., Hauton, C., and Queries, A. (2015). Developments since 2005 in understanding potential environmental impacts of CO_2 leakage from geological storage. International Journal of Greenhouse Gas Control *40*, 350–377.

[21] Intergovernmental Oceanographic Commission of UNESCO, I.-U. the Marine spatial planning programme.

[22] Menegon, S., Depellegrin, D., Farella, G., Sarretta, A., Venier, C., and Barbanti, A. (2018). Addressing cumulative effects, maritime conflicts and ecosystem services threats through msp-oriented geospatial webtools. Ocean Coastal Management *163*, 417–436.

[23] Boyd, A.D., Liu, Y., Stephens, J.C., Wilson, E.J., Pollak, M., Peterson, T.R., Einsiedel, E., and Meadowcroft, J. (2013). Controversy in technology innovation: Contrasting media and expert risk perceptions of the alleged leakage at the Weyburn carbon dioxide storage demonstration project. International Journal of Greenhouse Gas Control *14*, 259–269.

[24] Maeda, Y., Shitashima, K., and Sakamoto, A. (2015). Mapping observations using AUV and numerical simulations of leaked CO_2 diffusion in sub-seabed CO_2 release experiment at Ardmucknish Bay. International Journal of Greenhouse Gas Control *38*, 143–152.

[25] Greenwood, J., Craig, P., and Hardman-Mountford, N. (2015). Coastal monitoring strategy for geochemical detection of fugitive CO_2 seeps from the seabed. International Journal of Greenhouse Gas Control *39*, 74–78.

[26] Hvidevold, H.K., Alendal, G., Johannessen, T., Ali, A., Mannseth, T., and Avlesen, H. (2015). Layout of ccs monitoring infrastructure with highest probability of detecting a footprint of a CO_2 leak in a varying marine environment. International Journal of Greenhouse Gas Control *37*, 274–279.

[27] Hvidevold, H.K., Alendal, G., Johannessen, T., and Ali, A. (2016). Survey strategies to quantify and optimize detecting probability of a CO_2 seep in a varying marine environment. Environmental Modelling and Software *83*, 303–309.

[28] Alendal, G. (2017). Cost efficient environmental survey paths for detecting continuous tracer discharges. Journal of Geophysical Research-Oceans *122*, 5458–5467.

[29] Alendal, G., Blackford, J., Chen, B., Avlesen, H., and Omar, A. (2017). Using Bayes Theorem to Quantify and Reduce Uncertainties when Monitoring Varying Marine Environments for Indications of a Leak. Energy Procedia *114*, 3607–3612.

[30] Blackford J.,Alendal, G., Artioli, Y.,Avlesen,H.,Cazenave, P., Chen, B.,Dale, A., Dewar, M.,Gundersen, K., Haeckel, M., Khajepor, S., Lessin, G., Oleynik, A., Saleem, U., García-Ibáñez, M.I., Omar A.M. (2018). Ensuring efficient and robust offshore storage − the role of marine system modelling, *this issue*.

[31] Gundersen, K., Oleynik,A., Alendal, G., Skaug,H.J., Avlesen, H.,Berntsen,J., Blaser,N., Blackford J.,Cazenave, P. (2018). Ensuring efficient and robust offshore storage − use of models and machine learning techniques to design leak detection monitoring, *this issue*.

[32] Hasanov Hasanoğlu, A., and Romanov V.G. (2017). Introduction to inverse problems for differential equations (Springer International Publishing).

[33] Tarantola, A. (2005). Inverse problem theory and methods for model parameter estimation (Society for Industrial; Applied Mathematics)

[34] Sweby, P. (1984). High resolution schemes using flux limiters for hyperbolic conservation laws. SIAM J. Numer. Anal. *21*, 995–1011.

[35] Haidvogel, D., and Beckmann, A. (1999). Numerical ocean circulation modeling (Imperial College Press).

[36] Berntsen, J. (2000). Users guide for a modesplit σ-coordinate numerical ocean model (Johs. Bruns gt.12, N-5008 Bergen, Norway: Dept. of Applied Mathematics, University of Bergen).

[37] Berntsen, J., Xing, J., and Alendal, G. (2006). Assessment of non-hydrostatic ocean models using laboratory scale problems. Continental Shelf Research *26*, 1433–1447.

[38] Yang, H., and Przekwas, A. (1992). A comparative study of advanced shock-capturing schemes applied to Burgers equation. Journal of Computational Physics *102*, 139–159.

[39] Neal, R.M. (2011). MCMC using Hamiltonian dynamics. In Handbook of Markov Chain Monte Carlo, G. L. J. Steve Brooks Andrew Gelman and X.-L. Meng, eds. (Chapman; Hall/CRC), pp. 113–162.

[40] Nocedal, J., and Wright, S.J. (2006). Numerical optimization second. (New York, NY, USA: Springer).

The stoichiometric C_{seep} method as a tool to distinguish CO_2 seepage signal from the natural variability

A. M. Omar[a]*, M. I. García-Ibáñez[a], and G. Alendal[b]

[a]Uni Research, Bjerknes Centre for Climate Research, Bergen, Norway
[b]University of Bergen, Bergen, Norway

Abstract

For CO_2 Capture and Storage (CCS) technologies to be classified as a climate change mitigation option, an efficient, safe and enduring storage needs to be verified through site-specific monitoring programs, which is required by the international and national regulations. In the case of offshore geological storage, the high spatiotemporal natural variability of seawater CO_2 hampers the interpretation of a seepage signal. Therefore, the characterization of the spatiotemporal natural variability of seawater CO_2 through baseline studies is required when designing an efficient monitoring program.

Here we present a stoichiometric method called C_{seep} for the determination of excess seeped CO_2 dissolved in the water column. The method takes advantage of the fact that the production and consumption of seawater CO_2 by natural process can be predicted from variables that are not impacted by CO_2 seepage. For instance, biological production of CO_2 is always associated with a certain amount of oxygen consumption and nutrient production while CO_2 seepage has no specific effect on oxygen and nutrient levels in seawater. We discuss the applicability of the C_{seep} method as an offshore CCS monitoring tool around the Goldeneye area – a potential offshore CCS site in the Northern North Sea. We also evaluate how the choice of measured parameters influences the sensitivity/accuracy of the C_{seep} calculations. The results (partly preliminary) show that the C_{seep} method clearly minimizes the effect of natural variability on seawater DIC measurements while highlighting the simulated seepage signal. Moreover, C_{seep} values computed using data achievable with autonomous sensors can have an uncertainty similar to C_{seep} values obtained with highly accurate benchtop instrumentation, implying that the method can be fully automated.

Keywords: CCS monitoring; CO_2 seepage; geochemical tracer; C_{seep} method.

1. Introduction

For CO_2 Capture and Storage (CCS) technologies to be categorized as a climate change mitigation option, they have to demonstrate an efficient, safe and enduring storage of CO_2 [e.g., 1,2]. Therefore, monitoring and verification is required at storage sites by national and international regulations [e.g., 3,4,5]. Primary monitoring of storage

---

* Corresponding author. Tel.: (+47) 55584264.
 E-mail address: Abdir.Omar@uib.no

reservoirs is based on seismic techniques imaging CO_2 through the overburden [6]. However, the detection threshold of such techniques may be of the order of 10^3 t CO_2 [6]. Therefore, possible seepage at low levels may not be detected and monitoring for emissions at the surface provides an important secondary monitoring strategy.

Globally many potential CCS storage reservoirs are located offshore [7], and a number of subsea storage demonstration projects are in operation worldwide [8]. Since CO_2 is a naturally occurring gas in seawater, with dynamic concentration in both space and time [e.g., 9,10], and ocean dynamics is highly variant, e.g. due to tides and local conditions [e.g., 11], seeps will generate varying and highly anisotropic signals [12] with concentrations that may be within the range of natural variability of seawater CO_2. Therefore, water column monitoring with the purpose of detecting possible seepage from unknown locations is challenging in many aspects. Environmental changes, e.g. changes in bottom fauna or in the pelagic ecosystems [13,14], bubble detection using ship sonars [15,16], or measurements of elevated concentration of dissolved gases [17,18,19], can be used as indicators of unintended gas releases from the offshore CCS storage. The challenge in detecting seeps using surface monitoring techniques is to be able to distinguish the seepage signal from the "noise" created by the natural variability. Therefore, baseline characterization is crucial to understand which environmental anomalies are associated with natural processes and which are related to CCS seepages, while minimizing the chance for false positives. It is also important to determine what degree of anomaly will mobilize the more expensive confirmation and localization monitoring, i.e., the anomaly threshold.

In the case of concentration-based monitoring, a cost-efficient monitoring design maximizing seep detection also requires the knowledge of seep morphology. Marine system models can simulate a wide variety of "seepage" scenarios, including multi-phase simulations modelling the dynamics of bubble plumes as well as the dissolved phase, and seepage morphology, in particular the nature of flow across the sediment-water interface [e.g., 20,21,22]. Models can also determine the optimal sensor combinations and deployment strategies [7,23]. Baseline statistics and predictions of discharge characteristics proved successful to design cost-efficient deployment of fixed sensors on the seafloor [24,25,26,27] and survey pathway of Autonomous Underwater Vehicles (AUVs) for detecting anomalies in water column CO_2 concentration [28]. However, the design of cost-efficient monitoring for surface detection relies on the definition of anomaly thresholds.

Defining anomaly thresholds for geochemical monitoring of the water column is challenging due to the complexity of the seawater CO_2 system [e.g., 7,9,10]. When CO_2 dissolves in seawater, it reacts with it forming carbonic acid (H_2CO_3), which rapidly dissociates into bicarbonate ions (HCO_3^-; Eq. 1), which in turn can also dissociate into carbonate ions (CO_3^{2-}; Eq. 2) according to the following equilibrium reactions:

$$CO_2 + H_2O \leftrightarrow H_2CO_3 \leftrightarrow HCO_3^- + H^+ \qquad (1)$$
$$HCO_3^- + H^+ \leftrightarrow CO_3^{2-} + H^+ \qquad (2)$$

Natural processes, such as photosynthesis/respiration, biosynthesis/dissolution of calcium carbonate ($CaCO_3$) and changes in temperature and salinity, affect the complex seawater CO_2 system. Therefore, the seawater CO_2 content is highly dynamic in both space and time, thus hampering the discrimination of seepage signals from natural variability signals. Consequently, the ability to detect possible CO_2 seepages from offshore storage requires the characterization of the natural variability of the seawater CO_2 system and its drivers through site-specific baseline studies.

Here we discuss the applicability of the C_{seep} method [29] as a CCS monitoring tool around the Goldeneye area (centered at 58.00°N 0.35°W) – a potential offshore CCS site in the Northern North Sea (Fig. 1). The C_{seep} method minimizes the effect of natural variability on water column DIC measurements, allowing easy detection of CO_2 excess originating from a seepage. The C_{seep} method uses knowledge of the seawater CO_2 system [e.g., 9,10], as well as, the natural processes affecting it. A similar procedure has proved successful to estimate the oceanic uptake of excess CO_2 from the atmosphere [e.g., 30]. The C_{seep} method assumes that there is a nearly constant theoretical background DIC concentration (C_b) in seawater, which is dictated by the history and physical properties of the water, and a fluctuating DIC component (ΔC) governed by natural variability and/or seeps, which is superimposed to the theoretical background so that:

$$C_m = C_b + \Delta C \qquad (5)$$

where C_m is the measured DIC concentration. The ΔC term can be further decomposed into biology-driven variability (ΔC_{bio}), air-sea exchange-driven variability (ΔC_{ase}), mixing-driven variability (ΔC_{mix}) and impact of seeps (C_{seep}).
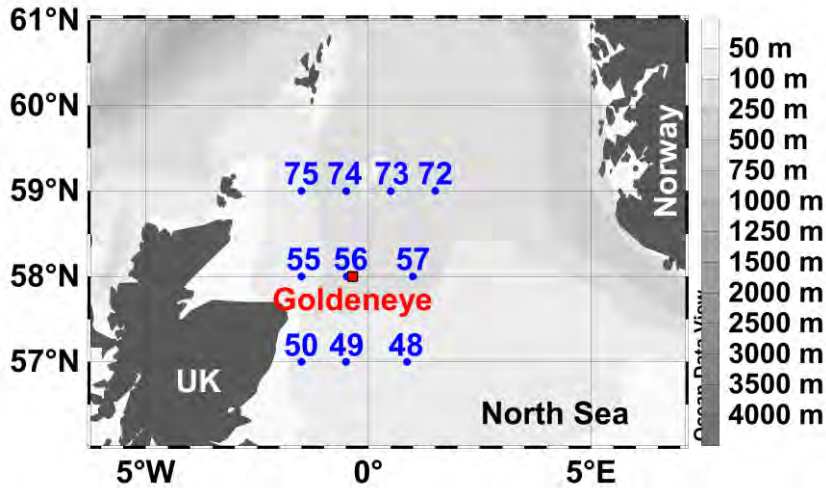

Fig. 1. Map of the Northern North Sea with the position of Goldeneye (red square). Blue dots indicate sampling locations (stations) and numbers refer to station numbers.

2. Measurements of the seawater CO₂ system

The seawater CO_2 system can be characterized by four measurable master variables [10]: total alkalinity (TA), total dissolved inorganic carbon (DIC), partial pressure of CO_2 (pCO_2), and pH. These master variables can be measured using a wide variety of methods [31].

Seawater TA is related to the charge balance in seawater and has units of moles per kilogram of solution. It can be approximated by the expression:

$$TA = [HCO_3^-] + 2[CO_3^{2-}] + [B(OH)_4^-] + [OH^-] - [H^+] \tag{6}$$

TA is determined by acidimetric titration and currently discrete sampling and benchtop instrumentation gives the highest precision.

Seawater DIC is the sum of the concentrations of all inorganic carbon compounds dissolved in seawater. It is expressed in moles per kilogram of solution and is given by the expression:

$$DIC = [CO_2]^* + [HCO_2^-] + [CO_3^{2-}] \tag{7}$$

where $[CO_2]^*$ accounts for the concentrations of dissolved CO_2 and H_2CO_3. Similar to TA, DIC is determined by acidimetric titration and currently discrete sampling and benchtop instrumentation gives the highest precision.

The pCO_2 in an air sample in equilibrium with a seawater sample is given by the expression:

$$pCO_2 = xCO_2\, p \tag{8}$$

where xCO_2 is the mole fraction of the CO_2 in the air sample and p is the total pressure of the gases. Both xCO_2 and p are usually measured directly. Several sensors measuring pCO_2 *in situ* at high frequency and in an autonomous mode exist and present satisfactory precision and accuracy.

The hydrogen ion concentration in seawater ($[H^+]$) is reported as a pH:

$$pH = -\log_{10}([H^+]) \tag{9}$$

Seawater pH can be determined by a potentiometric or spectrophotometric techniques. For this variable, as for pCO_2, there are sensors that can measure *in situ* at high frequency and in an autonomous mode with satisfactory precision and accuracy.

By measuring any two of the above-mentioned four master variables characterizing the seawater CO_2 system (along with temperature, salinity, pressure and with the knowledge of other non-CO_2 acid-base systems in seawater), it is possible to calculate those not measured. The selection of the appropriate two measured parameters can produce uncertainties in the computed parameters that are the same order of magnitude as their experimental errors [32].

3. Modeling the natural variability of the seawater CO_2 system

Natural processes affecting the seawater CO_2 system on seasonal to decadal time scales are adequately known. Water column DIC distribution is usually controlled by (i) air-sea exchange (followed by downward transport), (ii) biological processes of photosynthesis/respiration and formation/dissolution of $CaCO_3$ and (iii) mixing of water masses. In order to detect the CO_2 seeped from offshore CCS reservoirs using water column DIC measurements, a model that determines the effect of each of the above-mentioned natural processes on seawater DIC is necessary to filter out fluctuations arising from natural processes.

Photosynthesis takes up CO_2 and primary nutrients from seawater and produces oxygen (O_2) and organic matter. Inversely, degradation of organic matter through respiration uses O_2 and releases CO_2 and nutrients back to the water column. The changes in DIC, dissolved O_2 and nutrients through photosynthesis and respiration take place in constant proportions called Redfield ratios [33]. Therefore, the change in seawater DIC related to photosynthesis and respiration can be quantified from changes in nutrients or O_2 and the knowledge of the Redfield ratios [e.g., 33,34].

Similarly, *in situ* formation (dissolution) of $CaCO_3$ structures removes (releases) CO_3^{2-} from (to) seawater, therefore decreasing (increasing) TA and DIC in a 2:1 ratio [9]. Consequently, measurements of TA can be used to (i) monitor the *in situ* $CaCO_3$ changes and (ii) quantify the impact of such changes on water column DIC [e.g., 35].

The change in DIC due to air-sea exchange is driven by differences in pCO_2 between air and seawater. The effect of this process on seawater DIC can be estimated from direct pCO_2 measurements in air and seawater along with observations of wind speed (10 m above sea surface), sea surface temperature, sea surface salinity, and mixed layer depth.

Mixing of water masses changes the distribution of DIC and TA in the water column. In the presence of two water masses with known conservative properties (e.g., temperature and salinity), then a conservative mixing line can be constructed from a property-property plot to estimate the water mass fractions that make up the sample. Given these fractions, together with the DIC concentrations of the water masses, the DIC changes arising from mixing of varying water mass fractions can be estimated. Mixing between more than two water masses can be treated similarly, but it requires additional data from other conservative tracers. The addition/removal of freshwater also changes DIC and TA in the water column. The impact of this freshwater flux is minimized by a salinity normalization procedure, which adjusts seawater CO_2 system parameters to one reference salinity – often set to the mean salinity of the study area [e.g., 34].

From the above discussion it is understood that changes in seawater DIC due to natural processes can be modeled using variables that are assumed to be unaffected by CO_2 seepage. This is the motivation of the C_{seep} method.

4. The C_{seep} method

Once the drivers of the natural variability are 'modeled' as described in the previous section, we can rewrite Eq. (5) as:

$$C_m - \Delta C_{bio} - \Delta C_{mix} - \Delta C_{ase} = C_b + C_{seep} \quad (10);$$

in which the terms of the left-hand side are known and those of the right-hand side are unknown. To determine C_b, we need measurements at a reference station, i.e., a station with no seeps and therefore with $C_{seep}=0$. Assuming that C_b is identical at the reference station and the monitored area, C_{seep} is estimated using Eq. (10).

To ensure that C_b is identical in both the reference station and the monitored area, a sound site-specific baseline characterization is needed. This baseline study should include the same measurements at both the reference station and the monitored area during a period of time long enough to capture the seasonal and annual variability. It would also be desirable that the baseline characterizes the long-term trends (i.e. change in seawater CO_2 system due to the uptake of atmospheric CO_2 released by human activities) in both locations.

5. Application of the C_{seep} method in the Goldeneye area

We applied the C_{seep} method to publicly available seawater CO_2 system measurements around Goldeneye (Fig. 1; https://www.nodc.noaa.gov/ocads/oceans/GLODAPv2/cruise_table.html, cruises 661–665), a potential geological storage formations for CCS in the Northern North Sea. To test the ability of C_{seep} for seep detection, we created an artificial seep by adding extra DIC (34 µmol kg^{-1}) to one of the sampling locations (station 56) per cruise. This extra DIC added is within the range of the natural variations of DIC in the area. As reference station, we chose station 57. All other stations were treated as monitored stations.

The 'seepage' signal is obscured by the natural variability in the DIC around Goldeneye (Fig. 2a), where in some cases the DIC value of the seepage station equals to that in a non-seep station (see for example Fig. 2a, sampling period 11/2001). This problem is minimized when applying the C_{seep} methodology (Fig. 2b). The C_{seep} method clearly minimizes the effect of natural variability on seawater DIC measurements (Fig. 2), and highlights the seepage signal.
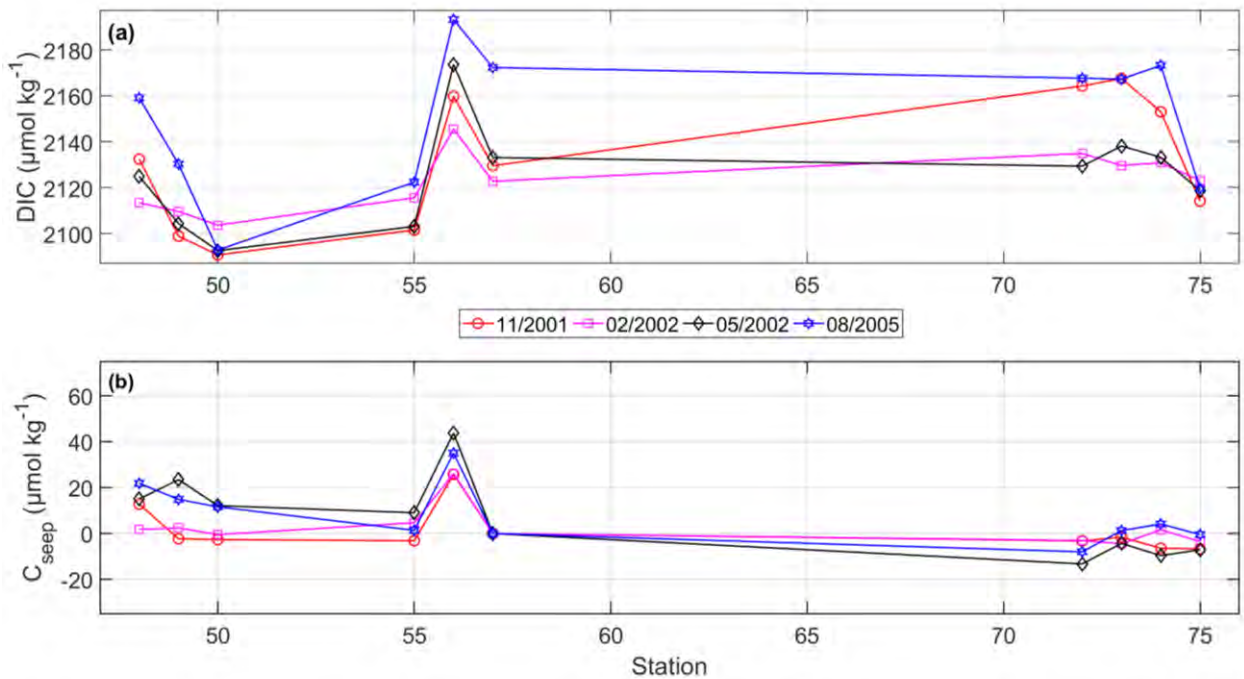

Fig. 2. (a) Natural variability of dissolved inorganic carbon (DIC) in the near-bottom samples at stations around Goldeneye (Fig. 1) during four cruises: 11/2001, 02/2002, 05/2002 and 08/2005. (b) C_{seep} values resulting from solving Eq. (10) for the near-bottom DIC measurements in (a). In both plots, an artificial seepage was created by adding a constant DIC value of 34 µmol kg^{-1} to station 56.

Except at station 56 (the station with the simulated seep), C_{seep} values at the monitored stations should be zero since there is no seep occurring at those stations. Therefore, non-zero C_{seep} values are indicative for the uncertainty associated with the C_{seep} calculations. This uncertainty has two components: a random component indicated by the spread of the C_{seep} values at each station, and a systematic component determined from station-to-station differences. The former depends on how well we estimate the impact of natural processes affecting seawater DIC (ΔC_{bio}, ΔC_{mix}, and ΔC_{ase}); while the latter depends on how identical is C_b in the reference station and the monitored area.

6. Automation of the C_{seep} method

The C_{seep} method was originally demonstrated using discrete sampling and highly accurate benchtop instrumentation for DIC and TA [29]. However, the combination of discrete sampling and benchtop instrumentation is resource intensive and time-consuming, which makes it a non-ideal technique for CCS monitoring purposes. Therefore, work is underway to optimize the C_{seep} method for working with measurements of autonomous sensors measuring at high frequency.

Preliminary results show that the choice of measurement parameters and associated uncertainty influences the sensitivity/accuracy of the C_{seep} calculations. By evaluating all the possible parameter combinations in the C_{seep} calculations for the Goldeneye area (Fig. 1), we found that the uncertainty of the C_{seep} values computed using pH and TA estimated from salinity have similar uncertainty to those resulting from highly accurate benchtop measurements of DIC and TA. Both pH and salinity can be measured at high frequency and in an autonomous mode using sensors, which makes these parameters suitable for CCS monitoring purposes. Therefore, the C_{seep} method can be fully automated using measurements from sensors and algorithms. Sensors necessary for the C_{seep} computations can be placed in both fixed stations and mobile platforms (e.g., AUVs), of which placement and pathways, respectively, can be optimized using statistical modeling [24,25,26,27,28].

7. Conclusions and further remarks

The application of the C_{seep} method as an offshore CCS monitoring tool around the Goldeneye area shows promising results. The method seems to adequately model the processes governing the natural variability of the seawater CO_2 system, which allows minimizing their influence on water column DIC measurements and isolating the artificially induced CO_2 seepage signal. Therefore, the C_{seep} method can be used to define DIC detection threshold. Besides, the C_{seep} method can be automated with *in situ* sensor-based measurements and algorithms. Therefore, the C_{seep} method is a potential CCS monitoring technique to be applied to geochemical water column measurements.

Site-specific baseline with high spatiotemporal resolution is needed to accurately parameterize the natural drivers of the variability in seawater DIC at a specific location. Sound baseline studies will also enable choosing the best reference station needed for the application of the C_{seep} method. The reference station must be representative of the monitored area and not affected by seeps. The careful selection of appropriate reference station will contribute to reduce uncertainty in the computed C_{seep} values and, hence, minimize the occurrence of false positives.

The implementation of the C_{seep} method needs a further careful site-specific evaluation of the main sources of uncertainty associated with the computed C_{seep} values. These include the evaluation of (i) the Redfield ratios parameterizing the DIC variability due to photosynthesis/respiration; (ii) the water masses encountered at both the reference station and the monitored area; and (iii) the trends in ocean acidification (i.e. change in seawater CO_2 content due to the uptake of atmospheric CO_2 released by human activities) in both the reference station and the monitored area.

Acknowledgements

References

[1] Haugan PM, Joos F. Metrics to assess the mitigation of global warming by carbon capture and storage in the ocean and in geological reservoirs. Geophys. Res. Lett. 2004; 31:L18202.

[2] IPCC. IPCC Special Report on Carbon Dioxide Capture and Storage. Prepared by Working Group III of the Intergovernmental Panel on Climate Change. [Metz B, Davidson O, de Coninck HC, Loos M, Meyer LA, (editors)]. Cambridge, United Kingdom and New York, NY, USA: Cambridge University Press; 2005.

[3] U.S. EPA. Federal Requirements under the Underground Injection Control (UIC) Program for Carbon Dioxide (CO_2) Geologic Sequestration (GS) wells. Federal Regulation, vol. 75, no. 237: 2010. p. 77230–77303.

[4] European Commission. Implementation of Directive 2009/31/EC on the Geological Storage of Carbon Dioxide: Guidance Document 2, Characterisation of the Storage Complex, CO_2 Stream Composition, Monitoring and Corrective Measures; 2011.

[5] Environmental Protection Agency. Geologic Sequestration of Carbon Dioxide. Draft Underground Injection Control (UIC) Program Class VI well testing and monitoring guidance. Office of Water (4606M). EPA 816-D-10-009; 2012.

[6] Jenkins C, Chadwick A, Hovorka SD. The state of the art in monitoring and verification-ten years on. Int. J. Greenh. Gas Control 2015; 40:312–349.

[7] Blackford J, Artioli Y, Clark J, de Mora L. Monitoring of offshore geological carbon storage integrity: Implications of natural variability in the marine system and the assessment of anomaly detection criteria. International Journal of Greenhouse Gas Control 2017; 64:99–112.

[8] IEAGHG. International Energy Agency Greenhouse Gas Research & Development Programme, "Assessment of Sub Sea Ecosystem Impacts", Report No. 2008/8; 2008.

[9] Zeebe RE, Wolf-Gladrow DA. CO_2 in seawater: equilibrium, kinetics and isotopes. Amsterdam: Elsevier Science, B.V.; 2001.

[10] Dickson AG. The carbon dioxide system in seawater: equilibrium chemistry and measurements. In: Riebesell U, Fabry VJ, Hansson L, Gattuso JP, editors. Guide to Best Practices for Ocean Acidification Research and Data Report. Luxembourg: Publications Office of the European Union; 2010. P. 17–40.

[11] Alendal G, Bernsten J, Engum E, Furnes GK, Kleiven G, Eide LI. Influence from 'Ocean Weather' on near seabed currents and events at Ormen Lange. Mar. Pet. Geol. 2005; 22(1–2): 21–31.

[12] Ali A, Frøysa HG, Avlesen H, Alendal G. Simulating spatial and temporal varying CO_2 signals from sources at the seafloor to help designing risk-based monitoring programs. J. Geophys. Res. Oceans 2016; 121:745–757.

[13] Wegener G, Shovitri M, Knittel K, Niemann H, Hovland M, Boetius A. Biogeochemical processes and microbial diversity of the Gullfaks and Tommeliten methane seeps (Northern North Sea). Biogeosci. Discuss. 2008; 5(1): 971–1015.

[14] Blackford JC, Widdicombe S, Lowe D, Chen B. Environmental risks and performance assessment of carbon dioxide (CO_2) leakage in marine ecosystems. In: Maroto-Valer MM, editors. Developments and Innovation in Carbon Dioxide (CO_2) Capture and Storage Technology, Carbon Dioxide (CO_2) Storage and Utilisation, vol. 2. Cambridge, U. K.: Woodhead Publ. Ltd.; 2010. P. 344–373.

[15] Brewer PG, Chen B, Warzinki R, Baggeroer A, Peltzer ET, Dunk RM, Walz P. Three-dimensional acoustic monitoring and modeling of a deep-sea CO_2 droplet cloud. Geophys. Res. Lett. 2006; 33:L23607.

[16] Noble RRP, Stalker L, Wakelin SA, Pejcic B, Leybourne MI, Hortle AL, Michael K. Biological monitoring for carbon capture and storage— A review and potential future developments. Int. J. Greenhouse Gas Control 2012; 10:520–535.

[17] Alendal G, Drange H. Two-phase, near-field modeling of purposefully released CO_2 in the ocean. J. Geophys. Res. 2001; 106:1085–1096.

[18] Drange H, Alendal G, Johannessen O. Ocean release of fossil fuel CO_2: A case study. Geophys. Res. Lett. 2001; 28:2637–2640.

[19] Vielst€adte L, Karstens J, Haeckel M, Schmidt M, Linke P, Reimann S, Liebetrau V, McGinnis DF, Wallmann K. Quantification of methane emissions at abandoned gas wells in the Central North Sea. Mar. Pet. Geol. Part B 2015; 68:848–860.

[20] Dewar M, Wei W, McNeil D, Chen B. Small-scale modelling of the physiochemical impacts of CO_2 leaked from sub-seabed reservoirs or pipelines within the North Sea and surrounding waters. Marine Pollution Bulletin 2013; 73:504–-515.

[21] Dewar M, Saleem U, Khajepor S, Chen B. Prediction of Greenhouse Gas Leakages from Potential North Sea Storage Sites into Coastal Waters by an Unstructured, Multi-Scale and Multi-Phase Flow Model, this issue.

[22] Saleem U, Dewar M, Chen B. Numerical Modelling of CO_2 Flow through Sediments into Water Column, this issue.

[23] Blackford J, Alendal G, Artioli Y, Avlesen H, Cazenave P, Chen B, Dale A, Dewar M, Gundersen K, Haeckel M, Khajepor S, Lessin G, Oleynik A, Saleem U, García-Ibáñez MI, Omar AM. Ensuring efficient and robust offshore storage–the role of marine system modelling, this issue.

[24] Hvidevold HK, Alendal G, Johannessen T, Ali A. Mannseth T, Avlesen H. Layout of CCS monitoring infrastructure with highest probability of detecting a footprint of a CO_2 leak in a varying marine environment. Int. J. Greenhouse Gas Control 2015; 37:274–279.

[25] Hvidevold HK, Alendal G, Johannessen T, Ali A. Survey strategies to quantify and optimize detecting probability of a CO_2 seep in a varying marine environment. Environ. Modell. Software 2016; 83:303–309.

[26] Gundersen K, Oleynik A, Alendal G, Skaug HJ, Avlesen H, Berntsen J, Blackford J, Blaser N, Cazenave P. Combining models and machine learning techniques to design leak detection monitoring, this issue.

[27] Oleynik A, Gundersen K, Alendal G, Skaug HJ, Avlesen H, Berntsen J, Blackford J, Blaser N, Cazenave P. Simplified modelling as a tool to locate and quantify fluxes from a CO_2 seep to marine waters, this issue.

[28] Alendal G. Cost efficient environmental survey paths for detecting continuous tracer discharges. J. Geophys. Res. Oceans 2017; 122:5458–5467.

[29] Botnen H, Omar AM, Throseth I, Johannessen T, Alendal G. The impact of submarine CO_2 vents on seawater: implications for detection of subsea carbon sequestration leakage. Limnology and Oceanography 2015; 60:402–410.

[30] Gruber N, Sarmiento JL, Stocker, T. An improved method for detecting anthropogenic CO_2 in the oceans. Glob. Biogeochem. Cycl. 1996; 10:809–837.

[31] Dickson AG, Sabine CL, Christian JR. Guide to best practices for ocean CO_2 measurements. Sidney, British Columbia: North Pacific Marine Science Organization; 2007.

[32] Millero FJ. The Marine Inorganic Carbon Cycle. Chemical Reviews 2007; 107 (2):308–341.

[33] Redfield AC. On the Proportions of Organic Derivatives in Sea Water and Their Relation to the Composition of Plankton. James Johnstone Memorial Volume, University Press of Liverpool 1934; 176-192.

[34] Anderson LA, Sarmiento JL. Redfield ratios of remineralization determined by nutrient data analysis. Glob. Biogeochem. Cycl. 1994; 8:65–80.

[35] Brewer PG. Direct observation of the oceanic CO_2 increase. Geophys. Res. Lett. 1987; 5:997–1000.

[36] Friis K, Kortzinger A, Wallace DWR. The salinity normalization of marine inorganic carbon chemistry data. Geophys. Res. Lett. 2003; 30:1085.

Establishing an effective environmental baseline for offshore CCS

Steve Widdicombe[a]*, Veerle A.I. Huvenne[b], James Strong[b], Jerry Blackford[a], Gavin Tilstone[a]

aPlymouth Marine Laboratory, Prospect Place, Plymouth, PL1 3DH, UK
bNational Oceanography Centre, University of Southampton Waterfront Campus, Southampton, SO14 3ZH, UK

Abstract

The proposed storage of CO_2 in sub-seabed geological reservoirs, known as Carbon dioxide Capture and Storage (CCS), could make a practical and significant contribution to reducing atmospheric CO_2 emissions thereby alleviating environmental and ecological damage due to climate change and ocean acidification. However, before any new marine activity is conducted, it is standard procedure for any environmental risks potentially posed by that activity to be considered. In particular, understanding what is 'natural' or 'normal' for an area is essential when looking to establish criteria against which potential environmental impacts can be identified, monitored and quantified. To that end, all offshore CCS projects would benefit from constructing an effective environmental baseline prior to the start of storage. However, due to the large spatial extent of storage complexes and the expectation that storage of the CO_2 will be permanent, there are a number of financial, logistical and methodological issues associated with constructing such baselines.

Firstly, sub-seabed storage complexes are sizeable structures. Whilst individual leakage events themselves are likely to be rare and have a small spatial impact, it might be considered that anywhere above the storage complex could potentially be the location of a leakage event. In reality very few areas will be at any risk from leakage but for the sake of public reassurance and in line with the precautionary principle, constructing an environmental baseline which covered the whole complex footprint would be prudent. However, assessing such large areas does raise certain challenges. The marine environment in general is highly spatially variable in terms of its physical, chemical and biological makeup with scales of variability ranging from the sub-metre scale corresponding to benthic patchiness, to dynamic boundaries between water masses of different origins, which may stretch for many kilometres. Consequently, the large area of marine environment that sits above a CCS reservoir will inevitably contain a mosaic of different seabed habitats and biological communities. It will also consist of varying water masses and pelagic biomes. This large spatial extent and high level of spatial variability, raises problems of affordability when attempting to construct the type of environmental baseline required to comprehensively assess any potential environmental risks associated with CCS activities.

In addition to the problems associated with assessing environmental heterogeneity over large spatial scales, described above, the marine environment also displays high levels of temporal variability. This is particularly relevant to many of the environmental parameters that may be directly used to identify and monitor CO_2 leakage events, such as changes in carbonate chemistry parameters which can undergo large and rapid fluctuations as a result of naturally occurring biological and physical processes. In addition to shorter term fluctuations, the marine environment is being exposed to longer-term changes in environmental conditions driven by man-made pressures such as climate change and changes in human activities (e.g. fishing, resource extraction, pollution). These gradual, chronic changes are especially important when considering the typical life-span of a CCS project. With the intention of storing CO_2 permanently it is essential that future long-term changes in environmental conditions are understood and such changes are not falsely attributed to CCS activities. All of this means that collecting sufficient amounts of observational data to adequately account for tidal, seasonal, annual and decadal trends and cycles, prior to starting any CCS activities would be impractical using traditional methods and would delay the rapid deployment of CCS projects, thus reducing this technology's potential contribution to reducing CO_2 emissions.

To meet the challenges of constructing effective environmental baselines that adequately account for large spatial and temporal scales, and thereby provide public reassurance that any potential risks are both identified and managed, new approaches in baseline data collection and analysis are needed. In this paper we illustrate a generic framework that combines some new and existing approaches and opportunities to extend environmental baselines through time and expand their spatial coverage. In doing so we illustrate how baseline data can be collected in a cost-effective and appropriate manner.

---

* Corresponding author. Tel.: +44 1752 633100; fax: +44 1752 633101.
  E-mail address: swi@pml.ac.uk

1. Introduction

In establishing effective marine environmental baselines for CCS operations there are generally three related objectives. The first is an assessment of any potential environmental risk faced by the marine environment in the unlikely event CO_2 was to escape from the storage complex and reach the overlying marine ecosystem. For this there is a need to identify the structure, function and potential sensitivities of those marine ecosystems above the storage complex. The second objective is to construct baselines that enable efficient and rapid yet rigorous CO_2 release detection or assurance monitoring. For this an understanding of seep dispersion and resulting chemical signatures is crucial. The third objective is to enable impact (or lack of impact) assessment, for which understanding the footprint of potentially damaging hypothetical seeps must be considered alongside an understanding of habitat variability and sensitivity to external pressures not related to storage. In the current paper we deal with the collection of information and data that could potentially contribute to each of these objectives. We are mindful, however, that here we only consider the upper seafloor and overlaying water column and do not consider deeper geological assessments.

The purpose of this paper is to highlight a series of approaches that could be used to create an effective environmental baseline specifically for industrial-scale, offshore Carbon dioxide Capture and Storage (CCS) projects. Whilst some of the actual data collection methods proposed in the paper are not new, the specific use of these data to describe environmental conditions across larger spatial and temporal domains in the context of CCS are. It is the challenge of scaling up across space and time while maintaining an appropriate level of detail that reflect a major difference between the requirements of CCS environmental baselines when compared to more traditional environmental surveys. An additional complication associated with CCS activities is that the potential contaminant involved is carbon dioxide (CO_2) which, as an abundant and naturally occurring compound in the marine environment, is a fundamental part of the marine ecosystem and is involved in a myriad of biological and chemical processes. Consequently, discriminating between natural variability in CO_2 related processes or parameters and any changes to the environment specifically due to CO_2 leakage from CCS, as well as predicting the potential risks and impacts associated with leaks, requires a far greater understanding of baseline conditions than were needed for previous industrial activities (e.g. oil and gas extraction).
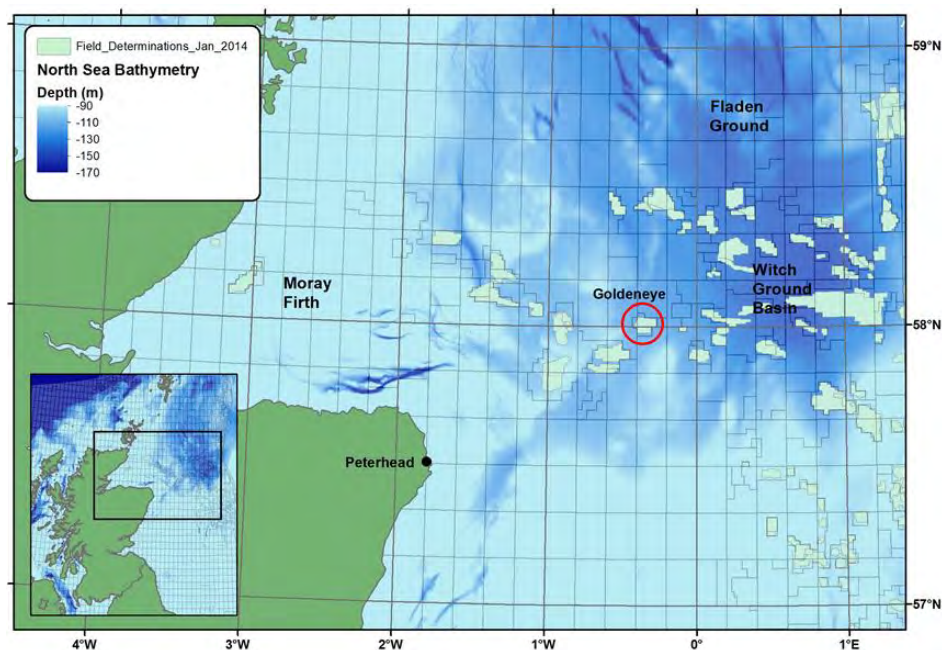

Fig. 1. Location map of the Goldeneye study site, NE of Peterhead, Scotland.

Whilst the approaches presented in this paper are intended to be generic and applicable to the majority of offshore CCS projects we have used a specific location to demonstrate how these approaches can be applied to a real world situation. The location we selected was the Goldeneye Field in the Central North Sea (fig. 1). Goldeneye is a depleted gas field operated by project partner Shell, and was operational from 2004 till 2011. It was planned that this site would be used as an industrial scale demonstration project for CCS but due to changes in UK government policy and funding these plans have yet to be realized.

It should however be noted that marine systems are characterised by high levels of heterogeneity, such that different storage sites will have different baseline variability and therefore different strategies for anomaly detection and different environmental sensitivities. So whilst in this paper Goldeneye is used as an exemplar for the application of the approaches we propose, the specific results we present cannot be directly applied to other storage areas.

2. Generic methodological framework

In this paper we propose a generic methodological framework that can be used effectively in CCS environmental baseline data acquisition and baseline construction (fig. 2). This framework suggests three main steps, each involving a series of activities. The first step is the initial site characterization which will use a combination of broad-scale acoustic surveys, remote sensing observations and computer based modelling to define and map the potential type and extent of marine habitats, biomes and features that exist within the area above the CCS complex. Once these areas have been defined the second step is to use this information to guide the collection of biological, physical and chemical data to confirm the accuracy of these maps, validate the remote sensing algorithms and model predictions and to generate greater understanding of marine environment above the CCS complex. This greater understanding will then underpin the next step which is to use existing acoustic and remote sensing data, plus computer model hind-casts and forecasts to recreate detailed multi-year baselines specific to the storage complex. It will also be used to extrapolate between point sources of data to provide a more extensive spatial coverage than can be achieved from sampling alone.
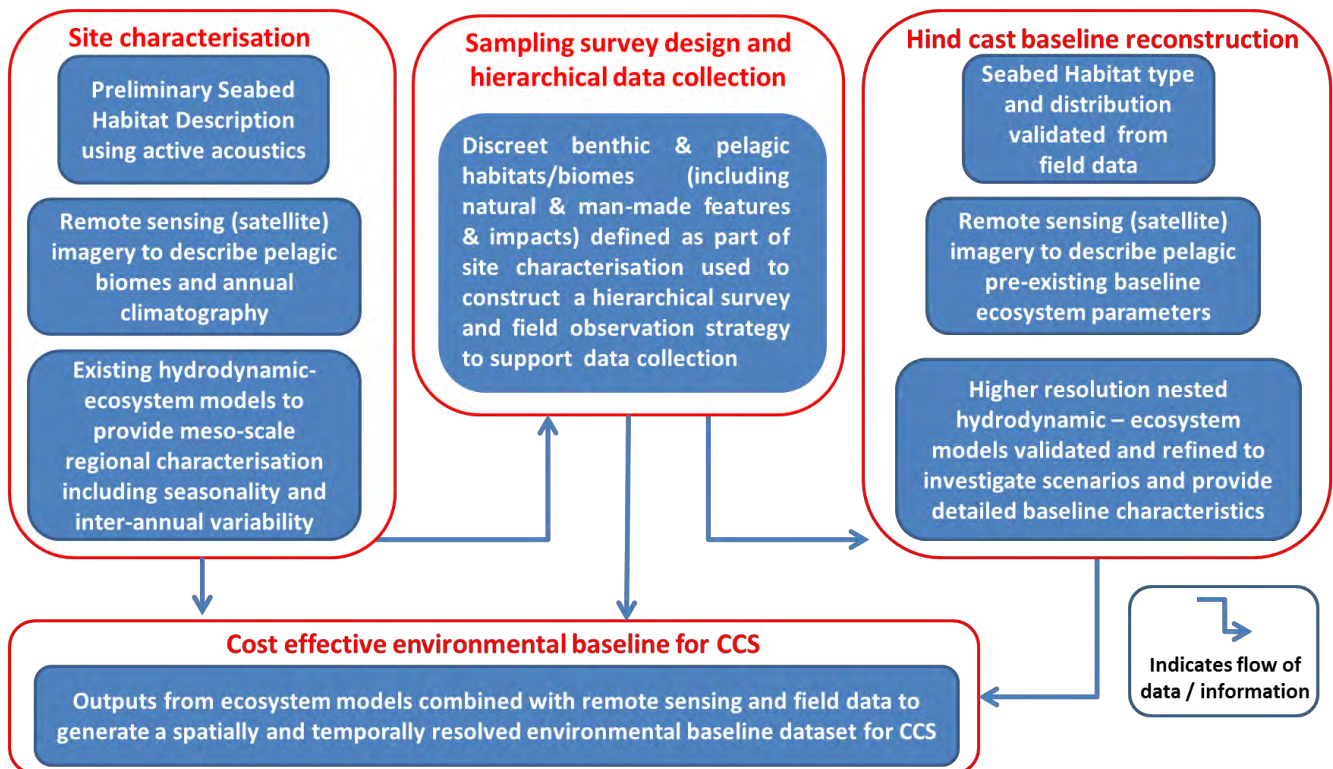

Fig. 2. A proposed generic framework for building a cost effective, CCS environmental baseline.

Both the initial site characterization and the subsequent hind cast baseline reconstruction activities in fig.2 involve aspects of seabed mapping, remote sensing and computer based modelling. Whilst, in practice, these 3 activities are strong linked, both with each other and with the data collection activity, for ease of presentation these activities will be discussed separately. However, before these methodologies are discussed it is important to consider a cost effective strategy by which baseline data collection can be prioritized and thus avoiding the collection of excess data and wasting resources.

3. Adopting a hierarchical approach to data collection

The marine environment that sits above a typical CCS complex is likely to be extremely large, possibly covering tens to hundreds of square kilometers. Consequently, collecting a broad suite of environmental data from across the entire area would be prohibitively expensive and time consuming. In order to ensure effective environmental baselines can be constructed we propose CCS projects should adopt a hierarchical approach to data collection with four distinct Tiers of data collection. These Tiers would

be based on a nested set of geographic areas with data at the broadest scale (Tier 1) being largely generated from existing, modelled or remotely sensed data (as described above), whilst data collected at the finest spatial and temporal scales (Tier 4) would involve more direct collection of environmental data.

- **Understanding the wider geographical context of storage complex by exploring processes out to the furthest extent of potential influence or impact [Tier 1].**

This would be done at the beginning of the CCS project but could also be updated every 10 years as new data and information become available. These repeated assessments would be useful for ensuring the continued validity of the original model projections and for monitoring changes in the primary production climatology of the area. Outputs from Tier 1 assessments would help to identify important biogeographic features (such as functionally different ecosystems or water bodies) that might exist above the storage complex. Examples of Tier 1 outputs include; Ecosystem modelling of baseline carbonate chemistry data (hindcast and projections) and remote sensing to reconstruct primary production climatology of the area.

- **Initial broad-scale mapping of the marine environment directly above the entire extent of the geological complex within which the predicted storage site is located (including seabed, water column and human uses) [Tier 2].**

This broad-scale mapping exercise could be conducted once at the start of the baseline parameters collection activity. The results from this mapping exercise would identify the specific locations that would require Tier 4 data collection (e.g. CO_2 injection well, old or existing wells, identified geological features that facilitate transport, specifically sensitive biological features). Collection of field data would involve surveys that combine side scan sonar from towed fish (or Automated Underwater Vehicles) with ship based multi-beam echosounder surveys to describe the seabed environment. Habitat definitions would be ground-truthed with point source samples where required. Visual (photography or video) surveys documenting physical features, type and conspicuous organisms or biogenic structures could also be conducted. Using this approach it is also possible to map human, physical structures and artefacts (e.g. munitions dumps, oil infrastructure, pipeline strengthening material location, litter, ship wreck location, fishing impacts and trawl tracks) as well as natural structures (e.g. Pock marks, reefs and rocks, natural gas bubble streams and fields) that might be of interest. It may be useful to undertake soundscape mapping should passive acoustic monitoring for bubbles become an accepted monitoring tool. Desk-based data gathering could be undertaken to identify other (potentially conflicting or consequential) users of the marine environment above the whole geological storage complex. In addition, existing (or relic) wells, chimneys, geological weaknesses, potential sources of current or historical contamination should be identified. Collecting shallow seismic data on seabed (including uppermost layers of overburden) structure, type and anomalies (including both natural e.g. fractures and chimneys, and manmade e.g. existing exploration, extraction or injection wells) to identify potentially high risk pathways for leakage would help identify Tier 4 areas.

- **Using fine scale computer based modelling, validated by targeted field observations, to describe the structure and function of those habitats occurring directly above the maximum expected spatial extent of CO_2 storage [Tier 3].**

Using high-resolution 3D local models, with simulations of hypothetical CO_2 seep scenarios, to identify potential perturbation footprints and contribute to EIA and development of monitoring strategies. Higher resolution modelling of the Tier 2 biogeochemical dynamics would enable validation and development using targeted observations and sample collection. This validation should be done at a spatial and temporal frequency sufficient to capture the variability predicted in the model projections. Validation data should ideally be collected regularly to maintain confidence on model predictions.

- **Detailed spatially and temporally resolved surveys in all habitats located above the expected storage site which are considered to be at the highest risk from leakage (i.e. have the highest probability of leakage or greatest potential sensitivity to leakage impact) [Tier 4]**

These areas are considered at highest risk from CCS leakage so should be assessed at the greatest level of detail. Observations of organisms or processes that could be impacted by CO_2 release should be made seasonally and annually resolved with the highest possible frequency sampling across 3 successive years. These data should be repeatedly collected every 10 years. The purpose of these data is not primarily to detect or monitor for CO_2 leakage but to provide a baseline against which the impact of a leakage event could be assessed in the unlikely event that a leak should occur.

4. Seabed Habitat Description

We propose that an important step in constructing an effective environmental baseline should be to collect broad scale seafloor morphological and sedimentological/substrate information. The most cost effective way of doing this over a large area is to use active acoustic seabed mapping techniques. Currently available and widely used techniques can be used to define seabed 'landscapes' as derived from geo-morphological classifications [1]. These landscapes can cover areas of 10's km at a resolution

of 5-10m and are therefore appropriate for providing information at the Tier 1 level. In addition, using ship or Autonomous Underwater Vehicle (AUV) based acoustics with point observations (ground-truthing) for model calibration and validation, seabed habitats can be defined by using geo-spatial models to extrapolate point observations. Using this approach habitat maps can be constructed over areas from 1-10 km with a resolution of $1 - 5$ m. This would support the assessment of seabed habitats from above the storage complex (Tier 2).

Data collected using multi-beam echosounders provide information about depth (i.e., bathymetry) and seabed acoustic reflectivity (i.e. backscatter, which is a useful proxy for substratum) [2]. Also sidescan sonar (for seafloor reflectivity) and seismic techniques (for bathymetry and reflectivity) can be used to map seabed characteristics to a certain extent. These datasets form the backbone of any physical and geo-morphological mapping that will support the baseline, plus they are essential for the planning of further operational activities in the area. For CCS projects that are using previously exploited oil and gas reservoirs, these acoustic data may already be available. However, existing data may not always be of adequate resolution, extent or quality for more fine-scale discrimination of seabed features (Tier 3 or 4). This was the case at the Goldeneye site were analysis was carried out on existing high-resolution datasets, which unfortunately had limited spatial extent. We also used the first return (depth and amplitude) from a 3D seismic dataset to contribute to the seafloor morphological maps. However, the quality of the seismic data did not allow for anything greater than a Tier 2 analysis, which meant further data had to be acquired for Tier 4.

Ideally, for smaller (less than 1km^2) areas that have been identified as needing the greater levels of data coverage (Tier 4), comprehensive multibeam echosounder or sidescan sonar surveys should be carried out around each area. For the Goldeneye example, using a ship-mounted multi-beam system, surveying at 8 knots, would produce a 5 m x 5 m bathymetric grid. This resolution would provide a good quality dataset to interpret seafloor morphology, but may miss fine-scale changes in seabed bathymetry potentially associated with slow and diffuse gas seeps. For even finer resolutions at this water depth (~110 m) an AUV could be used, with a similar multibeam system, to achieve a pixel resolution of 1 m x 1 m. To enable the most detailed seabed characterisation (spatial distribution of sediment type, seabed disturbance from fishing (trawl marks) and from hydrocarbon extraction activities (e.g. cuttings piles, seafloor infrastructure, scars)), high resolution sidescan sonar surveys (~400 kHz) are required. To achieve full habitat maps, the acoustic data will have to be combined, using geo-spatial statistics, with direct observations of the seabed (ground-truthing) i.e. seabed photographs, video data, grab samples or cores that will provide real information on sediment type and faunal communities. However, given that it is not possible to image or sample the entire seafloor, the acoustic maps form the main vehicle to extrapolate robustly the point-source information gained from seabed samples into a full coverage map [3].

5. Using remote sensing (satellite) imagery to define the spatial extent of pelagic marine ecosystems and understanding seasonal patterns in ecosystem function

Much of the natural spatial and temporal variability seen in seabed ecosystems and marine biogeochemistry is driven by seasonal patterns in phytoplankton blooms which can vary in their structure, timing, intensity and duration. In addition, phytoplankton blooms have the capacity to take up CO_2 from seawater through the process of photosynthesis and can therefore influence the local carbonate chemistry dynamics. All of this means that understanding the primary production characteristics of an area is an important part of any initial site characterisation. This is especially important when assessing large spatial areas that could be influenced by more than one water mass each of which could have different physical, chemical and biological properties. In addition, an understanding of the primary production climatology of an area will help describe the overall ecosystem structure and function and can usefully inform the ecosystem level models described in section 6 below. Due to the scale over which satellite observations can be collected, ocean colour data can make a significant contribution to providing both Tier 1 and Tier 2 level data.

An example of ocean colour time series for the region is given in fig. 3. An initial assessment, integrating more than 10 years of existing remote sensing data from across the Goldeneye area, has demonstrated the value in using satellite derived ocean colour products to generate a detailed historic climatology for the area. Specifically, the Goldeneye storage complex was shown to sit below two functionally different pelagic marine ecosystems. The boundary between these ecosystems appears to run roughly NW to SE through the Goldeneye platform area. However, the precise location of this boundary is highly variable from year to year and could cause considerable inter-annual variability in Chl *a* and Primary Production (PP) across the sites. Future baseline data collection at this site should be mindful of this boundary area and should endeavor to collect data from each of these two contrasting ecosystems.
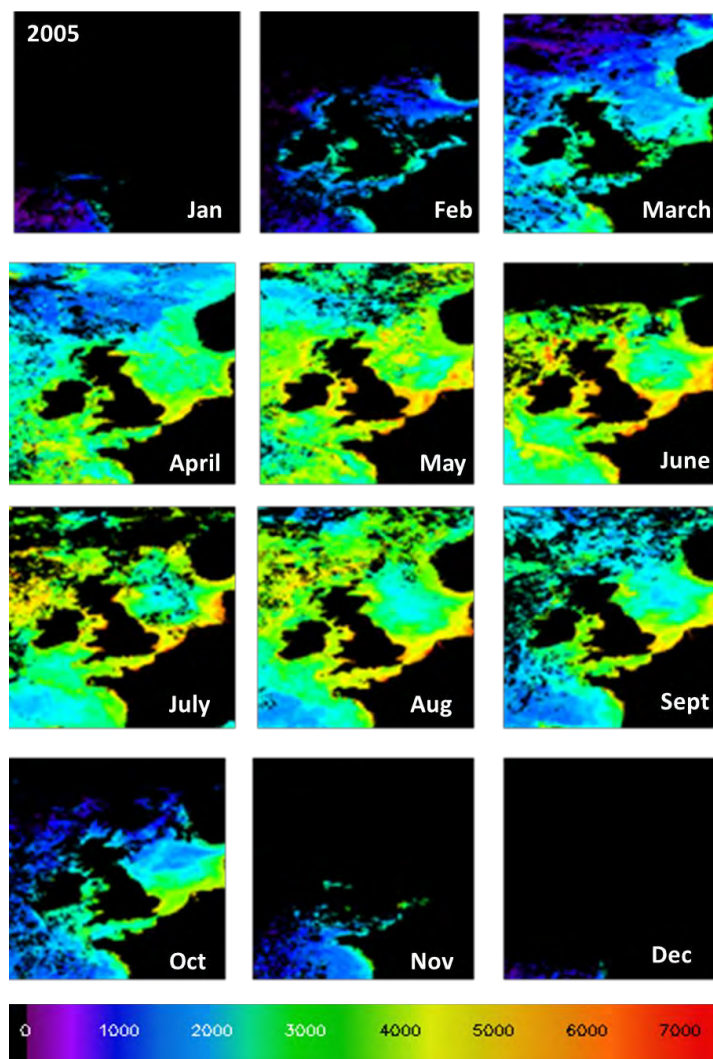
Fig. 3. Climatology in SeaWiFS Chlorophyll-a (mg m^{-3}) at Golden Eye from 1998 to 2010. SeaWiFS Chlorophyll-a can be used to compute primary production [4,5,6,7]. Analysis of historic ocean colour data can provide the baseline which can then be used to monitor perturbation in primary production around the CCS site.

As previously mentioned, the close coupling between primary production and carbonate chemistry [8,9,10,11] underpins the importance of understanding natural phytoplankton patterns and processes in areas overlaying CCS complexes. However this is not just limited to understanding the natural function of marine ecosystems and describing the short-term temporal and spatial heterogeneity existing above CCS complexes. In light of continuingly increasing levels of atmospheric CO_2, and the corresponding phenomena of ocean acidification, it is critical that long-term changes in pelagic ecosystems are not falsely attributed to CO_2 release from CCS. For example, in diatoms, some cyanobacteria and coccolithophorids, elevated CO_2 can lead to an increase in photosynthesis especially in large chain forming diatoms [12,13], *Synechococcus* spp. [14] and *Emiliania huxleyi* [15], suggesting that these taxa will behave differently in a future ocean with elevated levels of CO_2.

Measures of primary production are already being used to describe ecosystem health. Recently the European Union Marine Strategy Framework Directive has identified the maximum peak in Primary Production (PP) during the growing season, and the Productivity (PP/Chlorophyll a biomass) as appropriate indicators of changes in the environment and the ecosystem. The collection of long time series on primary production has helped to implement a seasonal reference baseline and ascertain evolution and the carrying capacity of the ecosystem. This has been termed 'Baseline Indicator FW2: Phytoplankton Production'. Threshold levels are determined for each OSPAR sub-region by annual primary production that should not exceed 300 gC m^{-2} yr^{-1} in coastal ecosystems with daily values of primary production should be less than 2-3 gC m^{-2} d^{-1} during phytoplankton blooms. It is essential that, should areas around CCS projects fail to meet these measures of ocean health in the future, such a failure should not be falsely attributed to CO_2 seepage. Remote sensing could be a powerful tool in demonstrating that changes are operating over spatial scales that couldn't possibly be attributable to CCS seepage.

In conclusion we propose that the use of remote sensing and satellite derived ocean colour data is an increasingly powerful

tool for understanding both the short-term (intra-annual) and long-term (inter-annual to decadal) patterns in pelagic production. This information will be important for i) defining the geographic extent of functionally different marine ecosystem and how these boundaries shift through time, and ii) understanding the changes in marine ecosystem functioning those caused by other environmental and anthropogenic drivers and differentiate these from changes that could be attributed to CCS activities.

6. Using ecosystem models to supplement environmental data acquisition and sampling design.

As previously discussed a comprehensive environmental baseline for CCS activities should ideally contain several years of data prior to the start of any storage activity in order to quantify (climate driven) inter-annual variability as well as a full annual description that resolves the significant seasonal cycles in the system and their (weather driven) variability. Variability at tidal to sub diurnal timescales can also be important, especially for detection monitoring. These data need to cover a broad geographical area equivalent to the storage complex and surrounding areas of influence. The data also needs to be multivariate; information on currents and mixing, CO_2 chemistry, key chemical components such as nutrients and oxygen, basic biological metrics such as production, sediment distributions, bottom morphology and key species information are all necessary or useful. Unfortunately this will rarely be possible to derive from direct observations for both logistical and financial reasons; direct observation data of marine systems, especially when requiring ship-borne deployments is expensive and consequently available data is sporadic and sparse, confined to a sub-set of the variables of interest, worse for near sea-bed data. Earth observation data provides excellent spatio-temporal coverage but of a very limited variable set limited to the surface ocean. Marine biogeochemical models however can provide high resolution, depth resolved, multivariate, internally consistent hindcast and forecast data [16], (fig 4). Generally models deliver hydrodynamic, chemical and basic biological metrics but not information on sediments, morphology and specific species. Of course models are not perfect representations of reality with errors due to the concatenation of thousands of individual species and processes into perhaps tens of functional groups and hundreds of mathematically defined processes. Never-the-less models are common research tools in international oceanography and the majority of the globes' oceans are described by pre-existing and often fairly sophisticated, evaluated model systems [17].
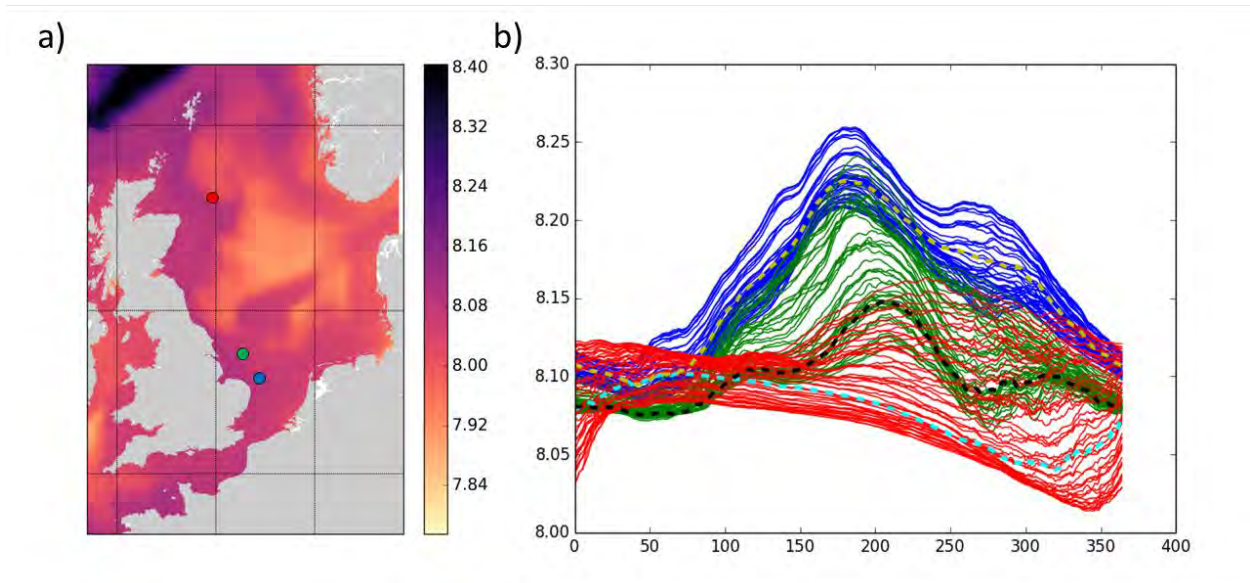

Fig. 4. (a) Modelled annual mean pH (indicating CO_2 concentration) in the North Sea, (b) multiple annual cycles of modelled pH from three different sites as indicated in (a).

In order to provide some utility for CCS operations, marine models require a reasonable characterisation of hydrodynamic mixing, including tidal processes and a biogeochemical or ecosystem model which describes changes in carbonate (CO_2) chemistry due to bio-physical processes and the basic biological components of the system, namely primary production, consumers and ideally benthic processes.

Initially and at minimal cost, off-the-peg regional model simulations are able to provide hind- and forecasts of physical-biogeochemical data which, alongside E.O. data can quantify how baselines may be naturally changing due to drivers that are unconnected with CCS activities. For example, climate change, eutrophication, deoxygenation and changes in fishing pressure are all factors that could impact upon the environment above a CCS complex that could drive change that could falsely be attributed to CCS [17]. The model data will further assist in the planning of detailed observational strategies.

A second, potential investment requiring stage is to nest high-resolution model domains describing specific storage sites at sub

kilometre to metre scale, which enable the simulation of speculative leak scenarios [18,19,20,21,22]. By understanding the dynamics and dispersion of the resulting plumes and their associate chemistry we can define impact footprints as part of a EIA risk analysis [23] as well as plan detailed detection monitoring strategies including the identification of site-specific anomaly criteria [24,25] and optimal platform deployment [26,27,28].

Thirdly, models are always improved by "real" data, such that assimilating or entering a model evaluation – development cycle utilising the site specific observations could improve model fidelity.

Finally, models can indicate some features of ecosystem response to perturbation from high CO_2 [29], but they are not yet sufficiently developed to be able to comprehensively predict ecological impacts of CO_2 seeps.

When used in conjunction with field data collection, ecosystem models provide us with powerful tools to supplement a lack of observational data with a modelled understanding of the marine ecosystem and an in-silico testbed for deriving monitoring strategies.

7. Managing the information and creating an integrated environmental baseline database

All spatial data gathered for baseline studies will need efficient and effective data management. Given its spatial nature, the use of Geographical Information Systems (GIS), effectively spatial databases, is strongly recommended. GIS systems allow the user to work with datasets of different scales, sources and types of coverage (full coverage raster datasets and spatially explicit vector datasets), and hence are perfect to move seamlessly between the different Tiers. They also provide functionality to combine or convert datasets recorded in differing coordinate systems (datum and projection). GIS also provides the framework for combining survey data (remote sensing, acoustic surveys and point observations collected for model calibration and validation) with additional spatial data sets. In order to represent the distribution and intensity of fishing effort with the study area, spatial grids of Vessel Monitoring System data (locational monitoring of larger fishing vessels whilst fishing) were imported into the Goldeneye GIS project. The Vessel Monitoring System data were used to stratify the Goldeneye site according to fishing effort, and thereby potentially proportion environmental or biological change induced by multiple and overlapping anthropogenic activities. Furthermore, GIS files stating the location of oil and gas seafloor infrastructure (e.g. well heads, jackets and pipelines) can be buffered to account for historical contamination, cutting piles and scour pits that might also compromise the detection of impacts specific related to gas leakage. Finally, GIS also provides the required tools for comparing overlapping surveys over time. For example, topographic changes in pockmark morphology may indicate the location of gaseous seeps. Ultimately, the GIS environment allows the user to combine pelagic and benthic data sets, with modelled data, and multiple sources of anthropogenic information into one, integrated framework. Overlap analysis can then be used to identify (i) consistent pelagic and benthic environments requiring specific baselines, (ii) overlapping anthropogenic activities that might confound the quantification and attribution of impacts, (iii) the identification of information gaps and data shortcomings that need to be addressed for full site characterisation and impact detection.

8. Summary

To meet the challenges of constructing environmental baselines that adequately account for large spatial and temporal scales, and thereby provide public reassurance that any potential risks are both identified and managed, new approaches in baseline data collection and analysis are needed. In this paper we have illustrated a framework that combines a series of new and existing approaches. This provides CCS operators with an opportunity to combine a variety of data types to extend environmental baselines through time and expand their spatial coverage. We propose this integrated framework as a supportive approach to constructing an effective environmental baseline, suitable for supporting offshore CCS activities in terms of leak detection monitoring, environmental risk assessment and impact quantification. This approach uses existing data, acoustic surveys, satellite, remote sensing and model derived data to map and describe habitat distributions, environmental conditions and ecosystem functioning across large areas. Coupled ecosystem-biogeochemical models can also be used to extrapolate data through space and time in order to determine monthly, seasonal or inter-annual modes of variability and trends in the biochemical and biological parameters of these areas. Results from broad-scale surveys, observations and models can be used to cost-effectively design and implement *in-situ* data collection activities, to ensure data are collected at the most appropriate locations and frequencies. Whilst each potential CCS site will have its own unique baseline requirements due to in-situ bio-physical characteristics, the baseline quantification techniques and approaches presented here are designed to be generic, allowing them to be applied to the majority of offshore storage sites located within coastal shelf seas. Their implementation should allow for a more practical and rapid assessment of baseline conditions thus allowing potential CCS projects to proceed more quickly.

Acknowledgements

References

[1] Hogg OT, Huvenne VAI, Griffiths HJ, Dorschel B, Linse K. (2016). Landscape mapping at sub-Antarctic South Georgia provides a protocol for underpinning large-scale marine protected areas. Scientific Reports,2016; 6: 33163

[2] Le Bas TP, Huvenne VAI. Acquisition and processing of backscatter data for habitat mapping - Comparison of multibeam and sidescan systems. Appl Acoust 2009;70(10):1248-1257.

[3] Brown CJ, Smith SJ, Lawton P, Anderson JT. Benthic habitat mapping: a review of progress towards improved understanding of the spatial ecology of the seafloor using acoustic techniques. Estuar Coast Shelf Sci 2011;92:502-520.

[4] Smyth TJ, Tilstone GH, Groom SB. Integration of radiative transfer into satellite models of ocean primary production. J. Geophys Res-Oceans, 2005;110.

[5] Tilstone GH, Smyth TJ, Gowen RJ, Martinez-Vicente V, Groom SB. Inherent optical properties of the Irish Sea and their effect on satellite primary production algorithms. J Plank Res 2005;27:1127-1148.

[6] Tilstone G, Smyth T, Poulton A, Hutson R. Measured and remotely sensed estimates of primary production in the Atlantic Ocean from 1998 to 2005. Deep-Sea Res II 2009;56:918-930.

[7] Tilstone GH, Taylor BH, Blondeau-Patissier D, Powell T, Groom SB, Rees AP, Lucas MI. Comparison of new and primary production models using SeaWiFS data in contrasting hydrographic zones of the northern North Atlantic. Remote Sens Env 2015;156:473-489.

[8] Brading P, Warner ME, Davey P, Smith DJ, Achterberg EP, Suggett DJ. Differential effects of ocean acidification on growth and photosynthesis among phylotypes of Symbiodinium (Dinophyceae). Limnol Oceanogr 2011;56:927-938.

[9] Feng Y, Hare CE, Leblanc K, Rose JM, Zhang Y, DiTullio GR, Lee PA, Wilhelm SW, Rowe JM, Sun J, Nemcek N, Gueguen C, Passow U, Benner I, Brown C, Hutchins DA. Effects of increased pCO_2 and temperature on the North Atlantic spring bloom. I. The phytoplankton community and biogeochemical response. Mari Ecol Prog Ser 2009;388:13-25.

[10] Feng Y, Warner ME, Zhang Y, Sun J, Fu F-X, Rose JM, Hutchins DA. Interactive effects of increased pCO_2, temperature and irradiance on the marine coccolithophore Emiliania huxleyi (Prymnesiophyceae). Euro J Phycol 2008;43:87-98.

[11] Flynn KJ, Clark DR, Mitra A, Fabian H, Hansen PJ, Glibert PM, Wheeler GL, Stoecker DK, Blackford JC, Brownlee C. Ocean acidification with (de)eutrophication will alter future phytoplankton growth and succession. Proc Roy Soc B 2015;282.

[12] Tortell PD, Morel FMM. Sources of inorganic carbon for phytoplankton in the eastern Subtropical and Equatorial Pacific Ocean. Limnol Oceanogr 2002;47:1012-1022.

[13] Tortell PD, Payne CD, Li Y, Trimborn S, Rost B, Smith WO, Riesselman C, Dunbar RB, Sedwick P, DiTullio GR. CO_2 sensitivity of Southern Ocean phytoplankton. Geophys Res Letts, 2008;35.

[14] Fu F.-X, Warner ME, Zhang Y, Feng Y, Hutchins DA. Effects of increased temperature and CO_2 on photosynthesis, growth, and elemental ratios in marine Synechococcus and Prochlorococcus (Cyanobacteria). J Phycol 2007;43:485-496.

[15] Leonardos N, Geider RJ. Elevated atmospheric carbon dioxide increases organic carbon fixation by Emiliania huxleyi (Haptophyta), under nutrient-limited high-light conditions. Journal of Phycology, 2005;41:1196-1203.

[16] Ciavatta, S., Kay, S., Saux-Picart, S., Butenschon, M., Allen, J.I., 2016. Decadal reanalysis of biogeochemical indicator and fluxes in the North West European shelf-sea ecosystem. *Journal of Geophysical Research – Oceans* 121, 1824–1845. doi:10.1002/2015JC011496

[17] Holt, J., Schrum, C., Cannaby, H., Daewel, U., Allen, J.I., Artioli, Y., Bopp, L., Butenschon, M., Fach, B.A., Harle, J., Pushpadas, D., Salihoglu, B., Wakelin, S., 2016. Potential impacts of climate change on the primary production of regional seas: A comparative analysis of five European seas. *Progress in Oceanography* 140, 91–115. doi:10.1016/j.pocean.2015.11.004

[18] Blackford, J.C., Jones, N., Proctor, R., Holt, J.T., 2008. Regional scale impacts of distinct CO_2 additions in the North Sea. *Marine Pollution Bulletin* 56, 1461–1468. doi:10.1016/j.marpolbul.2008.04.048

[19] Phelps, J.J.C., Blackford, J.C., Holt, J.T., Polton, J.A., 2015. Modelling Large-Scale CO_2 Leakages in the North Sea. *International Journal of Greenhouse Gas Control* 38, 210–220. doi:10.1016/j.ijggc.2014.10.013

[20] Blackford, JC; Torres, R; Artioli, Y; Cazenave, P. 2013. Modelling dispersion of CO_2 plumes in sea water as an aid to monitoring and understanding ecological impact. *Energy Procedia* 37, 3379–3386. doi:10.1016/j.egypro.2013.06.226

[21] Dewar, M., Saleem, U., Khajepor, S., Chen, B. Prediction of Greenhouse Gas Leakages from Potential North Sea Storage Sites into Coastal Waters by an Unstructured, Multi-Scale and Multi-Phase Flow Model, *this issue*.

[22] Dewar, M., Wei, W., McNeil, D., Chen, B., 2013. small-scale modelling of the physiochemical impacts of CO_2 leaked from sub-seabed reservoirs or pipelines within the North Sea and surrounding waters. *Marine Pollution Bulletin* 73, 504–515. doi:10.1016/j.marpolbul.2013.03.005

[23] Jerry Blackford, Guttorm Alendal, Yuri Artioli, Helge Avlesen, Pierre W. Cazenave, Baixin Chen, Andrew W. Dale, Marius Dewar, Maribel I. García-Ibáñez, Jonas Gros, Kristian Gundersen, Matthias Haeckel, Sorush Khajepor, Gennadi Lessin, Anna Oleynik, Abdirahman M. Omar, Umer Saleem. Ensuring efficient and robust offshore storage – the role of marine system modelling. Proceedings of the 14th International Conference on Greenhouse Gas Control Technologies, GHGT-14

[24] Blackford, J.C., Artioli, Y., Clark, J., de Mora, L., 2017. Monitoring of offshore geological carbon storage integrity: implications of natural variability in the marine system and the assessment of anomaly detection criteria. *International Journal of Greenhouse Gas Control* 64, 99–112. doi:10.1016/j.ijggc.2017.06.020

[25] Ali, A., Frøysa, H.G., Avlesen, H., Alendal, G., 2016. Simulating spatial and temporal varying CO_2 signals from sources at the seafloor to help designing risk-based monitoring programs. *Journal of Geophysical Research-Oceans 121*(1), 745–757. doi:10.1002/2015JC011198

[26] Alendal, G. (2017). Cost efficient environmental survey paths for detecting continuous tracer discharges. *Journal of Geophysical Research-Oceans*, *122*(7), 5458–5467. http://doi.org/10.1002/2016JC012655

[27] Greenwood, J., Craig, P., Hardman-Mountford, N., 2015. Coastal monitoring strategy for geochemical detection of fugitive CO_2 seeps from the seabed. *International Journal of Greenhouse Gas Control* 39, 74–78. doi:10.1016/j.ijggc.2015.05.010

[28] Alendal, G., Blackford, J., Chen, B., Avlesen, H., & Omar, A., 2017. Using Bayes Theorem to Quantify and Reduce Uncertainties when Monitoring Varying Marine Environments for Indications of a Leak. *Energy Procedia*, *114*, 3607–3612. http://doi.org/10.1016/j.egypro.2017.03.1492

[29] Lessin, G., Artioli, Y., Queirós, A.M., Widdicombe, S., Blackford, J.C., 2016. Modelling impacts and recovery in benthic communities exposed to localised high CO_2. *Marine Pollution Bulletin* 109, 267–280. doi:10.1016/j.marpolbul.2016.05.071